Intensity interferometry in subatomic physics

David H. Boal

Department of Physics, Simon Fraser University, Burnaby, British Columbia, Canada V5A 1S6

Claus-Konrad Gelbke

Department of Physics and Astronomy and National Superconducting Cyclotron Laboratory, Michigan State University, East Lansing, Michigan 48824

Byron K. Jennings

TRIUMF, 4004 Wesbrook Mall, Vancouver, British Columbia, Canada V6T 2A3

The intensity interferometry technique, commonly referred to as the Hanbury-Brown/Twiss effect, has been applied to nuclear and elementary-particle collisions as a method of investigating their space-time evolution. In this review the theoretical framework of the technique is presented, describing the formulations in common use. A survey is made of its application to subatomic collisions, ranging from high-energy elementary-particle reactions to low-energy nuclear reactions. Results derived from experimental data analysis are compiled and discussed. A critique is made of the interpretational difficulties associated with the use of the technique in reaction studies.

CONTENTS

I. INTRODUCTION

The technique of intensity interferometry has its origins in astrophysics, but has seen significant theoretical development and widespread application in subatomic physics. It has been used to investigate the space-time evolution of elementary-particle and nuclear collisions. The method involves the construction of a two-particle correlation function from the distribution of particles radiated from a hot, spatially localized source. In the original astrophysics applications of the technique, the source was a distant radio-wave emitter. In applications involving the collision of nuclei or particles, the source is the reaction region. The particles used to construct the correlation function can be pions, protons, or even nuclei.

Intensity interferometry was developed by Hanbury-Brown and Twiss in the 1950s, as a means of determining the dimension of distant astronomical objects. They first used the technique to examine radio-wave sources in the galaxies Cygnus and Cassiopeia (Hanbury-Brown, Jennison, and Das Gupta, 1952), and subsequently applied the method to a measurement of the angular diameter of Sirius (Hanbury-Brown and Twiss, 1956b). The theory of the effect was presented and refined in a series of papers also written by these authors (Hanbury-Brown and Twiss, 1954, 1957a, 1957b). Initially, the technique did not receive universal acceptance, and a number of terrestrial experiments were performed to confirm it (Hanbury-Brown and Twiss, 1956a, 1956c, 1957b; see also Purcell, 1956). The method of intensity interferometry is now commonly referred to as the Hanbury-Brown/Twiss effect.

The difference between *intensity* interferometry and conventional *amplitude* interferometry is illustrated in Fig. 1 (the mathematical treatment of this example can be found in Chaps. 1–3 of Klauder and Sudarshan, 1968). A finite-size source emits indistinguishable particles (for example, from positions S_α and S_β), and the particles are later observed at positions P_1 and P_2. Both emission points contribute to both observation points.

In *amplitude* interferometry each of the "detectors" at P_1 and P_2 could be a slit through which the emitted par-

Copyright ©1990 The American Physical Society

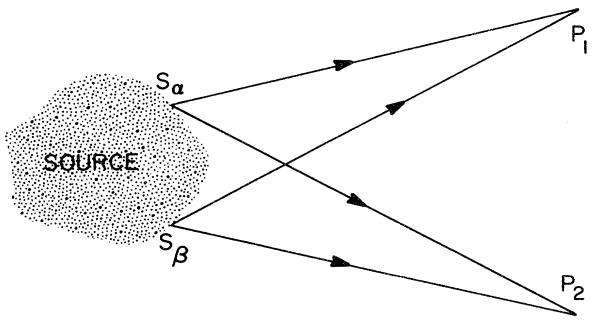

FIG. 1. Schematic representation of the emission of two indistinguishable particles from two points (S_α and S_β) on a source. The particles are observed at points P_1 and P_2.

ticles pass. The particles could then produce an interference pattern, perhaps on a screen located on the opposite side of the slits from the source, to use a traditional example. The interference pattern so produced depends on the relative phase of the particles' amplitudes as measured at P_1 and P_2.

In *intensity* interferometry a correlation function $R(\mathbf{r}_1,\mathbf{r}_2)$ is constructed from the number of counts n_1 and n_2 measured at P_1 and P_2:

$$R(\mathbf{r}_1,\mathbf{r}_2)=(\langle n_{12}\rangle/\langle n_1\rangle\langle n_2\rangle)-1\ , \tag{1.1}$$

where n_{12} denotes the number of counts in which particles are observed at P_1 and P_2. The correlation function is proportional to the intensity (i.e., the complex square of the amplitude) of the particles at P_1 and P_2. Because of the symmetrization (or antisymmetrization) of their wave function, identical particles can have a nonzero correlation function even if the particles are otherwise noninteracting.

One of the limitations to stellar diameter measurements using amplitude interferometry is the phase shift induced in the incident waves' amplitudes near P_1 and/or P_2 due to atmospheric effects. The further apart P_1 and P_2 are, the greater the potential for phase changes, and hence the poorer the resolution of the amplitude interferometer. Intensity interferometry was developed to reduce the importance of these phase changes.

Although the original application of the Hanbury-Brown/Twiss effect used photons as the detected particles, it was rapidly realized that the technique could be generalized to include correlation measurements for other bosons, and fermions as well. Within a decade, correlations between identical pions were used to investigate elementary-particle reactions. Subsequently the technique of intensity interferometry has also been applied to the interpretation of correlations between (identical and nonidentical) nuclear fragments: for simplicity we shall refer to the general technique of intensity interferometry as the Hanbury-Brown/Twiss (or HBT) effect hereafter. Today there is not only a substantial experimental literature on the technique's applications, but also a large number of theoretical papers on correlations dealing with final-state interactions and with different models for the source region.

In order to review the extensive literature on the effect and its applications we divide the topics in the following fashion. Theoretical and experimental work are separated into three sections each, with the theoretical background appropriate for a given group of experiments given first. In Sec. II we develop a theoretical framework for interferometry based on the existing literature. We present general formalisms, rather than models that may be more specific in their application. A significant number of models have been developed to characterize the space-time evolution of the radiating source and the degree to which particle emission is coherent. Models that are most relevant for pion emission are discussed in Sec. III, while those more important for proton and nuclear cluster emissions are treated in Sec. VI.

In subatomic physics the formalism has been applied to reactions ranging from high-energy collisions of elementary particles to low-energy collisions of nuclei. For review purposes we have grouped the experimental work into three sections which contain common themes. The first measurements of the Hanbury-Brown/Twiss effect in subatomic physics came from elementary-particle reactions. The results from these early experiments, as well as more extensive measurements performed recently, are summarized in Sec. IV. The role of interferometry in relativistic heavy-ion collisions is described in Sec. V, where more recent applications may be related to the detection of the quark-gluon plasma. Low- and intermediate-energy nuclear reactions are discussed in Sec. VII. The lower-energy reactions have also exploited correlations between clusters, for which the Coulomb and strong-interaction effects may be more important than interference arising from wave-function symmetries imposed by quantum mechanics.

There remain many interpretational questions associated with the application of the Hanbury-Brown/Twiss effect to subatomic reactions. We address these issues throughout the review and finally summarize the results in Sec. VIII.

Two final comments are in order. First, there is little uniformity of notation among authors for the correlation function or its characterization. Here we choose that notation which appears to us to be most commonly quoted. In particular the correlation function will be defined so that it vanishes when the correlations between particles vanish, as in Eq. (1.1). Readers are urged to use caution in comparing results from different papers. Second, we have generally avoided quoting conference proceedings, preprints, and other nonrefereed literature except for a very few cases that bring up new directions. We have tried to be thorough in our summaries, but there is undoubtedly work that has escaped our attention. To authors of such work we apologize.

II. THEORY OF INTENSITY INTERFEROMETRY

Theoretical development of the Hanbury-Brown/Twiss (HBT) technique has fallen into several broad categories. Much work has been done on the general formulation of the technique, and such work is the subject of this section of the review. However, a good deal of effort has gone into the development of model characterizations and into incorporating the effects of particle interactions on the correlation function. Such work is addressed in Secs. III and VI.

In astrophysics applications of the Hanbury-Brown/Twiss effect, the spatial characteristics of the particle-emitting source are assumed to have no strong time dependence over the time scale of the measurements. This is also true of the x-ray scattering applications investigated by Goldberger, Lewis, and Watson (1963, 1966). The situation is very different in applications of the HBT effect to reactions of subatomic particles. Here the system is evolving with time, and the technique is used to investigate the system's spatial and temporal characteristics.

A typical intensity interferometry study in subatomic reactions involves a measurement of cross sections $d^6\sigma/d^3p_1 d^3p_2$ for simultaneously observing a pair of particles with momenta $\mathbf{p}_1$ and $\mathbf{p}_2$ [the units used in this review are $(h/2\pi)=c=1$, so that p is used interchangeably to denote momentum and wave vector]. A correlation function $R(\mathbf{p}_1,\mathbf{p}_2)$ can be constructed from the pair cross section and the single-particle cross section $d^3\sigma/d^3p$ by

$$R(\mathbf{p}_1,\mathbf{p}_2)=\frac{\langle n\rangle^2}{\langle n(n-1)\rangle}\frac{\sigma_0 d^6\sigma/d^3p_1 d^3p_2}{(d^3\sigma/d^3p_1)(d^3\sigma/d^3p_2)}-1. \tag{2.1}$$

In this expression, $\langle n\rangle$ is the particle multiplicity and σ_0 is defined by the normalization condition chosen for the integrals of the inclusive cross sections. In many practical applications these prefactors are combined into one overall normalization constant. For example, this is necessary when the even multiplicity is unknown.

The individual momenta $\mathbf{p}_1$ and $\mathbf{p}_2$ may be combined to form other kinematic variables:

$$\mathbf{P}=\mathbf{p}_1+\mathbf{p}_2,\quad \mathbf{Q}=\mathbf{p}_1-\mathbf{p}_2,\quad \mathbf{q}=(\mathbf{p}_1-\mathbf{p}_2)/2\ .$$

In the literature, the pair $\mathbf{P},\mathbf{Q}$ are commonly used for high-energy reactions and the pair $\mathbf{P},\mathbf{q}$ for low-energy reactions. This review adopts the set $\mathbf{P},\mathbf{q}$. Caution should be used in comparing results from different areas of the literature.

The first investigation of Bose-Einstein symmetrization effects in subatomic reactions came from a study of pion emission in proton-antiproton annihilation (Goldhaber *et al.*, 1959). To analyze this data, Goldhaber, Goldhaber, Lee, and Pais (1960) adopted a static statistical model for particle emission and determined the consequences of Bose-Einstein statistics to the angular distributions of pions in such a system. The effect became known for some time in the particle physics literature as the Goldhaber (or GGLP) effect. The interpretation of pion emission in terms of intensity interferometry was pursued more than a decade later by Shuryak (1973a, 1973b) and Cocconi (1974). Another possible boson interferometry application in reaction studies is correlated photon emission. While this possibility has been investigated theoretically (Neuhauser, 1986), difficulties associated with small cross sections and/or detection efficiencies have restricted its experimental applications.

The early 1970s also saw the further development of formalisms to handle not only pion emission (Kopylov and Podgoretskii, 1972, 1973; Kopylov, 1974), but also interference in resonant decay (Grishin, Kopylov, and Podgoretskii, 1971a, 1971b; Kopylov and Podgoretskii, 1971; Kopylov, 1972). The early work on pion correlations omitted effects arising from final-state interactions, since low-energy $\pi\pi$ scattering has a slowly varying $I=2$ s-wave phase shift. However, calculations of correlations involving protons or nuclei must take into account strong final-state interactions. The effects of strong interactions have been investigated for pion emission (Suzuki, 1987; Bowler, 1988), proton emission (Koonin, 1977; Nakai and Yokomi, 1981; Ernst, Strayer, and Umar, 1985), and cluster emission (Jennings, Boal, and Shillcock, 1986).

In Secs. II.A and II.B below, we discuss correlations due to symmetrization (antisymmetrization) of the two-particle wave function of identical bosons (fermions). We outline a theoretical framework for describing correlation functions based upon a formalism for pion emission developed by Gyulassy, Kauffmann, and Wilson (1979; see also Bartnik and Rzazewski, 1978, for incoherent pion production, and Horn and Silver, 1971, for coherent pion production). Correlations due to strong or Coulombic interactions between particles are discussed in Secs. II.C and II.D.

A. Coherence and incoherence

While the main focus of this review is the two-particle correlation function, it is instructive to discuss symmetrization effects by considering an experiment in which only one particle is measured in the final state. Suppose that the particle can be emitted from one of a number of discrete sources, each of which has a probability amplitude $f_i(\mathbf{x})$ that is a delta function in coordinate space: $f_i\delta(\mathbf{x}-\mathbf{x}_i)$. Later, we shall consider models in which the amplitudes f_i are not static—for example, expanding sources in heavy-ion collisions as considered by Pratt (1984). It should be stressed throughout this section that we have assumed that the source can be described by a particular distribution. If this distribution changes with impact parameter, and if the measurement of the correlation function averages over impact parameter, then further averages must be taken beyond those indicated here (see, for example, Gyulassy, 1982).

In the present case, the total probability $P(\mathbf{p})$ of ob-

serving the particle with momentum $\mathbf{p}$ from these sources is obtained from a sum over i of the product of the source amplitude with the particle's wave function $\psi(\mathbf{x})$. The sum may be either coherent, i.e., $P_C(\mathbf{p})=|\Sigma_i\psi(\mathbf{x}_i)f_i|^2$, or incoherent, $P_I(\mathbf{p})=\Sigma_i|f_i\psi(x_i)|^2$, depending on the nature of the experiment. The first choice, P_C, is used if it cannot be determined (for example, by measuring the remainder of the reaction products) which source i emitted the particle. The second choice, P_I, is used if the source i can be determined.

Suppose now that the source is continuous in space so that the sum is replaced by an integral. Suppose further that the wave function of the particle is a plane wave, $\psi_p(\mathbf{x})\sim\exp(i\mathbf{p}x)$. Then the probability of emission from a coherent source is $P_C(\mathbf{p})=|\int\psi_p(\mathbf{x})f(\mathbf{x})d^3x|^2$. We see that the momentum dependence of $P_C(\mathbf{p})$ is determined by the spatial dependence of the emitting region: it is proportional to the Fourier transform of $f(\mathbf{x})$. However, in the same limit, $P_I(\mathbf{p})$ will have no momentum dependence, since it simply becomes $P_I(\mathbf{p})=\int|f(\mathbf{x})|^2d^3x$.

The detection of two bosons can be treated by a similar method. The coherent sum for the probability $P(\mathbf{p}_1,\mathbf{p}_2)$ of observing identical bosons with momenta $\mathbf{p}_1$ and $\mathbf{p}_2$ simultaneously can be written as

$$\begin{aligned}P_C(\mathbf{p}_1,\mathbf{p}_2)&=\tfrac{1}{2}\left|\int d^3x_1d^3x_2\psi_{12}(\mathbf{x}_1,\mathbf{x}_2)f_C(\mathbf{x}_1)f_C(\mathbf{x}_2)\right|^2\\&=\tfrac{1}{2}\left|\int d^3x_1d^3x_2\frac{1}{\sqrt{2}}(e^{i\mathbf{p}_1\cdot\mathbf{x}_1}e^{i\mathbf{p}_2\cdot\mathbf{x}_2}+e^{i\mathbf{p}_1\cdot\mathbf{x}_2}e^{i\mathbf{p}_2\cdot\mathbf{x}_1})f_C(\mathbf{x}_1)f_C(\mathbf{x}_2)\right|^2\\&=|\tilde{f}_C(\mathbf{p}_1)\tilde{f}_C(\mathbf{p}_2)|^2\ .\end{aligned}\tag{2.2}$$

Here the tilde denotes a Fourier transform. Unnormalized plane waves have been used for the two-particle wave function (the normalization constant of the plane waves disappears in the calculation of the correlation function). The factor of $\frac{1}{2}$ in Eq. (2.2) comes from the fact that the particles are indistinguishable. Note that a coherent state cannot be constructed for fermions: antisymmetrization of the wave function ψ in Eq. (2.2) leads to a null result. We see that the coincidence probability factorizes into contributions from each momentum separately. However, in most situations this momentum dependence of $P_C(\mathbf{p}_1,\mathbf{p}_2)$ is influenced more by energy and momentum conservation than the geometry of the source. In any event when Eq. (2.2) is used to construct a correlation function from

$$R(\mathbf{p},\mathbf{p}_2)=[P(\mathbf{p}_1,\mathbf{p}_2)/P(\mathbf{p}_1)P(\mathbf{p}_2)]-1\ ,\tag{2.3}$$

one can see that there is no correlation between the two momenta: $R_C(\mathbf{p}_1,\mathbf{p}_2)=0$.

Repeating the above argument for the incoherent sum we have

$$\begin{aligned}P_I(\mathbf{p}_1,\mathbf{p}_2)&=\int d^3x_1d^3x_2|\psi_{12}(\mathbf{x}_1,\mathbf{x}_2)f_I(\mathbf{x}_1)f_1(\mathbf{x}_2)|^2\\&=|\tilde{F}_I(0)|^2\pm|\tilde{F}_I(\mathbf{p}_1-\mathbf{p}_2)|^2\ ,\end{aligned}\tag{2.4}$$

where $F_I(\mathbf{x})\equiv f_I(\mathbf{x})^*f_I(\mathbf{x})$. This expression is valid for both bosons (+) and fermions (−). Here, P_I has no dependence on the total momentum $P=\mathbf{p}_1+\mathbf{p}_2$, but there is a correlation between the two individual momenta

$$R_I(\mathbf{p}_1,\mathbf{p}_2)=\pm|\tilde{F}_I(\mathbf{p}_1-\mathbf{p}_2)/\tilde{F}_I(0)|^2\ .\tag{2.5}$$

It is from such an incoherent source that correlations can arise (Hanbury-Brown and Twiss, 1954, 1957a, 1957b; Goldhaber, Goldhaber, Lee, and Pais, 1960). If the momentum difference vanishes, $R_I(\mathbf{p},\mathbf{p})=+1$ (-1) for bosons (fermions).

Let us summarize the results so far. Two different processes that contribute to the same measured final state add incoherently if additional measurements along with the original one could uniquely determine the initial state. Alternatively, incoherence can be considered to result from phase averaging (see discussion below). Otherwise, the processes add coherently. If the different parts of the source contribute only coherently, the two-particle correlation function in momentum vanishes. On the other hand, if the sources contribute incoherently, there is a nonzero two-particle correlation function (but it has no dependence on the total momentum of the particle pair if the sources are static). Strong and Coulomb two-body interactions may be included by using distorted waves for the two-body wave function, rather than the plane waves we have used thus far.

The problem of coherence can be approached from another point of view. For the observation of one particle, the coherent sum, $P_C(\mathbf{p})=|\Sigma_i\psi(\mathbf{x}_i)f_i|^2$, can be expanded as

$$P_C(\mathbf{p})=\sum_i|\psi(\mathbf{x}_i)|^2|f_i|^2+\sum_i\sum_{j\neq i}\psi(\mathbf{x}_i)\psi^*(\mathbf{x}_j)f_i^*f_j\ ,\tag{2.6}$$

where the first sum on the right-hand side is recognized as just $P_I(\mathbf{p})$. Thus for $P_C(\mathbf{p})$ to behave like a completely incoherent sum (and possess the full nonvanishing correlations associated with symmetrization) it is necessary for the cross terms in Eq. (2.6) to vanish.

If the f_i involve extra degrees of freedom and are orthogonal in these degrees of freedom, then the cross terms vanish if the corresponding observables are not measured (i.e., the degrees of freedom are summed over). This is precisely the incoherent case discused above. One may consider the vanishing of the cross terms as arising from an averaging over some quantity or quantities. If the f_i fluctuate randomly in the variables being averaged over, then the average will tend to be small. This method

of generating orthogonality has led to the name "chaotic" for such incoherent processes. However it is possible to generate incoherent processes without anything being random or chaotic. The elimination of the cross terms is frequently referred to as phase averaging.

The effects of phase averaging on two-particle distributions have been discussed by Shuryak (1973a, 1973b), Gyulassy, Kauffmann, and Wilson (1979), and Bowler (1985). The coherent sum for the two-particle case is given by [see Eq. (2.2)]

$$\begin{aligned} P_C(\mathbf{p}_1,\mathbf{p}_2) &= \tfrac{1}{2}\left|\sum_{i,j}\psi_{12}(\mathbf{x}_i,\mathbf{x}_j)f_i f_j\right|^2 \\ &= \tfrac{1}{2}\sum_{i,j,k,l}\psi_{12}(\mathbf{x}_i,\mathbf{x}_j)f_i f_j\psi_{12}^*(\mathbf{x}_k,\mathbf{x}_l)f_k^* f_l^* \\ &= \tfrac{1}{2}\sum_{i,j}|\psi_{12}(\mathbf{x}_i,\mathbf{x}_j)|^2|f_i|^2|f_j|^2 \\ &\quad + \tfrac{1}{2}\sum_{i,j}\psi_{12}(\mathbf{x}_i,\mathbf{x}_j)\psi_{12}^*(\mathbf{x}_j,\mathbf{x}_i)|f_i|^2|f_j|^2 \\ &\quad + \tfrac{1}{2}\sum_{i,j\neq k,l}\psi_{12}(\mathbf{x}_i,\mathbf{x}_j)\psi_{12}^*(\mathbf{x}_k,\mathbf{x}_l)f_i f_j f_k^* f_l^* \ . \end{aligned} \tag{2.7}$$

If the wave function is symmetric, the sum of the first two terms equals the incoherent sum and we are left with

$$P_C(\mathbf{p}_1,\mathbf{p}_2) = P_I(\mathbf{p}_1,\mathbf{p}_2) + \tfrac{1}{2}\sum_{i,j\neq k,l}\psi_{12}(\mathbf{x}_i,\mathbf{x}_j)\psi_{12}^*(\mathbf{x}_k,\mathbf{x}_l)f_i f_j f_k^* f_l^* \ . \tag{2.8}$$

If the second term in Eq. (2.8) vanishes due to phase averaging, the incoherent sum is recovered.

From this discussion we also see that the two limits are not mutually exclusive: we can go continuously from the coherent to the incoherent situation depending on the degree of orthogonality between the f_i. In experiments, the observed value of $R(\mathbf{p},\mathbf{p})$ (i.e., the correlation function at zero momentum difference) is often interpreted as a measure of the incoherence of the source, and it is given the symbol $\lambda = R(\mathbf{p},\mathbf{p})$.[1] We refer to λ as the incoherence parameter, although it has been called a variety of other names. There are many other effects that cloud the interpretation of λ as a measure of incoherence and we return to them in Sec. III.E.

[1]The incoherence parameter λ is unity for an incoherent boson source from Eq. (2.5), and it is zero for a coherent source from Eq. (2.2). However, the suppression of the correlation in $R(q)$ from a coherent source comes about because of the large fluctuations that are present in the single-particle probability $P(p)$. Even with a coherent source, the function $P_C(P,q)$ has a correlation as a function of q characteristic of the source size. The correlation is retained in any analysis of $R(q)$ that assumes smooth behavior of the single-particle probability $P(p)$. This comment is due to G. Bertsch.

B. Sources of boson emission

The main issues raised in the previous section are (i) how does the symmetrization of a two-particle wave function lead to correlations in momentum and (ii) how does the coherence of the source manifest itself in the measurement of the correlation function? In this section we outline a more detailed treatment of the source for boson emission. We adopt the formulation of Gyulassy, Kauffmann, and Wilson (1979). The reader is referred to this article, as well as those of Kopylov and Podgoretskii (1972, 1973), Shuryak (1973a, 1973b), and Bartnik and Rzazewski (1978), for a more detailed treatment than can be accommodated here.

For definiteness we shall consider pion production. We would like to solve the following field equation for the pion field $\phi(x)$ (where we denote the four-dimensional x^μ simply by x in this subsection):

$$(\partial^\mu\partial_\mu + m_\pi^2)\phi(x) = J(x) \ . \tag{2.9}$$

In principle, the current $J(x)$ is coupled to the pion fields, and we would need to solve coupled equations in a self-consistent manner. As a first approximation one can treat the source as a c-number. The final pion state $|\phi\rangle$ produced by such a classical current source is a coherent state $|J\rangle$ given by (see, for example, pp. 202–207 of Bjorken and Drell, 1965)

$$\begin{aligned} |\phi\rangle &= |J\rangle \\ &= \exp\left[-\bar{n}/2 + i\int d^3p\,\tilde{J}(\mathbf{p})a^+(\mathbf{p})\right]|0\rangle \ , \end{aligned} \tag{2.10}$$

where

$$\tilde{J}(\mathbf{p}) = \int d^4x \frac{\exp(i\omega_p t - i\mathbf{p}\cdot\mathbf{x})}{[2\omega_p(2\pi)^3]^{1/2}} J(\mathbf{x},t) \tag{2.11}$$

is the on-mass-shell Fourier transform of the current, i.e., $\omega_{\mathbf{p}}^2 = \mathbf{p}^2 + m^2$. The pion multiplicity distribution is a Poisson distribution with mean

$$\langle n\rangle = \bar{n} = \int d^3p|\tilde{J}(\mathbf{p})|^2 \ , \tag{2.12}$$

which satisfies

$$\langle n\rangle^2 = \langle n(n-1)\rangle = \bar{n}^2 \ . \tag{2.13}$$

The density matrix

$$\rho_\pi = |J\rangle\langle J| \tag{2.14}$$

describes a pure coherent state ($\mathrm{Tr}\rho_\pi = \mathrm{Tr}\rho_\pi^2 = 1$). Since $|J\rangle$ is an eigenstate of the destruction operator, the m-pion inclusive distribution is easily calculated to be

$$\begin{aligned} P_m(\mathbf{p}_1,\ldots,\mathbf{p}_m) &= \mathrm{Tr}(\rho_\pi a^+(\mathbf{p}_1)\cdots a^+(\mathbf{p}_m)a(\mathbf{p}_m)\cdots a(\mathbf{p}_1)) \\ &= |\tilde{J}(\mathbf{p}_1)|^2\cdots|\tilde{J}(\mathbf{p}_m)|^2 \ . \end{aligned} \tag{2.15}$$

The two-particle correlation function, in this case, is simply $R(\mathbf{p}_1,\mathbf{p}_2) = 0$: the pions are uncorrelated in momen-

tum space. This is just what is expected from the coherent-sum example discussed above. Note also the dependence of $P_m(\mathbf{p}_1,\ldots,\mathbf{p}_m)$ on the individual momenta.

We now want to consider a more general situation in which there are a number N of independent sources. Each source may emit any number of pions, so N is not the number of pions produced in the reaction. The total source current is written as

$$J(x)=\sum_{i=1}^{N} J_i(x) . \tag{2.16}$$

Each $J_i(x)$ can be considered to represent a different inelastic nucleon-nucleon collision in a heavy-ion reaction or a different parton-parton collision in a high-energy hadron reaction. This approach is appropriate for either a cascade or a thermal model. Consider the situation in which the $J_i(x)$ depend only on the distance from the individual collision sites,

$$J(x)=\sum_{i=1}^{N} e^{i\phi_i} J_\pi(\mathbf{x}-\mathbf{x}_i,t-t_i) , \tag{2.17}$$

where we have allowed the possibility that the individual currents have variable phase. The on-shell Fourier transform of this equation is given by

$$\tilde{J}(\mathbf{p})=\tilde{J}_\pi(\mathbf{p})\sum_{i=1}^{N}\exp(i\phi_i+i\omega_p t_i-i\mathbf{p}\cdot\mathbf{x}_i) . \tag{2.18}$$

We now assume an incoherent sum (which is, in fact, an integral) over the location of the points $\mathbf{x}_i$. This corresponds to being able to distinguish where the collision centers are. It does not imply that we know exactly where the pions are produced. The density matrix can now be written as

$$\rho_\pi=\sum_N P_S(N)\int d^4x_1\rho(x_1)\cdots d^4x_N\rho(x_N)|J\rangle\langle J| , \tag{2.19}$$

where $P_S(N)$ is the probability that there are N collisions. The density $\rho(x)$ is normalized to one. Using our previous expression, Eq. (2.15), for the inclusive spectrum, we find that the m-pion inclusive distribution for the present case is given by

$$P_m(\mathbf{p}_1,\ldots,\mathbf{p}_m)=\sum_N P_S(N)\int d^4x_1\rho(x_1)\cdots d^4x_N\rho(x_N)\times|\tilde{J}(\mathbf{p}_1)|^2\cdots|\tilde{J}(\mathbf{p}_m)|^2 . \tag{2.20}$$

Using Eq. (2.18) we have

$$P_m(\mathbf{p}_1,\ldots,\mathbf{p}_m)=|\tilde{J}_\pi(\mathbf{p}_1)|^2\cdots|\tilde{J}_\pi(\mathbf{p}_m)|^2\sum_N P_s(N)\int d^4x_1\rho(x_1)\cdots d^4x_N\rho(x_N)\times\left\langle\sum_{i_1=1}^{N}\cdots\sum_{i_{2m}=1}^{N}\exp[ip_1(x_{i_1}-x_{i_2})]\cdots\exp[ip_m(x_{i_{2m-1}}-x_{i_{2m}})]\times\exp[i(\phi_{i_1}-\phi_{i_2})]\cdots\exp[i(\phi_{i_{2m-1}}-\phi_{i_{2m}})]\right\rangle_{[\phi]} . \tag{2.21}$$

The factors of $J_\pi(\mathbf{p}_i)$ on the right-hand side give the overall momentum dependence of the coincidence probability. The correlations, if any, come from the remaining sums and integrals. Consider first the one-pion inclusive distribution $m=1$ to illustrate coherence effects in Eq. (2.21). The Fourier transform of the density $\rho(x)$ is defined by

$$\tilde{\rho}(q)=\int d^4x\,\rho(x)\exp(iqx) . \tag{2.22}$$

Now, if the phases ϕ_i are random, then the double sum over the phases in Eq. (2.21) gives N diagonal elements plus an off-diagonal sum whose absolute value is also of the order N. Performing a further ensemble average over sets of phases, we obtain

$$P_1(\mathbf{p})=|\tilde{J}_\pi(\mathbf{p})|^2\langle N\rangle , \tag{2.23a}$$

where $\langle N\rangle$ is the average number of collisions. However, if all phases ϕ_i have the same value, there are an extra $N(N-1)$ terms in the sum over i_1 and i_2 (for $m=1$) in which $x_{i1}\neq x_{i2}$. These $N(N-1)$ terms each involve the Fourier transform of $\rho(x)$, so that Eq. (2.23a) becomes

$$P_1(\mathbf{p})=|\tilde{J}_\pi(\mathbf{p})|^2[\langle N\rangle+\langle N(N-1)\rangle|\tilde{\rho}(\mathbf{p},\omega_p)|^2] . \tag{2.23b}$$

Whether the $N(N-1)$ cross term in Eq. (2.23b) is important depends on the source size R_S. For short wavelengths $|\mathbf{p}|\gg R_S^{-1}$, the integrand in Eq. (2.22) oscillates rapidly and $|\rho(\mathbf{p})|^2\ll 1$. As a consequence the cross term can be neglected. On the other hand, for long wavelengths $|\mathbf{p}|\ll R_S^{-1}$, so that $\rho(k)=\rho(0,m_\pi)$, where m_π is the pion mass. For $m_\pi\to 0$, $\rho(0,m_\pi)$ goes to one and the interference term dominates for large N. As Gyulassy, Kauffmann, and Wilson (1979) point out, it is the zero-mass limit which is relevant for the Thompson scattering of photons. The interference term is responsible for the charge-squared dependence of the cross section. For finite-mass particles there is a difference due to the minimum energy scale in $\rho(0,m_\pi)$. If the source ρ has a

long lifetime, $\tau \gg m_\pi^{-1}$, then $\rho(0,m_\pi)$ is small and the cross term vanishes. On the other hand, if the lifetime is short, the cross terms remain.

This can be considered from another point of view. For long separations between emission times it is possible to tell which source i emitted the pion because the times of pion emission can be determined individually. This destroys the coherence. For short lifetimes, on the other hand, the uncertainty principle prevents time considerations from being used to tell which source emitted the particle. The size of the interference term can change from zero to its full size as a function of the source lifetime. The crucial point is the extent to which the source that emitted the particle can be distinguished from the other sources by additional measurements. For the rest of this discussion we shall assume that the cross terms between the different sources vanish whether because of time or ensemble averages.

Now we proceed to the two-particle distribution. Performing an average over the random phase ϕ_i as we did in Eq. (2.23a), we find that the two-particle distribution becomes

$$P_2(\mathbf{p}_1,\mathbf{p}_2)=|\tilde{J}_\pi(\mathbf{p}_1)|^2|\tilde{J}_\pi(\mathbf{p}_2)|^2[\langle N^2\rangle+\langle N(N-1)\rangle|\tilde{\rho}(p_1-p_2)|^2] . \tag{2.24}$$

The overall momentum dependence and the correlation effects have different origins; the overall momentum dependence comes from the properties of the individual collisions, while the correlations come from the properties of the region where the collisions take place. This is a general feature and not just a peculiarity of the model. The next features to note are the factors of $\langle N^2\rangle$ and $\langle N(N-1)\rangle$. These change the size of the correlations when the number of collisions is small. Hence we have

$$R(\mathbf{p}_1,\mathbf{p}_2)=\frac{\langle N(N-1)\rangle}{\langle N^2\rangle}|\tilde{\rho}(p_1-p_2)|^2 . \tag{2.25}$$

We see that the value of the correlation function at the origin is affected by more than just coherence (see also Sec. III.E). In this case the incoherence parameter $\lambda=R(\mathbf{p},\mathbf{p})$ is given by

$$\lambda=\frac{\langle N(N-1)\rangle}{\langle N^2\rangle} . \tag{2.26}$$

The full value of unity for λ is reached only when the number of collisions N is large. If the number of collisions is distributed according to Poisson statistics, then $\lambda=\langle N\rangle/(\langle N\rangle+1)$. For such a distribution in N, λ is reduced to one-half if $\langle N\rangle$ is one.

C. Final-state interactions

So far we have considered only the effect of symmetry on two-particle correlations. However, correlations can also arise from two-particle final-state interactions even if there are no symmetry-based correlations. As a generalization of Gyulassy, Kauffman, and Wilson (1979) we have the following expression for the two-particle probability distribution in the presence of distortions:

$$P_2(\mathbf{p}_1,\mathbf{p}_2)=\tfrac{1}{2}\sum_N P_S(N)\int d^3x_1\rho(x_1)\cdots d^3x_N\rho(x_N)\sum_{i=1}^{N}\sum_{j=1}^{N}\left|\int d^3y_1 d^3y_2 J_\pi(\mathbf{y}_1-\mathbf{x}_i)J_\pi(\mathbf{y}_2-\mathbf{x}_j)\psi_{12}(\mathbf{y}_1,\mathbf{y}_2)\right|^2 , \tag{2.27}$$

where we have assumed that the sources add incoherently. Further, we have assumed that the sources have zero lifetime so that the four-dimensional integrals in Eq. (2.20) become three dimensional in Eq. (2.27). Hence Eq. (2.27) can be rewritten as

$$\begin{aligned}P_2(\mathbf{p}_1,\mathbf{p}_2)=&\langle N\rangle\int d^3x\,\rho(\mathbf{x})\left|\int d^3y\,d^3y' J_\pi(\mathbf{y}-\mathbf{x})J_\pi(\mathbf{y}'-\mathbf{x})\psi_{12}(\mathbf{y},\mathbf{y}')\right|^2\\&+\langle N\rangle(\langle N\rangle-1)\int d^3x\,d^3x'\rho(\mathbf{x})\rho(\mathbf{x}')\left|\int d^3y\,d^3y' J_\pi(\mathbf{y}-\mathbf{x})J_\pi(\mathbf{y}'-\mathbf{x}')\psi_{12}(\mathbf{y},\mathbf{y}')\right|^2 .\end{aligned} \tag{2.28}$$

This equation reduces to our previous result, Eq. (2.24), in the plane-wave limit:

$$\psi_{12}(\mathbf{y},\mathbf{y}')=\frac{1}{\sqrt{2}}[\exp(i\mathbf{p}_1\mathbf{y})\exp(i\mathbf{p}_2\mathbf{y}')+\exp(i\mathbf{p}_1\mathbf{y}')\exp(i\mathbf{p}_2\mathbf{y})] . \tag{2.29}$$

We can rewrite Eq. (2.28) in momentum space as

$$\begin{aligned}P_2(\mathbf{p}_1,\mathbf{p}_2)=&\langle N\rangle\int d^3p\,d^3p'd^3p''d^3p'''\tilde{\rho}(\mathbf{p}-\mathbf{p}'+\mathbf{p}''-\mathbf{p}''')\tilde{J}_\pi(\mathbf{p})\tilde{J}_\pi(\mathbf{p}')\tilde{J}_\pi^*(\mathbf{p}'')\tilde{J}_\pi^*(\mathbf{p}''')\psi_{12}(\mathbf{p},\mathbf{p}')\psi_{12}^*(\mathbf{p}'',\mathbf{p}''')\\&+\langle N\rangle(\langle N\rangle-1)\int d^3p\,d^3p'd^3p''d^3p'''\tilde{\rho}(\mathbf{p}-\mathbf{p}'')\tilde{\rho}(\mathbf{p}'-\mathbf{p}''')\\&\times\tilde{J}_\pi(\mathbf{p})\tilde{J}_\pi(\mathbf{p}')\tilde{J}_\pi^*(\mathbf{p}'')\tilde{J}_\pi^*(\mathbf{p}''')\psi_{12}(\mathbf{p},\mathbf{p}')\psi_{12}^*(\mathbf{p}'',\mathbf{p}''') .\end{aligned} \tag{2.30}$$

Now if the $J_\pi(\mathbf{p})$ are sufficiently slowly varying functions of momentum, they can be taken outside the integral and evaluated at the asymptotic values of the momentum $\mathbf{p}_1$ and $\mathbf{p}_2$. The wave function $\psi_{12}(\mathbf{x}',\mathbf{x}'')$ depends implicitly on these two asymptotic momenta. This leads to the result

$$P_2(\mathbf{p}_1,\mathbf{p}_2)=|\tilde{J}_\pi(\mathbf{p}_1)|^2|\tilde{J}_\pi(\mathbf{p}_2)|^2[\langle N\rangle\int d^3x\,\rho(\mathbf{x})|\psi_{12}(\mathbf{x},\mathbf{x})|^2+\langle N(\langle N\rangle-1)\rangle\int d^3x\,d^3x'\rho(\mathbf{x})\rho(\mathbf{x}')|\psi_{12}(\mathbf{x},\mathbf{x}')|^2]\ , \tag{2.31}$$

which becomes, in the large $\langle N\rangle$ limit,

$$P_2(\mathbf{p}_1,\mathbf{p}_2)=\langle N\rangle^2|\tilde{J}_\pi(\mathbf{p}_1)|^2|\tilde{J}_\pi(\mathbf{p}_2)|^2\int d^3x\,d^3x'\rho(\mathbf{x})\rho(\mathbf{x}')|\psi_{12}(\mathbf{x},\mathbf{x}')|^2\ . \tag{2.32}$$

This expression is used in the next subsection (Sec. II.D), and it is commonly used in the literature.

If one-body distortions are included and two-body interactions are neglected, the wave function can be written as

$$\psi_{12}(\mathbf{x},\mathbf{x}')=\frac{1}{\sqrt{2}}[\psi_1(\mathbf{x})\psi_2(\mathbf{x}')\pm\psi_1(\mathbf{x}')\psi_2(\mathbf{x})]\ . \tag{2.33}$$

Here it is assumed that the individual wave functions are orthogonal (where the $\pm$ refers to the usual symmetry requirements). It has been pointed out by Gyulassy *et al.* (1979) that final-state interactions, even if only one-body, can affect the geometrical content of R.

D. The large-source-size limit

We have shown that the two-particle correlation function is affected by both symmetry and final-state interactions. In Secs. III and VI we provide a number of model parametrizations of the source that have been used for data fitting. In this subsection we consider an example in which the two-body interaction is of much shorter range than the size of the system. In this we follow the development of Jennings, Boal, and Shillcock (1986), which shares many similarities with other treatments of final-state interactions in correlation functions (Nakai and Yokomi, 1981; Ernst, Strayer, and Umar, 1985; Bowler, 1988). Using Eqs. (2.32) we can write the correlation function as

$$R(\mathbf{p}_1,\mathbf{p}_2)=\int d^3\mathbf{x}_1d^3\mathbf{x}_2\rho(\mathbf{x}_1)\rho(\mathbf{x}_2)[|\psi_{12}(\mathbf{x}_1,\mathbf{x}_2)|^2-1]\ , \tag{2.34}$$

where we use $\int d^3x\,\rho(x)=1$ and where we make the sources instantaneous. Equation (2.34) is valid for boson, fermion, or nonidentical particle pairs.

If we have only two-body interactions between equal-mass particles, the wave function $\psi_{12}(\mathbf{x}_1,\mathbf{x}_2)$ is just a plane wave in the center-of-mass coordinate $\mathbf{X}=(\mathbf{x}_1+\mathbf{x}_2)/2$, and $|\psi(\mathbf{x}_1,\mathbf{x}_2)|$ depends only on the relative coordinate $\mathbf{x}=(\mathbf{x}_1-\mathbf{x}_2)$. A relative function

$$g(\mathbf{x})=\int d^3X\,\rho(\mathbf{X}+\tfrac{1}{2}\mathbf{x})\rho(\mathbf{X}-\tfrac{1}{2}\mathbf{x})\ , \tag{2.35}$$

whose volume element is again one, can be obtained from $\rho(x)$. We can use this function in rewriting Eq. (2.34) as an expansion over partial waves. If $g(\mathbf{x})$ is spherically symmetric, cross terms between different angular momenta vanish, and we obtain

$$R(\mathbf{p}_1,\mathbf{p}_2)=4\pi\int dx\,x^2g(x)\left[2\sum_{l\ \text{even}}(2l+1)[\psi_l^2(x)-j_l^2(qx)]+j_0(2qx)\right]\quad\text{(bosons)}\ , \tag{2.36a}$$

$$R(\mathbf{p}_1,\mathbf{p}_2)=4\pi\int dx\,x^2g(x)\left[2\sum_{l\ \text{odd}}(2l+1)[\psi_l^2(x)-j_l^2(qx)]-j_0(2qx)\right]\quad\text{(fermions)}\ , \tag{2.36b}$$

$$R(\mathbf{p}_1,\mathbf{p}_2)=4\pi\int dx\,x^2g(x)\left[\sum_{l}(2l+1)[\psi_l^2(x)-j_l^2(qx)]\right]\quad\text{(nonidentical)}\ , \tag{2.36c}$$

where $j_l(x)$ is a spherical Bessel function and $\mathbf{q}=(\mathbf{p}_1-\mathbf{p}_2)/2$. Notice that $\mathbf{q}$ is the relative momentum rather than just the difference in momenta; hence the factor of one-half in the definition of $\mathbf{q}$ and the two in the spherical Bessel function $j_0(2qx)$. In deriving Eq. (2.36) we have used the identities (see Abramowitz and Stegun, 1964)

$$1=\sum_{l=0}^{\infty}(2l+1)j_l^2(qx) \tag{2.37}$$

and

$$j_0(2qx)=\sum_{l=0}^{\infty}(-1)^l(2l+1)j_l^2(qx)\ . \tag{2.38}$$

For this subsection we use $q=|\mathbf{q}|$ and the integrals are three dimensional. Equations (2.36a)–(2.36c) give the explicit expressions for three different particle combinations. For simplicity, the remaining derivations in this subsection up to Eqs. (2.46a)–(2.46c) are shown for bosons only.

One can show that the contributions to the correlation function from symmetrization and two-particle interactions are additive. In deriving this result, no approxima-

tions are required beyond those used in Eq. (2.34) and the assumption that $g(x)$ is spherically symmetric. The $j_0(2qx)$ term in Eq. (2.36) is the usual correlation function of Eq. (2.4). To see this we note that in the plane-wave case, Eq. (2.34) can be written as

$$R(\mathbf{p}_1,\mathbf{p}_2)=\int d^3x_1 d^3x_2 \rho(x_1)\rho(x_2)[2\cos^2(\mathbf{q}\cdot\mathbf{x})-1]$$
$$=\int d^3x\, g(x)\cos(2\mathbf{q}\cdot\mathbf{x}) \ . \tag{2.39}$$

Assuming $g(x)$ is spherically symmetric, the angular integration of Eq. (2.39) gives the $j_0(2qx)$ of Eq. (2.36).

We concentrate on the integral

$$I=\int dx\, x^2[\psi_l^2(x)-j_l^2(qx)]g(x) \ . \tag{2.40}$$

Adding and subtracting the asymptotic forms of $\psi_l(x)$ and $j_l(qx)$, we can rewrite this integral as

$$I=\int_0^\infty dx\, x^2[\psi_l^2(x)-\sin^2(qx-l\pi/2+\delta_l)/(qx)^2-j_l^2(qx)+\sin^2(qx-l\pi/2)/(qx)^2]g(x)$$
$$+\int_0^\infty dx\, x^2[\sin^2(qx-l\pi/2+\delta_l)/(qx)^2-\sin^2(qx-l\pi/2)/(qx)^2]g(x) \ , \tag{2.41}$$

where δ_l is the phase shift of the lth partial wave. For the first integral we may restrict the upper limit, since the quantity in square brackets goes to zero as $x\to\infty$. If $g(x)$ is sufficiently slowly varying (i.e., the source is sufficiently large) we may replace $g(x)$ by its value at the origin $g(0)$. The replacement requires both that the range of the force be small and that the momentum q be large, since the Bessel functions are being replaced by their asymptotic form. The integral can now be written as

$$I=g(0)\int_0^{R_0} dx\, x^2[\psi_l^2(x)-\sin^2(qx-l\pi/2+\delta_l)/(qx)^2-j_l^2(qx)+\sin^2(qx-l\pi/2)/(qx)^2]$$
$$+\int_0^\infty \frac{dx}{q^2}\sin(\delta_l)\sin(2qx-l\pi+\delta_l)g(x) \ , \tag{2.42}$$

where R_0 is assumed to be sufficiently large that $\psi_l(x)$ and $j_l(qx)$ have reached their asymptotic forms and sufficiently small that $g(x)$ can be replaced by a constant. The second integral has been simplified using trigonometric identities.

For the first term in Eq. (2.42) we follow a procedure very similar to that used in Appendix B-2 of Preston and Bhaduri (1975) for the effective range expansion. We define $u_l(x,q)=\psi_l(x)qx$ so that $u_l(x,q)$ satisfies the equation

$$\frac{d^2}{dx^2}u_l(x,q)-\left[m_\pi V(x)+\frac{l(l+1)}{x^2}\right]u_l(x,q)=-q^2u_l(x,q) \ . \tag{2.43}$$

The same equation (with q replaced by q') is satisfied by $u_l(x,q')$. Multiplying the first of these by $u_l(x,q')$, the second by $u_l(x,q)$, and taking the difference, we have, after an integration by parts

$$\left[u_l(x,q')\frac{d}{dx}u_l(x,q)-u_l(x,q)\frac{d}{dx}u_l(x,q')\right]_{x_a}^{x_b}=(q'^2-q^2)\int_{x_a}^{x_b}dx\, u_l(x,q)u_l(x,q') \ . \tag{2.44}$$

The procedure now is to divide through by (q'^2-q^2) and then let q' go to q. Combining with similar results for the Bessel function and taking $x_a\to 0$ and $x_b\to R_0$, we have

$$I=\frac{g(0)}{2q^2}\frac{d\delta_l}{dq}+\frac{\sin\delta_l}{2q^3}\int_0^\infty dx\cos(2qx-l\pi+\delta_l)\frac{dg(x)}{dx} \ . \tag{2.45}$$

The derivative with respect to q has arisen from taking the $q\to q'$ limit. For large source sizes the first term dominates. Through integration by parts we can show that the second term can be expanded in terms of derivatives of $g(x)$ evaluated at the origin. Successive terms are one power in $1/a$ smaller, where a is a length scale related to the size of the system. Thus for large source sizes $R(\mathbf{p}_1,\mathbf{p}_2)$ can be written as

$$R(\mathbf{p}_1,\mathbf{p}_2)=g(0)\frac{4\pi}{q^2}\sum_{l\ \text{even}}(2l+1)\frac{d\delta_l}{dq}+\int d^3x\, g(x)j_0(2qx) \quad \text{(bosons)} \ , \tag{2.46a}$$

$$R(\mathbf{p}_1,\mathbf{p}_2)=g(0)\frac{4\pi}{q^2}\sum_{l\ \text{odd}}(2l+1)\frac{d\delta_l}{dq}-\int d^3x\, g(x)j_0(2qx) \quad \text{(fermions)} \ , \tag{2.46b}$$

$$R(\mathbf{p}_1,\mathbf{p}_2)=g(0)\frac{2\pi}{q^2}\sum_l(2l+1)\frac{d\delta_l}{dq} \quad \text{(nonidentical)} \ . \tag{2.46c}$$

This expression breaks down for very large wavelegnths, as might be expected from the $1/q^2$. We see that in the large-source-size limit the effect of the interaction comes only through on-shell information, namely, the derivative of the phase shift.

This behavior is very similar to that obtained in thermal models (Jennings, Boal, and Shillcock, 1986). At a resonance the phase shift increases rapidly through $\pi/2$. The rapid increase in the phase shift leads to a peak in the correlation function whose height and width are determined by the width of the resonance. In general, repulsive potentials have a decreasing phase shift, at least for low momentum, which lowers the correlation function. An attractive potential has the opposite effect, provided the attraction is not strong enough to bind a state (in which case the result depends on how strong the binding is; see Sec. VI.A for a discussion of *pd* correlations in which the phase shift decreases with energy, although the potential is attractive).

III. MODEL SOURCES FOR PARTICLE EMISSION

In this section we review models for two-pion correlation functions at high energy. Experimental results at these energies are presented in Secs. IV and V. Relevant issues include model parametrizations of the source, the importance of the time evolution of the source, the magnitude of strong and electromagnetic effects in the correlation function, and the interpretation of the incoherence parameter λ. Many of the results presented in this section are also relevant to proton and cluster emission. Effects that are most important at lower energies, at which proton and cluster emission is measured, are discussed in Sec. VI. Correlations among three or more pions are not included in this review. The interested reader is referred to the literature for an introduction to this topic (Biyajima and Miyamura, 1978; Biyajima, 1981; Zajc, 1987a).

This section begins with a discussion of the two most commonly used parametrizations for particle emission. The Gaussian source distribution (used in applications by Goldhaber, Goldhaber, Lee, and Pais, 1960; Koonin, 1977; Yano and Koonin, 1978; Lednicky and Podgoretskii, 1979; Kvatadze, Moller, and Lorstad, 1988; Capella and Krzywicki, 1989) is the subject of Sec. III.A. Radiation from a sphere or disk, often referred to as the Kopylov-Podgoretskii parametrization (Kopylov and Podgoretskii, 1972, 1973; Cocconi, 1974; Kopylov, 1974; Podgoretskii and Cheplakov, 1986), is discussed in Sec. III.B. These two distributions represent time-invariant sources moving with uniform velocity. Expanding sources are discussed in Sec. III.C (Pratt, 1984, 1986b; Kolehmainen and Gyulassy 1986; Averchenkov, Makhlin, and Sinyukov, 1987; Machlin and Sinyukov, 1987; Hama and Padula, 1988).

In Sec. III.D we review the effects of Coulomb (Gyulassy, Kauffmann, and Wilson, 1979; Pratt, 1986a; Gersch, 1987) and strong final-state interactions (Bowler, 1987b; Suzuki, 1987) on the pion correlation function. Mention is also made of resonance decays (Grassberger, 1977; Thomas, 1977), although this topic is dealt with more thoroughly in Sec. VI. Final-state interactions between the measured pair and the emitting system have not yet been systematically investigated (Gyulassy, Kauffmann, and Wilson, 1979; Gyulassy and Kauffmann, 1981; see also Sec. VII).

The origin and interpretation of the incoherence parameter λ have attracted considerable attention (Fowler and Weiner, 1977, 1978, 1985; Bartnik and Rzazewski, 1978; Fowler, Stelte, and Weiner, 1979; Gyulassy, Kauffmann, and Wilson 1979; Biyajima, 1980, 1981, 1982; Gyulassy, 1982; Pratt, 1986; Fowler *et al.*, 1988; Vourdas and Weiner, 1988). This topic is reviewed in Sec. III.E.

Formalisms for the correlation function based upon the string model (Bowler, 1985, 1987a; Andersson and Hofmann, 1986); and other statistical and dynamical models (Biyajima and Miyamura, 1974; Miyamura and Biyajima, 1975; Ranft and Ranft, 1975a, 1975b; Giovannini and Veneziano, 1977; Engels and Schilling, 1978; Pratt and Tsang, 1987) and other applications of Bose-Einstein symmetrization (Bilic, Dadic, and Martinis, 1978; Carruthers and Shih, 1983, 1984) are discussed in Sec. III.F.

Data analysis has been performed with several different source parametrizations. To provide a uniform basis for comparison we adopt the most commonly used form—the Gaussian source—in the experimental sections of this review. In the discussion that follows, methods are developed to allow parameters extracted by a given method to be compared with those from the Gaussian model. Finally, we should also mention that we often adopt different notation from that used in the original literature in order to make the review self-consistent.

A. Gaussian source

The most extensively used parametrization corresponds to particle emission from a Gaussian source that may move with respect to the laboratory frame but does not otherwise evolve with time. The Gaussian-source model was formulated in investigations by Goldhaber, Goldhaber, Lee, and Pais (1960), Koonin (1977), and Yano and Koonin (1978); it has also been applied to a Regge-Mueller model by Capella and Krzywicki (1989). We begin our discussion of this model by considering a distribution with no time dependence at all. The static Gaussian model takes the distribution function $\rho(\mathbf{r})=F_I(\mathbf{r})=f_I(\mathbf{r})*f_I(\mathbf{r})$ of Eq. (2.4) to be [we replace $F_I(\mathbf{r})$ with $\rho(\mathbf{r})$ in the remainder of the review to facilitate comparison with the literature]

$$\rho(\mathbf{r})=\frac{1}{\sqrt{a_x^2a_y^2a_z^2\pi^3R^6}}\exp\{-[(x/a_x)^2+(y/a_y)^2+(z/a_z)^2]/R^2\}\ , \qquad (3.1)$$

where the a_i's are dimensionless constants that allow for nonspherical sources. The root-mean-square radius $r_{\rm rms}$ of this distribution is given by

$$r_{\rm rms}=[(a_x^2+a_y^2+a_z^2)/2]^{1/2}R \ . \tag{3.2}$$

When the two-body wave functions are plane waves, the correlation function for an incoherent source, Eq. (2.5), is given by the square of the Fourier transform of $F_I(\mathbf{r})$:

$$R(\mathbf{p}_1,\mathbf{p}_2)=\exp\{-2[(q_x a_x)^2+(q_y a_y)^2+(q_z a_z)^2]R^2\} \ . \tag{3.3}$$

The correlation function depends only on the width of the emitting region parallel to the direction of $\mathbf{q}=(\mathbf{p}_1-\mathbf{p}_2)/2$, and it goes to unity when $\mathbf{q}=0$. If $|\mathbf{p}_1|=|\mathbf{p}_2|$, then $\mathbf{q}$ is perpendicular to the direction of the total momentum of the particle pair $\mathbf{P}=\mathbf{p}_1+\mathbf{p}_2$ and the results depend only on the size of the emitting region transverse to $\mathbf{P}$. This aspect of the problem has been emphasized by Kopylov and Podgoretskii (1972, 1973).

The main quantities of interest in Eq. (3.3) are the magnitudes of R and a_i's. These are measurable through the width of the correlation function taken with respect to an axis, typically the beam axis. The use of Eq. (3.3) and its variants to determine spatial dimensions of anisotropic sources is discussed in Secs. IV, V, and VII. Other theoretical discussions of anisotropic sources can be found in Podgoretskii and Cheplakov (1986) and Kvatadze, Moller, and Lorstad (1988). Many authors choose to set $a_x=a_y=a_z=1$ in their analyses, often for simplicity or because of limited statistics. For such a spherical Gaussian source, $R\equiv r_0$ and $r_{\rm rms}=(\frac{3}{2})^{1/2}r_0$. It should be noted that one parametrization by Goldhaber, Goldhaber, Lee, and Pais (1960) used Eq. (3.1) with $a_x=a_y=a_z=\sqrt{2}$. This parametrization appears in sufficiently many papers that we define a corresponding radius parameter $R\equiv r_G=r_0/\sqrt{2}$.

Various refinements of the static single-Gaussian-source model have been proposed. For example, Lednicky and Podgoretskii (1979) consider a source composed of two Gaussians with different scales:

$$\rho(\mathbf{r})=\frac{\mu_1}{(\pi R_1^2)^{3/2}}\exp(-\mathbf{r}^2/R_1^2)+\frac{\mu_2}{(\pi R_2^2)^{3/2}}\exp(-\mathbf{r}^2/R_2^2) \ , \tag{3.4}$$

where $\mu_1+\mu_2=1$. One of the length scales could refer to direct pion production, while the second could refer to pions produced through resonance decay. The corresponding correlation function is

$$R(\mathbf{p}_1,\mathbf{p}_2)=\mu_1\exp[-(\mathbf{p}_1-\mathbf{p}_2)^2R_1^2/2]+\mu_2\exp[-(\mathbf{p}_1-\mathbf{p}_2)^2R_2^2/2] \ . \tag{3.5}$$

Evidence for such a two-length scenario has been cited in experiments by Åkesson *et al.* (1987b). The presence of two length scales could complicate the determination of the incoherence parameter λ: if measurements do not extend to sufficiently small momentum differences, the second Gaussian remains undetected and an incoherence parameter of $\lambda=\mu_1$ is determined.

Another refinement of the Gaussian-source model is the inclusion of a finite source lifetime. One model source distribution is given by (Koonin, 1977; Yano and Koonin, 1978)

$$\rho(\mathbf{r},t)=\frac{1}{\pi^2 r_0^3\tau}\exp\{-r^2/r_0^2-t^2/\tau^2\} \ . \tag{3.6}$$

The corresponding correlation function is, in the plane-wave limit,

$$R(\mathbf{p}_1,\mathbf{p}_2)=\exp\{-[(\mathbf{p}_1-\mathbf{p}_2)^2r_0^2/2]-[(E_1-E_2)^2\tau^2/2]\} \ . \tag{3.7}$$

As in the two-Gaussian case, $R(\mathbf{p}_1,\mathbf{p}_2)$ is affected by two scales r_0 and τ; as $\mathbf{q}$ is rotated with respect to $\mathbf{P}$, the source may appear anisotropic. Of course, a nonzero value for τ has no effect on the correlation function if the energies of the particles are the same.

A further time dependence of the source distribution is the translation of the source in the laboratory frame. The effect of this motion on the correlation function can be handled in a number of ways. Yano and Koonin (1978) use a Lorentz-invariant form of the Gaussian source:

$$\rho(x^\mu)=\frac{1}{\pi^2 r_0^3\tau}\exp[-B_1(x_\mu S^\mu)^2+B_2 x_\mu x^\mu] \ , \tag{3.8}$$

where B_1 and B_2 are source parameters and S_μ is the total 4-momentum of the source system. Repeated indices imply a summation and the Mandelstam variable s is given by $s=S_\mu S^\mu$. The choice for B_1 and B_2 of

$$B_1=(r_0^{-2}+\tau^{-2})/s, \quad B_2=r_0^{-2} \ , \tag{3.9}$$

gives the previous form for the correlation function if it is observed in the rest frame of the source. In the absence of final-state interactions, the correlation function corresponding to Eq. (3.8) has the form

$$R(\mathbf{p}_1,\mathbf{p}_2)=\exp[-2B_1r_0^2\tau^2(q_\mu S^\mu)^2+2q_\mu q^\mu/B_2] \ , \tag{3.10}$$

where $q^\mu=(p_1^\mu-p_2^\mu)/2$ as elsewhere in this review.

When the velocity of the source $\mathbf{V}_0$ is nonrelativistic, the source distribution reduces to [with the substitutions of Eq. (3.9)]

$$\rho(\mathbf{r},t)=\frac{1}{\pi^{3/2}r_0^3}\exp[-(\mathbf{r}-\mathbf{V}_0t)^2/r_0^2]\frac{1}{\pi^{1/2}\tau}\exp(-t^2/\tau^2) \ , \tag{3.11}$$

and the correlation function becomes

$$R(\mathbf{p}_1,\mathbf{p}_2)=\frac{1}{(2\pi)^{3/2}r_0^2 d}\int d^3r\,\exp\{-[r^2-(\mathbf{r}\cdot\mathbf{V}'\tau/d)^2]/2r_0^2\}|\psi|^2\ , \tag{3.12}$$

where ψ is the two-particle wave function. In these expressions, $\mathbf{V}'=\mathbf{V}-\mathbf{V}_0$ and $d=[r_0^2+(V'\tau)^2]^{1/2}$ where $\mathbf{V}$ is the velocity of the two-pion c.m. position. The presence of the term $(\mathbf{r}\cdot\mathbf{V}'\tau/d)^2$ in the exponential means that the distribution looks prolate *in a direction determined* by $\mathbf{V}'$. Note that even if the source is not moving, $\mathbf{V}_0=0$, a time dependence is still present in Eq. (3.12), as expected from Eq. (3.11). A stationary source of finite lifetime appears to be prolate in the direction of observation (i.e., the direction of $\mathbf{V}$). This can also be seen directly from Eq. (3.7) because of the on-mass-shell relationship between E and $\mathbf{p}$.

B. Kopylov-Podgoretskii model

Several other model source distributions that yield analytically tractable results have been proposed. In this subsection we discuss emission from either the interior or the surface of an ellipsoid (Kopylov and Podgoretskii, 1972, 1973; Cocconi, 1974; Kopylov, 1974; for a discussion of source shape analysis using this formalism, see Podgoretskii and Cheplakov, 1986).

Kopylov and Podgoretskii (1972, 1973) consider a two-step approach to pion production. In the first step an oscillator is excited. In the second step it deexcites by emitting a pion. The decay is assumed to take place statistically. In the original work two models are considered for the spatial region where the oscillators are produced. The first model uses an ellipsoidal region with the oscillators distributed uniformly inside the boundary, while the second model uses an ellipsoidal region with the oscillators excited only on the surface. Once excited, the oscillators move and decay. This approach differs from that presented in Sec. III.A: the spatial distribution of the source is different (although it would take a very precise experiment to detect this difference) and a two-step process is assumed for particle emission.

Following Kopylov and Podgoretskii (1972, 1973), we consider the amplitude $A(E,\mathbf{r})$ for detecting a particle at position $\mathbf{r}$ with energy E:

$$A(E,\mathbf{r})\propto\int g(\mathbf{r}',t')\exp(ip|\mathbf{r}-\mathbf{r}'|+iEt')\frac{d^3r'dt'}{|\mathbf{r}-\mathbf{r}'|}\ . \tag{3.13}$$

Note the absolute value in the exponential. The source $g(\mathbf{r}',t')$ is assumed to be a heavy pointlike oscillator with a proper frequency (i.e., frequency in the rest frame of the source) ω^* and lifetime $\tau^*=1/\Gamma^*$ (the corresponding laboratory quantities are ω and τ, respectively). The oscillator is assumed to move with constant velocity $\boldsymbol{\nu}$ and to be given excitation energy at the time t_0 when it passes through the origin. Thus the source is given by

$$g(\mathbf{r}',t')=g_0\delta[\mathbf{r}'-\boldsymbol{\nu}(t'-t_0)]\exp[-i\omega(t'-t_0)-(t'-t_0)/(2\tau)] \tag{3.14}$$

for $t'>t_0$ and is equal to zero otherwise. Combining Eqs. (3.13) and (3.14) and assuming that $\mathbf{r}'$ is much less than $|\mathbf{r}'-\mathbf{r}|$ we have, after neglecting slowly varying factors,

$$A(E,\mathbf{r})\propto\frac{\exp(ipr+iEt_0)}{E-\mathbf{p}\cdot\boldsymbol{\nu}-\omega+i/(2\tau)}\ . \tag{3.15}$$

The only space-time characteristics of the event are the instant t_0 when the oscillator is excited and its position at that instant.

The above argument can be repeated with two oscillators excited at times t_α and t_β with positions $\mathbf{r}_\alpha$ and $\mathbf{r}_\beta$, as in Fig. 1. The two emitted pions are detected at points $\mathbf{r}_1$ and $\mathbf{r}_2$. The distance between the oscillators, $\mathbf{r}_{\alpha\beta}=\mathbf{r}_\alpha-\mathbf{r}_\beta$, is assumed to be small compared to the other distances in the problem. The amplitude for detecting two particles now has two contributions: one contribution in which the pion emitted by oscillator α is detected at $\mathbf{r}_1$ and the pion emitted by oscillator β is detected at $\mathbf{r}_2$, the other contribution in which $\mathbf{r}_1$ and $\mathbf{r}_2$ are interchanged. Hence

$$A(E_1,E_2)\propto\frac{\exp(ip_1r_{\alpha1}+iE_1t_\alpha)}{E_1-\mathbf{p}_1\cdot\boldsymbol{\nu}_\alpha-\omega_\alpha+i\Gamma_\alpha/2}\cdot\frac{\exp(ip_2r_{\beta2}+iE_2t_\beta)}{E_2-\mathbf{p}_2\cdot\boldsymbol{\nu}_\beta-\omega_\beta+i\Gamma_\beta/2}+\frac{\exp(ip_2r_{\alpha2}+iE_2t_\alpha)}{E_2-\mathbf{p}_2\cdot\boldsymbol{\nu}_\alpha-\omega_\alpha+i\Gamma_\alpha/2}\cdot\frac{\exp(ip_1r_{\beta1}+iE_1t_\beta)}{E_1-\mathbf{p}_1\cdot\boldsymbol{\nu}_\beta-\omega_\beta+i\Gamma_\beta/2}\ . \tag{3.16}$$

The momenta $\mathbf{p}_{\alpha1}$ and $\mathbf{p}_{\beta1}$ are indistinguishable and are replaced by a single momentum $\mathbf{p}_1$ in Eq. (3.16); similarly $\mathbf{p}_{\alpha2}=\mathbf{p}_{\beta2}=\mathbf{p}_2$.

The probability of detecting two particles is the complex square of the amplitude. In addition, the unobserved energies ω_α and ω_β must be integrated out. This leads to the joint probability

$$P_{12}\approx1+\frac{\exp(i\Delta)}{2(\xi_\alpha-i)(\xi_\beta+i)}+\frac{\exp(-i\Delta)}{2(\xi_\alpha+i)(\xi_\beta-i)}\approx1+\frac{(1+\xi_\alpha\xi_\beta)\cos\Delta+(\xi_\alpha-\xi_\beta)\sin\Delta}{(1+\xi_\alpha^2)(1+\xi_\beta^2)}\ , \tag{3.17}$$

where we have used (note that these are not dot products)

$$\Delta = p_1 r_{\alpha 1} + p_2 r_{\beta 2} - p_1 r_{\beta 1} - p_2 r_{\alpha 2} - (E_1 - E_2)(t_\alpha - t_\beta) \tag{3.18}$$

and

$$\xi_{\alpha(\beta)} = [E_1 - E_2 - \nu_{\alpha(\beta)} \cdot (\mathbf{p}_1 - \mathbf{p}_2)]/\Gamma_{\alpha(\beta)} \ . \tag{3.19}$$

When the distance between the sources is small

$$\Delta \rightarrow (\mathbf{p}_1 - \mathbf{p}_2) \cdot (\mathbf{r}_\alpha - \mathbf{r}_\beta) - (E_1 - E_2)(t_\alpha - t_\beta) \ . \tag{3.20}$$

Note that Δ depends on the dot product of $\mathbf{r}_{\alpha\beta}$ and $\mathbf{q} = (\mathbf{p}_1 - \mathbf{p}_2)/2$.

In this subsection we consider the case in which the oscillators are excited at the same time $t_\alpha - t_\beta$, move with the same velocity $\nu_\alpha = \nu_\beta = \nu$, and have the same decay rate $\Gamma_\alpha = \Gamma_\beta = \Gamma$, so that $\xi_\alpha = \xi_\beta = \xi$. The oscillator positions must now be averaged over the source distribution. Kopylov and Podgoretskii (1973) consider two different source distributions. In their formalism the source is the region where the oscillators are formed and not the region from which the pions are emitted.

The first source region is a uniform ellipsoid and the correlation function is

$$R(\mathbf{p}_1, \mathbf{p}_2) = [3 j_1(\kappa)/\kappa]^2/(1 + \xi^2) \ , \tag{3.21}$$

where $j_1(\kappa)$ is a spherical Bessel function and

$$\kappa = 2[(q_x A_x)^2 + (q_y A_y)^2 + (q_z A_z)^2]^{1/2} \ . \tag{3.22}$$

The A_i are the semiaxes of the ellipsoid. As with the Gaussian source, the correlation $R(\mathbf{q})$ depends only on the source dimension parallel to $\mathbf{q}$.

As a second source distribution, Kopylov and Podgoretskii consider emission from an ellipsoidal surface. This gives the result

$$R(\mathbf{p}_1, \mathbf{p}_2) = [2 J_1(\kappa)/\kappa]^2/(1 + \xi^2) \ , \tag{3.23}$$

where $J_1(\kappa)$ is a cylindrical Bessel function. The interesting feature of this result is that it is indistinguishable from emission from a disk, even though it is derived from a three-dimensional shape. The interested reader is referred to Kopylov and Podgoretskii (1973) for the modification to the correlation function caused by relaxing the condition that the oscillator excitation times t_α be simultaneous.

To simplify the parametrization further, let the source be stationary ($\nu = 0$) and isotropic ($A_x = A_y = A_z = R_{\rm KP}$; the subscript is introduced to differentiate between this radius and those from other models). Then $\kappa = 2qR_{\rm KP}$ and Eqs. (3.21) and (3.23) become

$$R(\mathbf{p}_1, \mathbf{p}_2) = [3 j_1(2qR_{\rm KP})/(2qR_{\rm KP})]^2/[1 + (2q_0\tau)^2] \tag{3.24}$$

and

$$R(\mathbf{p}_1, \mathbf{p}_2) = [2 J_1(2qR_{\rm KP})/(2qR_{\rm KP})]^2/[1 + (2q_0\tau)^2] \ . \tag{3.25}$$

If $\tau > 0$ in these equations, then $R(\mathbf{p}_1, \mathbf{p}_2)$ has its maximum value at $q_0 = 0$ (i.e., $|\mathbf{p}_1| = |\mathbf{p}_2|$) for a given value of $|\mathbf{q}|$ and decreases as $|q_0| > 0$.

Equation (3.25) has been used extensively in data analysis. In order to provide a means of comparing extracted values of $R_{\rm KP}$ with r_0 of the Gaussian model we use the approximation suggested by Zajc (1987b):

$$\left| \frac{2 J_1(\rho)}{\rho} \right|^2 \approx \exp(-\rho^2/4) \tag{3.26}$$

(which can be seen by comparing the power-series expansions of each function) to obtain $R_{\rm KP}/\sqrt{2} = r_0$.

C. Time-evolving sources

In Secs. III.A and III.B we discuss sources of fixed geometry. In this subsection, results are presented for time-dependent source geometries, in particular, expanding sources. Resonance lifetime effects, which are complementary to the discussions here, are deferred to Sec. VI.

Pratt (1984) has developed a correlation function formalism based on Wigner functions, which he applies to particle emission from a spherically expanding shell. As a model calculation, pion emission is treated from a source whose Wigner function has the form

$$g(x, \mathbf{p}) = \delta(r - R_0) \exp(-t^2/\tau^2) \exp[-E'(\mathbf{p}, r)/T] \ , \tag{3.27}$$

where the pion is emitted at space-time coordinates $(R_0\mathbf{n}, t)$ from a spherical shell characterized by a radius R_0, lifetime parameter τ, and temperature T. The unit vector normal to the sphere's surface is denoted by $\mathbf{n}$. In a frame comoving with the shell at velocity $\nu\mathbf{n}$, the pion's energy is $E'(\mathbf{p}, \mathbf{r}) = (E_p - \nu\mathbf{n} \cdot \mathbf{p})(1 - \nu^2)^{-1/2}$. The corresponding correlation function has a form in which the apparent source size $R_S(\mathbf{P})$ depends on the total momentum of the pion pair $\mathbf{P} = \mathbf{p}_1 + \mathbf{p}_2$:

$$R_S(\mathbf{P}) = R_0[(z \tanh z)^{-1} - \sinh^{-2} z]^{1/2} \ , \tag{3.28}$$

where $z = P\gamma\nu/(2T)$ and γ is the usual Lorentz factor $\gamma = (1 - \nu^2)^{-1/2}$.

As an example, Fig. 2 shows $R_S(\mathbf{P})$ for an expanding source with $T/\gamma\nu = 100$ MeV. The apparent size decreases significantly with increasing $\mathbf{P}$. Pratt (1984) presents a simple explanation for this dependence: energetic particles are more likely to be emitted from a point on the shell expanding with a velocity in the direction of $\mathbf{P}$, whereas pairs with smaller $\mathbf{P}$ can come from more widely separated points. It should be pointed out that there are effects arising from the mean time between emissions that also result in decreasing apparent size with increasing $\mathbf{P}$; these effects are examined in Sec. VI.

A number of authors have explored the dependence of R on collective expansion at relativistic energies. Machlin and Sinyukov (1987) treat in a relativistically covari-

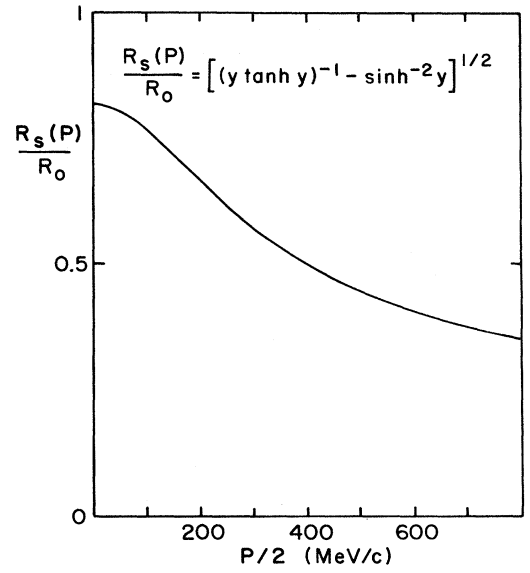

FIG. 2. Effective size of an expanding radial source with $T/\gamma v = 100$ MeV, shown as a function of the total momentum **P** of the two-particle pair (after Pratt, 1984).

ant manner a source with internal collective motion. Averchenkov, Makhlin, and Sinyukov (1987) then apply this approach to a variety of situations, in particular a scaling model of hydrodynamical expansion used in ultrarelativistic heavy-ion studies. In a different approach, Hama and Padula (1988) also investigate the apparent dimension of the source. Although their applications are more specific to the problem of quark-gluon plasma formation, they find the same general features of the correlation function as Pratt (1986b). Our treatment of expansion at ultrarelativistic energies uses a model by Kolehmainen and Gyulassy (1986), which is based upon the formalism of Sec. II.

Pion production in the Kolehmainen-Gyulassy (1986) approach is modeled after the inside-outside cascade dynamics in which the formation time of a secondary particle increases linearly with its energy due to time dilation. A natural set of kinematic variables are the longitudinal and transverse momenta $p_\parallel$ and p_T, and the transverse mass $m_T^2 = m^2 + p_T^2$, so that the particle's 4-momentum is $p^\mu = (m_T \cosh y, \mathbf{p}_T, m_T \sinh y)$. The particle production dynamics leads to a strong correlation between the average space-time point (z,t) of the particle emission and the longitudinal rapidity $y = (\frac{1}{2})\ln[(E+p_\parallel)/(E-p_\parallel)]$. This correlation can be expressed approximately by $z = \tau_0 \sinh y$ and $t = \tau_0 \cosh y$ (for further details see Kolehmainen and Gyulassy, 1986, and references therein).

The final interference reflects only the geometry at the proper time when the interactions have ceased. Using the source current approach described in Sec. II, Kolehmainen and Gyulassy write the correlation function as

$$R(\mathbf{p}_1,\mathbf{p}_2) = \frac{|G(\mathbf{p}_1,\mathbf{p}_2)|^2}{G(\mathbf{p}_1,\mathbf{p}_1)G(\mathbf{p}_2,\mathbf{p}_2)} , \tag{3.29}$$

where

$$G(\mathbf{p}_1,\mathbf{p}_2) = \int dy_0 \tilde{D}(\mathbf{p}_2 - \mathbf{p}_1, y_0) \tilde{J}_\pi^*(y_1 - y_0, \mathbf{p}_{1T}) \times \tilde{J}_\pi(y_2 - y_0, \mathbf{p}_{2T}) . \tag{3.30}$$

The distribution D comes from the space-time distribution of sources and is responsible for the two-particle correlation, while the J_π give the overall momentum dependence. This is like Eq. (2.27) with only one source. A simple characterization for the inside-outside cascade model is

$$D(z,t,\mathbf{r}_T,y_0) = (1/\pi R_T^2)\delta(t - \tau_0 \cosh y_0)\delta(z - \tau_0 \sinh y_0) \times \exp(-r_T^2/R_T^2) , \tag{3.31}$$

where y_0 is the source rapidity and the source distribution in the transverse direction is assumed to be a Gaussian with radius R_T. The functions D in Eqs. (3.30) and (3.31) are Fourier transforms of each other. To complete the determination of R it is necessary to give J_π. Of the two currents considered by Kolehmainen and Gyulassy, more analytically tractable results are found with the pseudothermal model,

$$\tilde{J}_\pi(y - y_0, p_T) = \exp[-(m_T/2T)\cosh(y - y_0)] = \exp(-E'/2T') , \tag{3.32}$$

where E' is the pion energy in the rest frame of the pion emitter. In this model, G is given by

$$G(\mathbf{p}_1,\mathbf{p}_2) = aK_0(\sqrt{u}\,)\exp(-q_T^2 \mathbf{R}_T^2/4) , \tag{3.33}$$

where K_0 is the modified Bessel function and the dynamical and geometrical contents are contained in the variable

$$u = 2m_{1T}m_{2T}(\tfrac{1}{4}T^2 + \tau_0^2)\cosh(\Delta y) + (m_{1T}^2 + m_{2T}^2)(\tfrac{1}{4}T^2 - \tau_0^2) + (i\tau_0/T)(m_{1T}^2 - m_{2T}^2) . \tag{3.34}$$

In this last expression, Δy is the rapidity difference $y_1 - y_2$. Unlike the Gaussian and Kopylov-Podgoretskii parametrizations discussed in Secs. III.A and III.B, Eq. (3.34) does not break up cleanly into components. Nevertheless, its parameters can be determined from measured correlation functions (Bamberger *et al.*, 1988). Kolehmainen and Gyulassy (1986) point out that their results are numerically similar to a model advanced by Pratt (1986b).

D. Pion final-state interactions

Several aspects of final-state interactions can be important for two-pion correlation functions. These include resonance decay as well as strong and Coulombic interactions at both the two- and three-body levels. Resonance decays are discussed more fully in Sec. VI, since correlations between clusters are observed to show strong resonance behavior. Interference between "prompt" pions

and those arising from resonance decay has been investigated by Grassberger (1977), who shows that such interference contributes to a narrow peak in the correlation function near $q=0$. Other effects of production dynamics on correlation functions have been considered by Thomas (1977).

Gyulassy, Kauffmann, and Wilson (1979) suggest a simple procedure for incorporating the Coulomb final-state interactions between the pions: the model pair probability without Coulomb interactions is multiplied by the Gamow factor to produce a Coulomb-corrected correlation function,

$$[R(\mathbf{p}_1,\mathbf{p}_2)+1]_{\text{theory+Coulomb}} = W(\mathbf{p}_1,\mathbf{p}_2)[R(\mathbf{p}_1,\mathbf{p}_2)+1]_{\text{theory}} . \quad (3.35)$$

The Gamow factor is the square modulus of the nonrelativistic Coulomb wave function at the origin (Gamow, 1928; Gurney and Condon, 1929; see Schiff, 1955, p. 141):

$$W(\mathbf{p}_1,\mathbf{p}_2)=2\pi\eta/[\exp(2\pi\eta)-1] \quad (3.36)$$

with

$$\eta=\alpha m_\pi/|\mathbf{p}_1-\mathbf{p}_2|, \quad \alpha=e^2/\hbar c . \quad (3.37)$$

The Gamow factor suppresses the model correlation function at small relative momenta. The factorization in Eq. (3.35) is only an approximation valid when the source radius is much less than the Bohr radius of the particle pair.

The Gamow correction procedure is frequently used for comparisons of experimental correlation functions with simple model parametrizations. Slightly different Coulomb corrections have been investigated by Pratt (1986a). A comparison with a classical Coulomb trajectory calculation is made by Gersch (1987).

Few two-pion correlation function analyses performed thus far have included strong-interaction corrections. Suzuki (1987) and Bowler (1988) have examined the strong-interaction contributions to the $I=0$ and $I=2$ $\pi\pi$ s-wave amplitudes (the $I=0$ phase shift may enter the $\pi^+\pi^+$ correlation function analysis if $\pi^+\pi^-$ pairs are used experimentally to normalize the $\pi^+\pi^+$ yields). The derivative of the $I=2$ phase shift $d\delta/dq$ is negative, whereas the $I=0$ value of $d\delta/dq$ is positive for small q. From the discussion of final-state interaction effects in Sec. II.D, one sees that the $I=2$ contribution tends to suppress the predicted correlation function for a given geometry. Unfortunately, there is considerable uncertainty in the measured phase shifts, so that the magnitude of the strong-interaction effects is not well determined. Both Suzuki (1987) and Bowler (1988) estimate that strong interactions may suppress the correlation function at $q=0$ by as much as 20%.

Suzuki (1987) also argues on the basis of an isospin decomposition of the $\pi^+\pi^0$ amplitudes that Bose-Einstein effects should be present in $\pi^+\pi^0$ correlations in spite of their being nonidentical particles. Bowler (1987b) performs a more general analysis of the amplitudes and arrives at the opposite and correct conclusion: there should be no Bose-Einstein correlations for $\pi^+\pi^0$.

The correlation function may be influenced by strong or Coulombic interactions between the emitted particles and their source. Gyulassy, Kauffmann, and Wilson (1979) have developed a formalism for treating these three-body-like interactions, but applications yielding analytical results are difficult to find. This is in contrast to the two-body situation, in which Gyulassy and Kauffmann (1981) examine the change in the single-particle inclusive spectra arising from Coulomb interaction of the particles with the emission region. Experimentally, correlation function distortions from final-state interactions with the source have received only modest attention for pion emission (Zajc *et al.*, 1984). Such distortions have been identified at lower bombarding energies. They are important if the emitted particles have different charge-to-mass ratios (see Sec. VII).

E. The incoherence parameter

In Sec. II the incoherence parameter λ is introduced as a means of describing boson-emitting sources that are neither fully coherent nor fully incoherent. As shown in Secs. IV and V, many experiments yield values for λ that are less than unity. Although the question of coherent emission is of fundamental interest in subatomic reactions, there are many factors that may make it an inappropriate concept. We begin this section by discussing aspects of coherent emission encountered in hadronic, and particularly nuclear, reactions.

The parameter $\lambda=R(\mathbf{p},\mathbf{p})$ is affected by many things other than source coherence. In the pion source model presented in Sec. II.B, $R(\mathbf{p},\mathbf{p})$ is affected by the number of source currents (Gyulassy, Kauffmann, and Wilson, 1979). The two-source model of Lednicky and Podgoretskii (1979) presented in Sec. III.A illustrates how phenomena such as long-time-frame decays (see, for example, Grassberger, 1977; Gyulassy and Padula, 1988) substantially alter $R(\mathbf{p},\mathbf{p})$. Thus, if a significant fraction of pions in a reaction results from resonance decays, the small amount of coherent production may be so masked as to be unobservable (Gyulassy, 1990). It may also happen that multiple scattering reduces initially coherent emission, in much the same way as a ground-glass screen is used in speckle interferometry from coherent laser light (Gyulassy, 1990). In high-energy reactions there is a question of the maximum coherence allowed by causality (Gyulassy, 1990). If particles are produced at small temporal, but large spatial, separation, then the production may not be coherent simply because the emission points cannot be causally connected.

As if all of these reaction effects were not enough, there are factors implicit in the measurement process that affect $R(\mathbf{p},\mathbf{p})$. Many measurements average over impact parameter, orientation of $\mathbf{q}$ with respect to $\mathbf{P}$, etc., and these averages may change $R(\mathbf{p},\mathbf{p})$. For example, Gyulassy (1982) shows in one particular dynamical

model that λ may even exceed unity because of impact-parameter averaging. As mentioned earlier, experimental averaging procedures may smooth out single-particle distributions [e.g., Eq. (2.23)] and lead to an apparent nonzero $R(\mathbf{p},\mathbf{p})$ even for a coherent source. Finally, as emphasized by Lednicky and Podgoretskii (1979), finite experimental resolution always tends to wash out peaks in $R(\mathbf{p},\mathbf{p})$ at small $\mathbf{q}$.

The critique in the preceding two paragraphs indicates that there are a significant number of difficulties in interpreting λ. Bearing these difficulties in mind we examine several methods for handling partially coherent sources. Gyulassy, Kauffmann, and Wilson (1979) decompose the pion source current $J(\mathbf{p})$ into coherent and incoherent contributions:

$$\tilde{J}(\mathbf{p})=\tilde{J}_{\rm coh}(\mathbf{p})+\tilde{J}_{\rm incoh}(\mathbf{p}) . \tag{3.38}$$

For real currents and source density, the corresponding correlation function becomes

$$\begin{aligned} R(\mathbf{p}_1,\mathbf{p}_2)=&[1-D(\mathbf{p}_1)][1-D(\mathbf{p}_2)]\tilde{\rho}^{\,2}(\mathbf{p}_1-\mathbf{p}_2) \\ &+2\{D(\mathbf{p}_1)D(\mathbf{p}_2)[1-D(\mathbf{p}_1)][1-D(\mathbf{p}_2)]\}^{1/2} \\ &\times\tilde{\rho}(\mathbf{p}_1-\mathbf{p}_2) . \end{aligned} \tag{3.39}$$

The momentum-dependent *degree of coherence* $D(p)$ is defined by

$$D(\mathbf{p})=\frac{|\tilde{J}_{\rm coh}(\mathbf{p})|^2}{P_1(\mathbf{p})}=\frac{n_{\rm coh}(\mathbf{p})}{n_{\rm coh}(\mathbf{p})+n_{\rm incoh}(\mathbf{p})} , \tag{3.40}$$

where $n_{\rm coh}(\mathbf{p})$ and $n_{\rm incoh}(\mathbf{p})$ are the number densities of coherently and incoherently produced pions with momentum $\mathbf{p}$. An expression for the incoherence parameter λ can be obtained from Eq. (3.39) when $\mathbf{p}_1=\mathbf{p}_2=\mathbf{p}$:

$$\lambda=1-\left[\frac{n_{\rm coh}(\mathbf{p})}{n_{\rm coh}(\mathbf{p})+n_{\rm incoh}(\mathbf{p})}\right]^2 . \tag{3.41}$$

Coherent and incoherent emission processes in particle physics are discussed by Fowler and Weiner (1977, 1978). They use a formalism similar to that of Gyulassy, Kauffmann, and Wilson (1979), but neglect the momentum dependence of the degree of coherence. The same expression for λ as Eq. (3.41) (again without the momentum dependence) in the Kopylov-Podgoretskii model is obtained by Biyajima (1980). Other formulations of λ in terms of the topological expansion model of Giovannini and Veneziano (1977) are made by Biyajima (1981, 1982).

The measured values of the incoherence parameter, which are summarized in Secs. IV and V, can be interpreted from many points of view (including the view that they have no interpretation). Fowler, Stelte, and Weiner (1979) propose two-pion interferometry as a signature for the formation of pion condensates. Possible directional dependence of λ on $\mathbf{P}$ has been interpreted by Fowler and Weiner (1985) in terms of the decay of an $N+\Delta$ baryon collective state. Determination of the incoherence parameter from multiplicity distributions (rather than the traditional two-particle correlation function) is investigated by Fowler *et al.* (1988) and Vourdas and Weiner (1988). However, given the cautionary notes at the beginning of this section, at present no unique interpretation for the extracted value of λ exists

F. Other formalisms and applications

Previous parts of Sec. III discuss the effects of source geometry on the shape of the correlation function. Alternative approaches to the calculation of correlation functions incorporate the reaction dynamics. For example, Pratt and Tsang (1987; see also Koonin, 1977) point out that the correlation function can be calculated from any dynamical theory in terms of its predicted single-particle Wigner function $f(\mathbf{P}/2,\mathbf{R};t)$ by means of

$$1+R(\mathbf{p}_1,\mathbf{p}_2)=\frac{\int d^3r\, F_K(\mathbf{r})\phi^*(\mathbf{q},\mathbf{r})\phi(\mathbf{q},\mathbf{r})}{\int d^3r\, F_K(\mathbf{r})} , \tag{3.42}$$

where $\mathbf{P}=\mathbf{p}_1+\mathbf{p}_2$ and $\mathbf{q}=(\mathbf{p}_1-\mathbf{p}_2)/2$ as usual. The appropriately symmetrized wave function is denoted by $\phi(\mathbf{q},\mathbf{r})$, and $F_K(\mathbf{r})$ is the relative Wigner function

$$F_K(\mathbf{r})=\lim(t\to\infty)\int d^3R\, f\left[\mathbf{P}/2,\mathbf{R}+\frac{\mathbf{r}}{2};t\right]f\left[\mathbf{P}/2,\mathbf{R}-\frac{\mathbf{r}}{2};t\right] . \tag{3.43}$$

The models describing the reaction dynamics were developed largely to interpret inclusive cross sections or other observables popular in their time. For example, in work performed in the 1970s, correlation functions were examined in the context of Regge-Mueller models (Biyajima and Miyamura, 1974; Miyamura and Biyajima, 1975), in which the properties of scattering amplitudes are assumed to be dominated by particle exchange. In a similar vein, Giovannini and Veneziano (1977) developed a framework for correlation functions based on dual topological expansions. Cluster and fireball models have been developed to describe high-energy particle production, and the correlation functions of such models have been investigated by Ranft and Ranft (1975a, 1975b) as well as Engels and Schilling (1978).

More recently, string models have become popular in high-energy reaction studies. Correlations within the string model context are investigated by Andersson and Hofmann (1986), Bowler (1985, 1986), and Osborne (1988). The relationship between different string model calculations is shown in Bowler (1987a). The string models have been primarily applied to e^+e^- annihilation

processes, although they have concepts, such as longitudinal growth, that are useful in other reactions as well.

Finally, Bose-Einstein symmetrization effects have been studied for observables other than correlation functions. In particular, their role has been investigated in multiplicity moments and inclusive particle production (Bilic, Dadic, and Martinis, 1978; Carruthers and Shih, 1983, 1984). The interested reader is referred to the original literature for further information on these investigations.

IV. PION EMISSION IN ELEMENTARY-PARTICLE COLLISIONS

Historically, the first observations of Bose-Einstein correlations in elementary-particle collisions were made by Goldhaber *et al.* (1959). Goldhaber, Goldhaber, Lee, and Pais (1960) interpreted the angular correlations among pions within the context of a statistical model in which the particles of the system were confined within a region of spatial dimension of the order 1 fm. Many of the experiments performed on two-pion correlations during the 1960s and early 1970s either determined parameters of the GGLP statistical formalism or used the GGLP model to deduce source volumes (Xuong and Lynch, 1962; Bartke *et al.*, 1967; Donald *et al.*, 1969; De Baere *et al.*, 1970; Boesebeck *et al.*, 1973; Oh *et al.*, 1975).

Kopylov and Podgoretskii (1972, 1973) developed a convenient formalism for interpreting two-particle correlation measurements in terms of the space-time extent of the particle-emitting source region (see Sec. III.B). Subsequent to this development, a sizable number of particle physics experiments were performed and interpreted in terms of the source geometry. In this section we subdivide these experiments into two categories. Experiments involving the collision of two hadrons (Bartke *et al.*, 1967; Donald *et al.*, 1969; Biswas *et al.*, 1976; Borreani *et al.*, 1976; Calligarich *et al.*, 1976; Deutschmann *et al.*, 1976, 1982; Grard *et al.*, 1976; Angelini *et al.*, 1977; Angelov *et al.*, 1977, 1981; Ezell *et al.*, 1977; Cooper *et al.*, 1978; De Wolf *et al.*, 1978; Goossens *et al.*, 1978; Loktionov *et al.*, 1978; Drijard *et al.*, 1979; Åkesson *et al.*, 1983, 1985, 1987a, 1987b; Breakstone *et al.*, 1985, 1987; Adamus *et al.*, 1988; Albajar *et al.*, 1989) are covered in Sec. IV.A. Only two lepton-hadron collision experiments (Arneodo *et al.*, 1986; Allasia *et al.*, 1988) have been performed; these are summarized in Sec. IV.B, along with measurements for lepton-lepton collisions (Aihara *et al.*, 1985; Althoff *et al.*, 1985, 1986; Avery *et al.*, 1985; Juricic *et al.*, 1989).

Almost all of the particles used in the correlation function measurements discussed in this section are relativistic. Unfortunately, most of the functional forms used to fit these data either use nonrelativistic kinematics or make assumptions about the velocity of the emitting source. The experimental correlation functions generally do not possess sufficient accuracy to test the assumed kinematics. In some analyses, arbitrarily chosen functional forms with Lorentz-invariant variables are used without regard for the fact that a variable such as $Q_\mu Q^\mu=(E_1-E_2)^2-(\mathbf{p}_1-\mathbf{p}_2)^2$ mixes together the time and space dimensions of the source (Zajc, 1987b).

A. Hadron-hadron collisions

The original paper of Goldhaber, Goldhaber, Lee, and Pais (1960) treated pion emission from $p\bar{p}$ annihilation. One of the links between correlations and geometry is also provided in their paper. However, experiments performed in the decade following GGLP often did not include a geometrical analysis or did not possess sufficient statistics to allow for an accurate determination of the source geometry (Xuong and Lynch, 1962; De Baere *et al.*, 1970; Boesebeck *et al.*, 1973; Oh *et al.*, 1975). Since the development of the Kopylov-Podgoretskii formalism (1972, 1973), a considerable number of hadron-hadron reactions have been investigated and interpreted geometrically.

Tables I and II summarize the parameters extracted from many of these experiments. We use the $2\pi+X$ notation to indicate that the source parameters are determined from 2π correlations. We do not use the notation to imply that only two pions are measured in the final state (often the experiment is far more exclusive). The size parameters quoted in the tables are extracted assuming an isotropic source. Results for anisotropic sources are not included in Tables I and II; they are discussed in more detail in the text below. It is often difficult to compare results from different experiments because of the many different data analysis methods. Analysis methodology is addressed more completely in Sec. VII, but the issues include the following:

(i) How is the correlation function normalized?

(ii) How is the denominator in Eq. (2.3) determined?

(iii) What source parametrization is chosen?

(iv) What experimental gates are placed on the data (e.g., multiplicity cuts, kinetic-energy cuts, etc.)?

As is shown in all of this review's experimental sections, the extracted parameters may be dramatically sensitive to the method of analysis and to the applied cuts and gating conditions.

In Tables I and II we convert the source radii from the original papers into equivalent values of r_0. The conversion factors are given in Sec. III. It must be stressed, however, that some of the analysis parametrizations include lifetime or incoherence parameters, while others do not, and the numerical values of r_0 are sensitive to the presence of these terms. With all of these caveats in mind let us examine the tables for trends.

Table I contains results for proton- and antiproton-induced reactions. Most values of r_0 are close to 1 fm, as expected. There are weak indications that the reaction volume increases with bombarding energy, perhaps reflecting the fact that the particle multiplicity increases with bombarding energy. A smaller size is observed with

TABLE I. Extracted Gaussian source dimensions for pp and $p\bar{p}$ collisions. The measured values have been converted to equivalent values of r_0 as described in the text.

Reaction	p_{lab} (GeV/c)	r_0 (fm)	λ
$pp \rightarrow 2\pi + X$[a]	1460	0.95±0.22	
$pp \rightarrow 2\pi + X$[b]	1500–2100	1.06±0.07	0.34±0.04
$pp \rightarrow 2\pi + X$[c]	2100	1.60±0.06	0.45±0.03
$p\bar{p} \rightarrow 2\pi + X$[d]	0	1.02±0.06	0.63±0.05
$p\bar{p} \rightarrow 2\pi + X$[e]	0–0.7	1.3±0.1	
$p\bar{p} \rightarrow K_s^0 K_s^0 + X$[f]	0.76	0.6±0.1	
$p\bar{p} \rightarrow 2\pi + X$[g]	1.2	0.4	
$p\bar{p} \rightarrow 2\pi + X$[h]	22.4	2.1±0.4	
$p\bar{p} \rightarrow 2\pi + X$[i]	2110	1.46±0.10	0.43±0.05
$\bar{p} + n \rightarrow 2\pi + X$[j]	1.0–1.6	0.87±0.06	

[a]Drijard *et al.*, 1979.
[b]Åkesson *et al.*, 1985.
[c]Breakstone *et al.*, 1985.
[d]Deutschmann *et al.*, 1982.
[e]Angelini *et al.*, 1977.
[f]Cooper *et al.*, 1978.
[g]Donald *et al.*, 1969.
[h]Loktionov *et al.*, 1978.
[i]Breakstone *et al.*, 1985.
[j]Borreani *et al.*, 1976.

KK pairs, as opposed to $\pi\pi$ pairs, although a systematic determination of this effect has not been performed (this large difference in source size between 2π and $2K$ pairs is not observed in heavy-ion reactions; see Sec. V). A comparison of Tables I and II shows that the extracted source size does not depend strongly on whether the projectile is a meson or baryon. Finally, the incoherence parameter λ is observed to be less than unity—in some cases substantially so (whether λ has a meaningful interpretation is discussed in Sec. III.E). The usual cautionary note should be made that the extracted parameters may be highly model dependent. For example, a study by Åkesson *et al.* (1987b) for the reaction $pp \rightarrow 2\pi + X$ at $\sqrt{s} = 63$ GeV shows that the incoherence parameter changes from $\lambda = 0.40 \pm 0.03$ using a single Gaussian source to $\lambda = 0.74^{+0.19}_{-0.14}$ using a two-Gaussian source (see Sec. III for a discussion).

Because of the many different source parametrizations

TABLE II. Extracted Gaussian source dimensions for πp and Kp collisions. The measured values have been converted to equivalent values of r_0 as described in the text.

Reaction	p_{lab} (GeV/c)	r_0 (fm)	λ
$\pi p \rightarrow 2\pi + X$[a]	4–25	$0.7^{+0.3}_{-0.1}$	
$\pi^+ p \rightarrow 2\pi + X$[b]	8	$1\frac{1}{2}$	
$\pi^- p \rightarrow 2\pi + X$[c]	11.2	0.74±0.07	
$\pi^+ p \rightarrow 2\pi + X$[d]	16	1.03±0.03	0.88±0.02
$\pi^- p \rightarrow 2\pi + X$[e]	40	1.2±0.2	
$\pi^- p \rightarrow 2\pi + X$[f]	40	1.0±0.2	
$\pi^- p \rightarrow 2\pi + X$[g]	200	1.34±0.15	
$\pi^+ p / K^+ p \rightarrow 2\pi + X$[h]	250	0.98±0.07	0.30±0.03
$K^+ p \rightarrow 2\pi + X$[i]	8.25	0.6±0.06	
$K^+ p \rightarrow 2\pi + X$[j]	16	$1\frac{1}{2}$	
$K^- p \rightarrow 2\pi + X$[d]	16	0.96±0.04	0.83±0.04
$K^+ p \rightarrow 2\pi + X$[k]	32	0.6±0.07	

[a]Deutschmann *et al.*, 1976.
[b]Bartke *et al.*, 1967.
[c]Calligarich *et al.*, 1976.
[d]Deutschmann *et al.*, 1982.
[e]Angelov *et al.*, 1977.
[f]Angelov *et al.*, 1981.
[g]Biswas *et al.*, 1976 (calculated in Bartnik and Rzazewski, 1978).
[h]Adamus *et al.*, 1988.
[i]Grard *et al.*, 1976.
[j]De Wolf *et al.*, 1978.
[k]Goossens *et al.*, 1978.

and fitting procedures used in data analysis, we have quoted values only for r_0 and λ in the tables. Some analyses extract lifetimes as well, using source distributions such as Eq. (3.6). Such fits generally obtain values of 1–2 fm/c for the lifetime.

The bombarding energy dependence of the source parameters has been investigated systematically by the UA1 collaboration (Albajar *et al.*, 1989) with high statistics in $p\bar{p}$ interactions over the c.m. energy range $\sqrt{s}=200$–900 GeV. Examples of the data are shown in Fig. 3 for $\sqrt{s}=630$ GeV and several charged-particle multiplicity ($N_{\rm ch}$), cuts: (a) $2<N_{\rm ch}\leq 10$; (b) $10<N_{\rm ch}\leq 20$; (c) $20<N_{\rm ch}\leq 30$; (d) $30<N_{\rm ch}\leq 40$; (e) $40<N_{\rm ch}\leq 50$. The kinematic variable Q_t is the projection of **Q** on the plane perpendicular to **P**. The smooth curves through the data are fits using a Gaussian source. Shown in Fig. 4 is the center-of-mass energy dependence of the extracted source radius at fixed charged-particle multiplicity for the reaction $p\bar{p}\rightarrow 2\pi+X$ (after Albajar *et al.*, 1989). Four different ranges of $N_{\rm ch}$ are shown, corresponding to (a)–(d) in Fig. 3. Larger source dimensions are extracted for high multiplicity than for low multiplicity. There is little variation of r_0 over the c.m. energy range shown. Similarly, the incoherence parameter λ also shows little variation over this energy range at fixed $N_{\rm ch}$.

The experiments quoted in Tables I and II involve averaging over many types of events and momentum

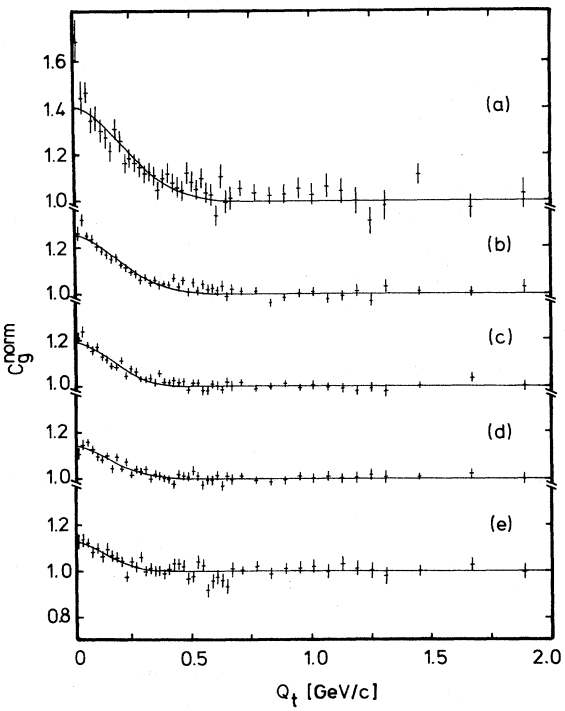

FIG. 3. Charged-particle-multiplicity ($N_{\rm ch}$) dependence of the correlation function for the reaction $p\bar{p}\rightarrow 2\pi+X$ at $\sqrt{s}=630$ GeV. Five different ranges of $N_{\rm ch}$ are shown: (a) $2<N_{\rm ch}\leq 10$; (b) $10<N_{\rm ch}\leq 20$; (c) $20<N_{\rm ch}\leq 30$; (d) $30<N_{\rm ch}\leq 40$; (e) $40<N_{\rm ch}\leq 50$. The smooth curves through the data are fits with a Gaussian source (after Albajar *et al.*, 1989).

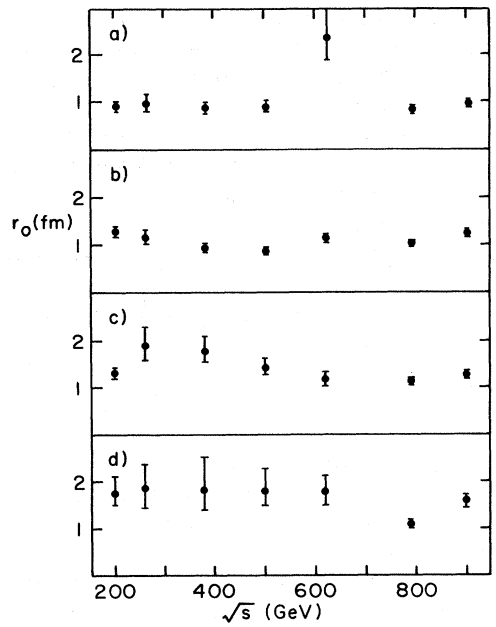

FIG. 4. Center-of-mass energy dependence ($\sqrt{s}$) of the extracted source radius at fixed charged-particle multiplicity $N_{\rm ch}$ for the reaction $p\bar{p}\rightarrow 2\pi+X$. Four different ranges of $N_{\rm ch}$ are shown: (a) $2<N_{\rm ch}\leq 10$; (b) $10<N_{\rm ch}\leq 20$; (c) $20<N_{\rm ch}\leq 30$; (d) $30<N_{\rm ch}\leq 40$ (after Albajar *et al.*, 1989).

orientations. A number of experiments attempt to determine the source anisotropy by analyzing the correlation function with the relative momentum vector $\mathbf{q}=(\mathbf{p}_1-\mathbf{p}_2)/2$ either parallel or perpendicular to the beam direction. The corresponding extracted source radii $r_\parallel$ and $r_\perp$ do not show a consistent trend in the early experiments. Deutschmann *et al.* (1976) find a source contracted in the beam direction, although the uncertainties are large. Similar observations are made by Ezell *et al.* (1977) in $pp\rightarrow 2\pi+X$ at $p_{\rm lab}=28.5$ GeV/c, who find $r_\parallel=0.52^{+0.07}_{-0.08}$ fm and $r_\perp=1.15^{+2.52}_{-0.70}$ fm, and also by Angelov *et al.* (1977) in $\pi^- p\rightarrow 2\pi+X$ at $p_{\rm lab}=40$ GeV/c, who find $r_\parallel=0.78\pm0.3$ fm and $r_\perp=1.3\pm0.3$ fm. In contrast, Loktionov *et al.* (1978) observe a source almost twice as long in the beam direction as in the perpendicular direction for the reaction $p\bar{p}\rightarrow 2\pi+X$ at $p_{\rm lab}=22.4$ GeV/c. In a higher-statistics experiment, Åkesson *et al.* (1987a) similarly find that $r_\parallel=1.82\pm0.17$ fm and $r_\perp=1.02\pm0.06$ fm in the reaction $pp\rightarrow 2\pi+X$ at $p_{\rm lab}=2100$ GeV/c.

In other studies, a "jet" axis is defined through kinematical cuts on the observed particles. Measurements of the correlation function are then made of the longitudinal and transverse dimensions (r_L and r_T) with respect to the jet axis, rather than the beam axis (the two axes are not necessarily coincident). One such study (Åkesson *et al.*, 1987b) shows no variation in the extracted radii in the reaction $pp\rightarrow 2\pi+X$ at $\sqrt{s}=63$ GeV: $r_L=0.93\pm0.07$ fm and $r_L=0.96\pm0.07$ fm.

High-statistics experiments have allowed extraction of

parameters for more restricted data sets that involve much less averaging over different event categories. In particular, it is hoped that multiplicity triggers will be able to provide data sets representing a narrower range of impact parameters. For example, Barshay (1983) associates an increase in N_{ch} with a decrease in impact parameter for elementary-particle interactions. Popular kinematic variables for relativistic events are the rapidity $y=(\frac{1}{2})\ln[(E+p_{\parallel})/(E-p_{\parallel})]$ or the pseudorapidity $\eta=-\ln\tan(\theta/2)$ (θ is the emission angle with respect to the beam axis). Events can be characterized by the charged-particle rapidity densities, $\Delta n/\Delta y$ or $\Delta n/\Delta\eta$.

In early work, Goossens *et al.* (1978) find that the incoherence parameter λ decreases with increasing multiplicity in the reaction $K^+p\rightarrow 2\pi+X$ at $p_{lab}=32$ GeV/c. In a high-statistics study of the reaction $pp\rightarrow 2\pi+X$ at $\sqrt{s}=31$, 44, and 62 GeV, Breakstone *et al.* (1987) find that the source size increases and the incoherence parameter decreases as a function of increasing $\Delta n/\Delta y$. This dependence of r_0 and λ on the charged-particle density $\Delta n/\Delta\eta$ has also been observed in the reaction $p\bar{p}\rightarrow 2\pi+X$ at $\sqrt{s}=630$ GeV by Albajar *et al.* (1989). An examination of Figs. 4(a)–4(d) shows that the source radii increase with increasing N_{ch}. Figure 5(a) shows more clearly the dependence of r_0 on $\Delta n/\Delta\eta$ at fixed c.m. energy $\sqrt{s}$. This trend has a simple interpretation, namely, that the source volume grows with the number of particles produced in a given reaction. Somewhat more surprising is the behavior of the incoherence parameter λ. Figure 5(b) shows the dependence of λ on the charged-particle rapidity density $\Delta n/\Delta\eta$ for the reaction $p\bar{p}\rightarrow 2\pi+X$ at $\sqrt{s}=630$ GeV (from Albajar *et al.*, 1989). Not only does λ decrease at high multiplicity, it is also small.

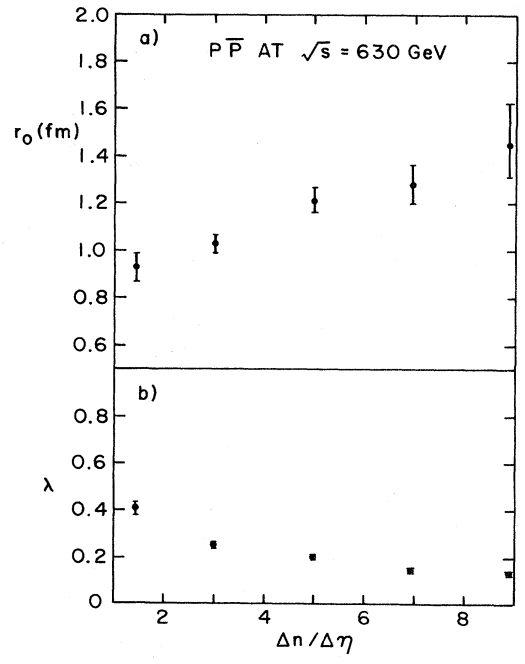

FIG. 5. Charged-particle density ($\Delta n/\Delta\eta$) dependence of (a) the extracted pion source dimension r_0 and (b) incoherence parameter λ for the reaction $p\bar{p}\rightarrow 2\pi+X$ at $\sqrt{s}=630$ GeV (after Albajar *et al.*, 1989).

B. Lepton-induced collisions

Data from lepton-induced reactions tend to be more limited than those from hadronic or nuclear reactions. Table III summarizes the available data; most investigations involve e^+e^- annihilation. Because of the small source sizes, the range of relative momenta **q** is large and the correlation function may be affected by particle resonance decay. Hence the Bose-Einstein contribution to the correlation function is more difficult to extract. Several analyses quoted in Table III use a model for hadron dynamics to simulate the strong-interaction and resonance-decay contributions to the correlation function, making the extracted source parameters less precise than would be expected from statistical errors alone. For example, the μp study by Arneodo *et al.* (1986) finds a considerable variability in extracted source parameter depending on how the hadronic contribution is handled; see Table III.

The measured correlations exhibit little sensitivity to the collision energy. Within errors, the extracted radius and incoherence parameters are constant. In general, measured radii are similar to those found in hadron-hadron collisions, but smaller than nucleus-nucleus collisions. The incoherence parameter values are similar as well, although the errors are large. Both Avery *et al.* (1985) and Juricic *et al.* (1989) argue that much of the deviation of λ from unity can be explained by resonance-decay effects.

Within large errors, Arneodo *et al.* (1986) find that the source is approximately spherical with respect to the direction of observation $\mathbf{P}=(\mathbf{p}_1+\mathbf{p}_2)$ as measured in μp collisions. Similar conclusions are reached for e^+e^- collisions by Aihara *et al.* (1985), Althoff *et al.* (1985), and Avery *et al.* (1985). These data have been analyzed in the string model context by Bowler (1985), and good agreement is found if decays of the η' resonance are neglected. Finally, it should be mentioned that both Althoff *et al.* (1985) and Juricic *et al.* (1989) perform analyses of pion triplets, although such correlations are not discussed in this review.

V. PARTICLE EMISSION IN HIGH-ENERGY NUCLEAR COLLISIONS

The use of interferometry in heavy-ion collisions began roughly a decade ago with the construction of the Bevalac accelerator complex at Lawrence Berkeley Laboratory. The first experiments (Fung *et al.*, 1978) were performed at beam kinetic energies per nucleon in the laboratory frame E/A in the 1.5–2.0-GeV range, and subsequent work has expanded the beam energies studied up to 200 GeV per nucleon and down to tens of MeV per nu-

TABLE III. Extracted Gaussian source dimensions for lepton-induced collisions. The measured values have been converted from the original analyses to equivalent values of r_0 as described in the text. Where two errors are quoted, the first is statistical and the second is systematic.

Reaction	$\sqrt{s}$ (GeV)	r_0 (fm)	λ
$\mu p \rightarrow 2\pi + X$[a]	23	0.65–1.19	0.60–1.08
$\nu(\bar{\nu})p \rightarrow 2\pi + X$[b]	<27	0.68±0.10	0.36±0.04
$e^+e^- \rightarrow 2\pi + X$[c]	3.095	1.09±0.03±0.06	0.69±0.03±0.06
$e^+e^- \rightarrow 2\pi + X$[c]	4.1–6.7	0.89±0.08±0.04	0.46±0.04±0.05
$e^+e^- \rightarrow 2\pi + X$[c]	29	1.06±0.04±0.06	0.28±0.02±0.04
$e^+e^- \rightarrow 2\pi + X$[d]	10.5	1.22±0.21	0.48±0.07
$e^+e^- \rightarrow 2\pi + X$[e]	29	0.92±0.06±0.07	0.61±0.05±0.06
$e^+e^- \rightarrow 2\pi + X$[f]	29–37	1.07±0.12	0.60±0.09

[a]Arneodo *et al.*, 1986.
[b]Allasia *et al.*, 1988.
[c]Juricic *et al.*, 1989 (unlike-sign reference set).
[d]Avery *et al.*, 1985.
[e]Aihara *et al.*, 1985.
[f]Althoff *et al.*, 1985.

cleon (see Sec. VII).

Studies at 400 MeV $< E/A <$ 1 GeV (Gustafsson *et al.*, 1984; Bock *et al.*, 1988; Dupieux *et al.*, 1988) are reported in Sec. V.A. These experiments use pions or protons to construct the two-particle correlation function. Extensive measurements involving predominantly pion pairs have been made at kinetic energies per nucleon of several GeV, using not only heavy-ion beams (Fung *et al.*, 1978; Angelov *et al.*, 1980; Lu *et al.*, 1981; Zarbakhsh *et al.*, 1981; Beavis *et al.*, 1983a, 1983b, 1986; Agakishiev *et al.*, 1984; Akhababian *et al.*, 1984; Zajc *et al.*, 1984; Liu *et al.*, 1986; Chacon *et al.*, 1988) but also *d* and He beams (Agakishiev *et al.*, 1984). These results and some aspects of their theoretical interpretation are presented in Sec. V.B.

Of particular theoretical interest are nucleus-nucleus collisions at ultrarelativistic energies $E/A > 100$ GeV, since such high-energy collisions may produce a plasma state of quarks and gluons. Unfortunately, existing experimental information at these energies is sparse. Section V.C contains a summary of experimental work published at the time of writing (Becker *et al.*, 1979; Åkesson *et al.*, 1983, 1985; De Marzo *et al.*, 1984; Bamberger *et al.*, 1988), as well as comparisons of these results with those from complementary elementary-particle reactions (discussed in Sec. IV). This subsection also contains theoretical interpretations of some of the results.

A. Collisions at 400 MeV $< E/A <$ 1 GeV

Experiments performed in the energy range $E/A = 400$ to 800 MeV use detectors with large-solid-angle coverage. Studies with equal-mass projectile and target nuclei have been performed with the Plastic Ball, which consists of 815 scintillator $\Delta E/E$ detectors covering the angular range of 9° to 160° in the laboratory frame (Gustafsson *et al.*, 1984; Bock *et al.*, 1988). Asymmetric mass systems have been investigated with Diogene, a cylindrically symmetric detector consisting of a pictorial drift chamber placed inside a magnetic field (Dupieux *et al.*, 1988). Charged particles are accepted in the angular range 20° to 132°. The Plastic Ball group has measured both two-proton and two-pion correlations, while the Diogene group has measured two-proton correlations only.

The two-pion correlation function is often fitted with a parametrization based on a stationary Gaussian-source density $\rho(r)$ of the form (Koonin, 1977; see Secs. III and VI)

$$\rho(\mathbf{r},t) = \frac{1}{\pi^2 r_0^3 \tau} \exp(-\mathbf{r}^2/r_0^2 - t^2/\tau^2) , \tag{5.1}$$

where the source parameter r_0 is a measure of the spatial dimension of the emitting region and the parameter τ is a measure of the source lifetime. Gustafsson *et al.* (1984) investigate the charged-particle multiplicity dependence of the correlation function for the reactions Ca+Ca and Nb+Nb at $E/A = 400$ MeV. By suitable kinematic cuts on the transverse momentum of the light particles (with respect to the beam direction), they obtain a quantity N_p which is approximately the charged-baryon multiplicity in the participant region. The participant region is defined as that part of phase space most likely to be filled by particles undergoing substantial momentum changes during the reaction, as opposed to the spectator region, which is close to the beam or target momentum per particle. In their fits, Gustafsson *et al.*, (1984) neglect the τ dependence in Eq. (5.1). The dependence of r_0 on N_p is shown in Fig. 6. The extracted radius parameter exhibits a slow increase as a function of multiplicity that is found to be consistent with an $N_p^{1/3}$ dependence on multiplicity. From this dependence the authors estimate that the reaction products "freeze out" (i.e., pass out of equilibrium) at a density of roughly 25% of normal nuclear matter density. As shown elsewhere in this section, this increase with multiplicity is often, but not always, seen experimentally.

Dupieux *et al.* (1988) extract zero-lifetime Gaussian radii for Ne-induced reactions on a variety of targets at $E/A = 400$ and 800 MeV. These radii, listed in Table IV, increase slowly with target mass in both energy ranges. Further, the radii either decrease or remain un-

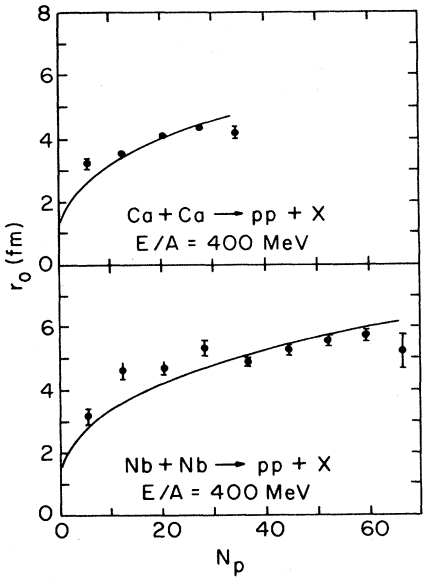

FIG. 6. Extracted Gaussian radii as a function of charged-baryon multiplicity, N_p, for the reactions Ca+Ca and Nb+Nb at $E/A=400$ MeV. The solid curves are proportional to $N_p^{1/3}$ (from Gustafsson *et al.*, 1984).

changed with increasing bombarding energy. Finally, the authors report that the radii do increase with multiplicity. However, for their published results, multiplicity and target change simultaneously and the systematic dependence on multiplicity for fixed target mass is not explored. A direct comparison with the results of Gustafsson *et al.* (1984) is therefore difficult.

Studies involving $\pi^+\pi^+$ correlations have also been done in this energy range (Bock *et al.*, 1988), although the average pion multiplicity per event is lower than those reported in Secs. V.B and V.C. The authors fit their measurements with a four-parameter function that includes a dependence on both the relative momentum $\mathbf{q}=(\mathbf{p}_1-\mathbf{p}_2)/2$ and the energy $q_0=(E_1-E_2)/2$ of the pion pair:

$$C(\mathbf{q},q_0)=C_\infty[1+\lambda\exp(-2r_0^2\mathbf{q}^2-2\tau^2q_0^2)] . \quad (5.2)$$

The correlation $C(\mathbf{q},q_0)$ is equal to $R(\mathbf{q},q_0)+1$ and C_∞ is a normalization constant. The Gaussian-source radii extracted by their method are shown in Table IV. They are similar to those determined by Dupieux *et al.* (1988). In contrast to the *pp* correlations measured by the Plastic Ball, the $\pi\pi$ radii do not show a charged-particle multiplicity dependence in this experiment, remaining relatively constant (within errors) over a substantial change in multiplicity.

The extracted source radii exhibit a pronounced dependence on the total momentum of the pion pair; see Table V. The correlations become stronger with increasing pion momentum in the projectile/target center-of-mass frame, leading to smaller apparent source sizes. For the Au+Au reaction the effect is dramatic. However, extracted source dimensions of the order of 1 fm are difficult to understand for such large collision partners. Strong dependence of the extracted source size on the total momentum of the particle pair has been noted for many different systems.

TABLE IV. Extracted Gaussian source dimensions for a variety of heavy-ion reactions with $E/A<1$ GeV.

Reaction	E/A (MeV)	r_0 (fm)
Ne+C→$2p+X$[a]	400	3.3±0.2
Ne+NaF→$2p+X$[a]	400	3.3±0.2
Ne+Nb→$2p+X$[a]	400	3.6±0.2
Ne+Pb→$2p+X$[a]	400	4.1±0.2
Nb+Nb→$2\pi^++X$[b]	650	3.4±0.4
Au+Au→$2\pi^++X$[b]	650	4.8±0.6
Ne+C→$2p+X$[a]	800	2.5±0.2
Ne+NaF→$2p+X$[a]	800	2.7±0.2
Ne+Nb→$2p+X$[a]	800	3.8±0.2
Ne+Pb→$2p+X$[a]	800	4.2±0.2

[a]Dupieux *et al.*, 1988.
[b]Bock *et al.*, 1988.

B. Relativistic collisions

Historically, the first correlation measurements performed with heavy-ion projectiles were done at kinetic energies per nucleon in the 1–2-GeV region. The detectors used in this region have generally been of the 4π type: streamer chambers or bubble chambers. Most experiments have measured correlations of π^- pairs, although there have been some measurements with π^+ pairs and proton pairs. Data now exist for a sufficiently large number of projectile-target combinations to allow the exploration of systematic effects.

However, several cautionary notes are in order. Since the extracted source parameters may depend upon the particle multiplicity of the event and the total momentum of the measured pair, meaningful comparisons between or within data sets must take these complications into account. Built-in biases from the detector or analysis technique can affect the extracted source param-

TABLE V. Extracted Gaussian source dimensions from the spatial dependence of the correlation function as a function of the pion momentum in the projectile/target c.m. frame for the reactions at $E/A=650$ MeV, as indicated (Bock *et al.*, 1988).

Reaction	Momentum range (MeV)	r_0 (fm)
Nb+Nb	0–80	4.6±0.6
	80–160	4.4±1.4
	160–350	3.2±1.3
Au+Au	0–80	10.7±1.2
	80–160	2.0±0.5
	160–350	1.0±0.2

eters. With these caveats in mind we examine the results that have been obtained thus far.

Table VI gives a summary of the equivalent Gaussian-source radii obtained from analysis of two-pion correlations in heavy-ion reactions at $E/A \approx 1.5-5$ (Fung *et al.*, 1978; Angelov *et al.*, 1980; Beavis *et al.*, 1983a; Agakishiev *et al.*, 1984; Akhabadian *et al.*, 1984; Zajc *et al.*, 1984; Chacon *et al.*, 1988). In most analyses, the data are first corrected for Coulomb effects and then the parameters are determined by fitting the correlation function with a simple functional form such as Eq. (5.2). An example is shown in Fig. 7, taken from Beavis *et al.* (1983a). The top and bottom parts of the figure show the uncorrected and corrected experimental correlation functions. The solid curves show fits with Eq. (5.2). Rather similar source dimensions are extracted from the corrected and uncorrected correlation functions, the major difference being the magnitudes of the parameter λ. For more details, see Beavis *et al.* (1983a). In other cases the data were fitted with the Kopylov-Podgoretskii formulation of a radiating disk or sphere (see Sec. III). In such instances the Gaussian parameters quoted in Table VI correspond to distributions with the same rms radii as the radiating disks or spheres. Compilations of equivalent rms radii, rather than Gaussian parameters, can be found in Bartke and Kowalski (1984), Bartke

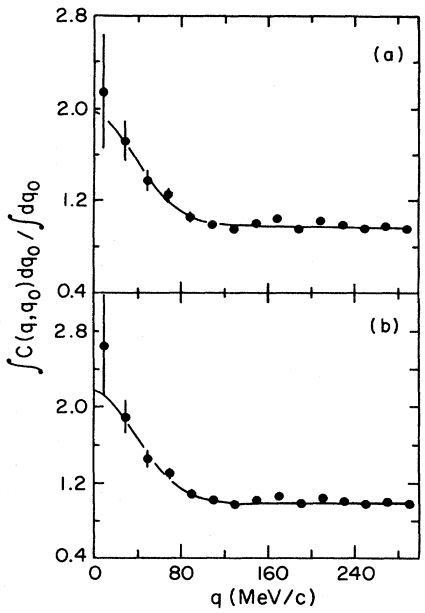

FIG. 7. Correlation function $C(\mathbf{q},q_0)$ for Ar+KCl collisions at $E/A=1.5$ GeV integrated over q_0. (a) Correlation function without Coulomb correction; (b) correlation function corrected for Coulomb effects using Eq. (3.36). The solid curves show calculations with Eq. (5.2) (after Beavis *et al.*, 1983a).

TABLE VI. Gaussian source dimensions extracted from two-pion correlations at kinetic energies in the range $1 < E/A < 4$ GeV.

Reaction	E/A (MeV)	r_0 (fm)	$c\tau$ (fm)	λ
C+C→$2\pi^-+X$[a]	3.4	2.3±0.6		
C+C→$2\pi^-+X$[a] (central)	3.4	3.1±0.7		
d+Ta→$2\pi^-+X$[b]	3.4	1.8±0.4		
α+Ta→$2\pi^-+X$[b]	3.4	2.4±0.3		
α+Ta→$2\pi^+ +X$[b]	3.4	2.0±.4		
C+Ta→$2\pi^-+X$[b]	3.4	2.8±0.3		
C+Ta→$2\pi^+ +X$[b]	3.4	2.3±0.3		
Ne+NaF→$2\pi^-+X$[c]	1.8	$1.8^{+0.8}_{-1.6}$	$3.0^{+0.9}_{-1.0}$	0.59±0.06
Ar+KCl→$2\pi^-+X$[c]	1.8	$2.9^{+0.5}_{-0.9}$	$3.3^{+1.4}_{-1.6}$	0.63±0.04
Ar+KCl→$2\pi^+ +X$[c]	1.8	$4.2^{+0.4}_{-0.5}$	$1.5^{+2.4}_{-1.5}$	0.69±0.06
Ar+KCl→$2\pi^-+X$[d]	1.5	4.7±0.5	$4.2^{+1.8}_{-4.2}$	1.2±0.2
Ar+KCl→$2\pi^-+X$[e]	1.2	3.8±0.5	5.4±1.8	0.74±0.17
Ar+BaI_2→$2\pi^-+X$[f]	1.8	3.1±1.1		
Ar+Pb_3O_4→$2\pi^-+X$[f]	1.8	3.3±0.9		
Ar+Pb_3O_4→$2\pi^-+X$[f] (central)	1.8	4.0±0.8		
Ar+Pb→$2\pi^-+X$[g]	1.8	5.5±0.4	0.0±2.5	0.99±0.13
Fe+Fe→$2\pi^-+X$[h]	1.5	4.0±0.5	1.7±1.7	0.66±0.05

[a]Akhabadian *et al.*, 1984.
[b]Agakishiev *et al.*, 1984.
[c]Zajc *et al.*, 1984.
[d]Beavis, *et al.*, 1983a (quoted in Beavis, *et al.*, 1983b).
[e]Beavis *et al.*, 1983b.
[f]Fung *et al.*, 1978.
[g]Beavis *et al.*, 1986.
[h]Chacon *et al.*, 1988 (quoted in Zajc, 1987b).

(1986), and Zajc (1987b).

A number of trends are worth noting. In general, the source dimensions increase with target or projectile mass. This can be seen in the work of Agakishiev *et al.* (1984) for various projectiles on a tantalum target and by the work of Zajc *et al.* (1984) for the reactions Ne+NaF and Ar+KCl. Similar trends emerge from other experimental work, but the error bars are too large to allow definitive conclusions. It should also be pointed out that not all of the data are fit with the same formula: in some cases the lifetime parameter is either omitted or set equal to a fixed value.

The source dimensions tend to increase for central collisions (i.e., collisions at small impact parameter). Detailed evidence of this trend is presented by Lu *et al.* (1981), who have examined the dependence of the radii on pion multiplicity in the reaction ^{40}Ar+Pb at $E/A=1.8$ GeV. Their results are shown in Fig. 8, in which the Gaussian-source parameter from $2\pi^-$ correlations is plotted against negative-pion multiplicity N_{π^-}. For comparison we have plotted the function $r_0=2.2(N_{\pi^-})^{1/3}$ (fm) to show the power-law dependence of r_0. The data are consistent with a $(N_{\pi^-})^{1/3}$ dependence, although other powers cannot be ruled out.

In Sec. V.A we discuss the dependence of r_0 on the total momentum of the particle pair used to form the correlation function. A similar dependence appears to be present here as well. Beavis *et al.* (1983a) find $r_0=6.0\pm1.1$ fm if both pions have a momentum (in the target/projectile c.m. frame) of less than 150 MeV/c, and this decreases to 4.1 ± 0.5 fm for momenta greater than 150 MeV/c (the incoherence parameter λ changes from 1.6 ± 0.5 to 0.9 ± 0.2 for the same momentum cuts).

A number of investigations have explored the source dimensions in directions parallel and perpendicular to the beam axis. The results reported by different groups are difficult to reconcile. Beavis *et al.* (1983a) and Chacon *et al.* (1988) rewrite Eq. (5.2) in the form

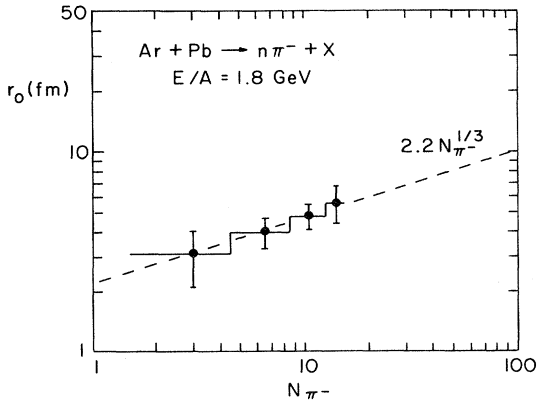

FIG. 8. Extracted Gaussian radii as a function of negative-pion multiplicity N_{π^-} for the reaction Ar+Pb$\rightarrow n\pi^-+X$ at $E/A=1.8$ GeV (data are from Lu *et al.*, 1981). Shown for comparison is the function $f(r_0)=2.2(N_{\pi^-})^{1/3}$ (fm).

$$C(\mathbf{q},q_0)=C_\infty[1+\lambda\exp(-2r_\parallel^2q_\parallel^2-2r_\perp^2q_\perp^2-2\tau^2q_0^2)]\ , \tag{5.3}$$

where r_0 has been replaced by two new parameters, $r_\parallel$ and $r_\perp$. The directions of $\mathbf{q}_\parallel$ and $\mathbf{q}_\perp$ are parallel and perpendicular to the beam, respectively. For the reaction Ar+KCl at $E/A=1.5$ GeV, Beavis *et al.* (1983a) find a spherical source: $r_\parallel=5.0\pm1.5$ and $r_\perp=5.0\pm1.5$ fm. On the other hand, Chacon *et al.* (1988) find a longitudinally contracted source $r_\parallel=1.5(+0.7/-1.5)$ and $r_\perp=4.6\pm0.2$ fm for the reaction Fe+Fe at $E/A=1.7$ GeV. The fitting procedure used by the two groups is slightly different: Chacon *et al.* allow the lifetime parameter to vary, whereas Beavis *et al.* fix it at 1.5 fm/c.

An attempt has been made by Humanic (1986) to use a computer simulation largely based upon classical mechanics to predict the pion source distribution. In general, the results of the simulation for averaged values of r_0 and τ are in fair agreement with the data, considering the errors in the data and the uncertainties in the simulation. The simulations predict that the sources in the reactions Ne+NaF at $E/A=1.8$ GeV and Ar+KCl at $E/A=1.2$–1.8 GeV should be isotropic within errors.

An experiment that measures both the longitudinal extension of the source and its dependence on the total momentum of the outgoing pair of particles has been performed by Beavis *et al.* (1986) for the reaction Ar+Pb at $E/A=1.8$ GeV. Events in which the c.m. momentum of the pion pair $\mathbf{P}=\mathbf{p}_1+\mathbf{p}_2$ is within a certain range are collected and analyzed according to Eqs. (5.2) and (5.3) separately. Their results are shown in Table VII. The average of P for the three momentum bins used is shown in the first column, while the results from the fits are shown in the remainder of the table. Looking first at the isotropic source fits, one can see the usual decrease in apparent source size with increasing particle pair energy. Further, the best fits from an anisotropic source parametrization indicate a source slightly elongated in the beam

TABLE VII. Gaussian source parameters extracted from the reaction Ar+Pb$\rightarrow2\pi^-+X$ at $E/A=1.8$ GeV. The parameters are shown as a function of the expectation of P, where $P=|\mathbf{p}_1+\mathbf{p}_2|$ is the momentum of the pion c.m. system (from Beavis *et al.*, 1986). The radii are quoted in fm.

$\langle P\rangle$ (MeV/c)	Isotropic source parameters	Anisotropic source parameters
203.6	$r_0=5.7\pm0.6$ $\lambda=0.96\pm0.18$	$r_\parallel=6.6\pm0.9$ $r_\perp=5.4\pm0.7$ $\lambda=1.03\pm0.21$
387.6	$r_0=5.7\pm0.6$ $\lambda=1.28\pm0.27$	$r_\parallel=5.9\pm0.8$ $r_\perp=6.2\pm0.8$ $\lambda=1.31\pm0.30$
645.8	$r_0=3.2\pm0.6$ $\lambda=0.68\pm0.23$	$r_\parallel=3.1\pm0.7$ $r_\perp=2.4\pm0.5$ $\lambda=0.49\pm0.15$

direction. However, within experimental errors, the results cannot exclude a spherical source.

Correlations among three pions have been studied by Liu *et al.* (1986) for the reactions $Ar+Pb_3O_4$ at $E/A=1.8$ GeV and Ar+KCl at $E/A=1.5$ GeV. The analysis was performed using a formalism developed by Biyajima (1980, 1981). Within experimental errors, the source radii extracted in the three-pion analysis agree with those found in the two-pion analysis of the same reactions.

Finally, we should mention the two-proton correlation measurement of Zarbakhsh *et al.* (1981) for the reaction Ar+KCl at $E/A=1.8$ GeV. They extract Gaussian-source radii in two regions of $p_\parallel$, the parallel component of the proton's momentum. For $p_\parallel$ near the beam momentum per nucleon, they find $r_0=2.2$ fm, which has a corresponding sharp sphere radius of 3.5 fm, similar to that of an Ar nucleus. For $p_\parallel$ near zero in the Ar+KCl c.m. frame, however, the value of r_0 *decreases* to 1.8 fm. If a sample multiplicity of five or more particles is placed on the events, the value of r_0 near zero c.m. momentum is reduced even further, to 1.5 fm. These results would not seem to be consistent with the picture of a large thermalized region being produced in the central region of a high-multiplicity event; the effect is not yet understood.

Experiments in this energy range find that the extracted source size decreases with increasing energy of the particle pair. As is shown in Sec. VII, similar observations are made at much lower bombarding energies as well. Taken at face value, this observation indicates that energetic particles are emitted from small sources early in the reaction. Given the computer simulation studies performed at lower energies (see, for example, Boal, 1987), such expansion is likely to take place in these reactions. However, the interpretation is not unique. Pratt (1984) has shown that a time-dependent expanding source can also give rise to such an energy dependence.

C. Ultrarelativistic collisions

Because of the large pion multiplicities produced at ultrarelativistic energies, typical experiments are designed to have the capability of measuring many particles simultaneously. For example, the NA35 group (Bamberger *et al.*, 1988) working at CERN uses a streamer chamber as a detector and records the track images on film. For the experimental gates of interest in their interferometry studies, this group uses events with π^- multiplicities on the order of 100. At such high multiplicities relatively few events suffice for the construction of a correlation function: less than 100 events are analyzed for the O+Au reactions at $E/A=200$ GeV. The number of two-pion pairs that can be constructed with 100 particles is sufficiently high that one can contemplate performing analyses with individual events.

We begin our discussion of reactions at ultrarelativistic energies with proton-induced reactions. De Marzo *et al.* (1984) have performed measurements of proton and antiproton reactions with H, Ne, Ar, and Xe targets at 200 GeV bombarding energy. Table VIII shows the parameters extracted for the hydrogen and xenon targets. De Marzo *et al.* use a modified Kopylov-Podgoretskii parametrization (see Sec. III):

$$R(\mathbf{p}_1,\mathbf{p}_2)=\lambda_1[2J_1(2q_TR_{\rm KP})/(2q_TR_{\rm KP})]^2/[1+(2q_0\tau)^2]\ , \tag{5.4}$$

where our definitions of $\mathbf{q}=(\mathbf{p}_1-\mathbf{p}_2)/2$ and $q_0=(E_1-E_2)/2$ remain as before and $\mathbf{q}_T$ is the component of $\mathbf{q}$ which is perpendicular to the two-particle c.m. momentum $\mathbf{P}=\mathbf{p}_1+\mathbf{p}_2$ (note that this $\mathbf{q}$ is half that used by Kopylov and Podgoretskii and many of the papers that use their formalism). We convert the radius $R_{\rm KP}$ in Eq. (5.4) to its equivalent r_0 value by using $r_0=R_{\rm KP}/\sqrt{2}$ (see Sec. III.B). The radii in Table VIII show little dependence on target, being roughly constant at 1.1 fm for both hydrogen and xenon targets. Similarly small radii are found from the measurements of Becker *et al.* (1979) for proton-induced reactions on nuclear targets at 28.5 GeV/c bombarding momentum. Larger radii, $r_0=2.6\pm0.6$ fm, are extracted by Angelov *et al.* (1981) for the reaction $\pi^-+C\rightarrow 2\pi^-+X$ at 40 GeV/c pion bombarding momentum (the parameters quoted in the original paper have been converted to equivalent Gaussian radii). Azimov *et al.* (1984) examine the dependence of r_0 on particle pair momentum $\mathbf{P}=\mathbf{p}_1+\mathbf{p}_2$ for the reaction $p+Ne$ at $p_{\rm lab}=300$ GeV/c. They find that r_0 increases with decreasing $\mathbf{P}$, similar to what is found in the heavy-ion reactions discussed previously, although their statistics do not allow an accurate determination of r_0.

The Axial Field Spectrometer group (Åkesson *et al.*, 1983, 1985) have measured both pion and kaon correlations from a variety of reactions: $p+p$ at $\sqrt{s}=63$ GeV, $p+\bar{p}$ at $\sqrt{s}=53$ GeV, and $\alpha+\alpha$ at $\sqrt{s}=126$ GeV (where $\sqrt{s}$ is the total energy in the c.m. system). For the $\alpha+\alpha$ reaction, the results for high-multiplicity gates

TABLE VIII. Source parameters from ultrarelativistic collisions ($E/A>100$ GeV). Several different parametrizations have been used in the data analysis. The value quoted for r_0 corresponds to the Gaussian distribution with the same rms radius as the original fits to the data.

Reaction	r_0 (fm)	λ_1	λ_2
$p+p\rightarrow 2\pi+X$[a]	1.17±0.03	0.96±0.08	
$\bar{p}+p\rightarrow 2\pi+X$[a]	1.07±0.06	1.30±0.20	
$p+Xe\rightarrow 2\pi+X$[a]	1.08±0.09	1.27±0.11	
$\bar{p}+Xe\rightarrow 2\pi+X$[a]	1.04±0.08	1.34±0.08	
$\alpha+\alpha\rightarrow 2\pi+X$[b] (high multiplicity)	1.8±0.3		0.16±0.04
$\alpha+\alpha\rightarrow 2K+X$[b] (high multiplicity)	1.6±0.4		0.60±0.28

[a]De Marzo *et al.*, 1984.
[b]Åkesson *et al.*, 1983, 1985.

are included in Table VIII. The source size increases with charged-particle multiplicity. It is interesting to note that the radii extracted from KK correlations are similar to those found from $\pi\pi$ analyses at similar multiplicity gates.

The NA35 experiment has measured both O+Au and S+S reactions at $E/A=200$ GeV, although only results from the O+Au reaction have appeared in the literature at the time of this writing. The group has analyzed their two-pion correlation functions using the conventional Gaussian source parametrization, as well as the Kolehmainen-Gyulassy (1986) formulation. For ease of comparison with results quoted in the other sections of this review we quote only the parameters extracted with the Gaussian source. The correlation functions measured by NA35 are fitted with three parameters: $r_\perp$, $r_\parallel$, and the incoherence parameter λ. The perpendicular and parallel radii $r_\perp$ and $r_\parallel$ correspond to directions with respect to the beam axis. The analysis is carried out using the rapidity, $y=(\frac{1}{2})\ln[(E+p_\parallel)/(E-p_\parallel)]$, of the particle pair as an experimental gate. The results for several ranges of y are shown in Table IX.

The emitting source is approximately spherical in shape, although it tends to be somewhat larger in the transverse direction than it is in the longitudinal direction. This behavior is not too different from that observed by Beavis *et al.* (1986); see Table VII. The source is largest for the intermediate rapidity region $2<y<3$. For a comparison of the rapidity scale, Bamberger *et al.* (1988) point out that a system composed of 16 oxygen nucleons and 50 gold nucleons from the geometrical overlap region has a rapidity of 2.5.

In this midrapidity region, the source is large—as is the number of negative pions per unit rapidity ($dN_{\pi^-}/dy\approx 35-40$). Taken together these results imply that a source with many pions is formed at midrapidity. The incoherence parameter λ appears to be larger in this rapidity region as well, compared with the regions nearer the beam and target rapidity. It should be emphasized that the event sample has a "centrality trigger" based on the energy flow into the projectile fragmentation region.

Possible relationships between two-pion correlations in ultrarelativistic collisions and the formation and decay of the QCD plasma state have been investigated by Lopez, Parikh, and Siemens (1984), Pratt (1986b), Bertsch, Gong, and Tohyama (1988), Gyulassy and Padula (1988), Hama and Padula (1988), and Bertsch (1989). The use of dilepton interferometry as a probe of the QCD plasma is discussed by Makhlin (1987). Bertsch, Gong, and Tohyama (1988) have made first quantitative predictions of the source characteristics for the NA35 results using a simulation of the mixed plasma/hadron phase. Gyulassy and Padula (1988) have compared several different simulation models to investigate the characteristics of the source: the inside-outside cascade model (Kolehmainen and Gyulassy, 1986), the resonance-gas-decay model and the Bertsch-Gong-Tohyama (1988) model. They conclude that none of the models can be ruled out by the present data set.

TABLE IX. Source parameters extracted from the reaction $^{16}O+Au\rightarrow 2\pi^-+X$ at $E/A=200$ GeV with a small impact-parameter gate. The fits are performed over several ranges of rapidity y for the pions. The perpendicular and parallel directions are with respect to the beam (from Bamberger *et al.*, 1988).

Rapidity interval	$r_\perp$ (fm)	$r_\parallel$ (fm)	λ
$1<y<4$	4.1 ± 0.4	$3.1^{+0.7}_{-0.4}$	$0.31^{+0.07}_{-0.03}$
$1<y<2$	4.3 ± 0.6	2.6 ± 0.6	$0.34^{+0.09}_{-0.06}$
$2<y<3$	8.1 ± 1.6	$5.6^{+1.2}_{-0.8}$	0.77 ± 0.19
$3<y<4$	$4.3^{+1.2}_{-0.8}$	5.8 ± 2.2	0.55 ± 0.20

The application of interferometry in plasma studies lies in determining the time scale for conversion of the plasma phase to hadrons (Pratt, 1986b; Bertsch, 1989). The idea is to measure the source size along two directions of **q** perpendicular to the beam axis. The "outward" direction is parallel to the pair momentum **P** when a frame is chosen such that **P** is perpendicular to the beam axis. The "sideways" direction is perpendicular to both the emission direction and the beam. A long lifetime for plasma-to-hadron phase conversion should make the apparent size in the outward direction much larger than in the sideways direction.

In this context a comparison with two-pion correlations measured in $p\bar{p}$ collisions by the UA1 collaboration (Albajar *et al.*, 1989, discussed in Sec. IV) is of interest. Although the mean multiplicity of the $p\bar{p}$ reaction is much lower than that of the O+Au reaction, a similar functional dependence of the extracted source radii on the charged-particle multiplicity per unit rapidity $\Delta n/\Delta y$ is observed for both data sets; see Fig. 9 (Albajar *et al.*, 1989; for the heavy-ion reactions, $\Delta n/\Delta y$ is assumed to be twice $\Delta N_{\pi^-}/\Delta y$). The straight line through the data is drawn to guide the eye; it suggests that the behavior of the source radii might be related. The incoherence parameters λ, extracted for the two reactions, are also shown in Fig. 9. Given the large statistical uncertainties of the NA35 data, no simple trend is apparent. Nevertheless, it is clear that a solid understanding of the relation between extracted source radii and $\Delta n/\Delta y$ must be in hand before any hard conclusions can be drawn about QCD plasma formation.

VI. FINAL-STATE INTERACTIONS AND RESONANCE DECAY

In the pion emission models discussed in Sec. III, strong-interaction effects are usually neglected because of the weakness of the $I=2\pi\pi$ phase shift (see Suzuki, 1987, and Bowler, 1988). For proton and cluster emission, however, there are resonances at low excitation energy that can have significant effects on the shape of the correlation function. Calculations incorporating strong final-state interactions have been performed by Koonin (1977)

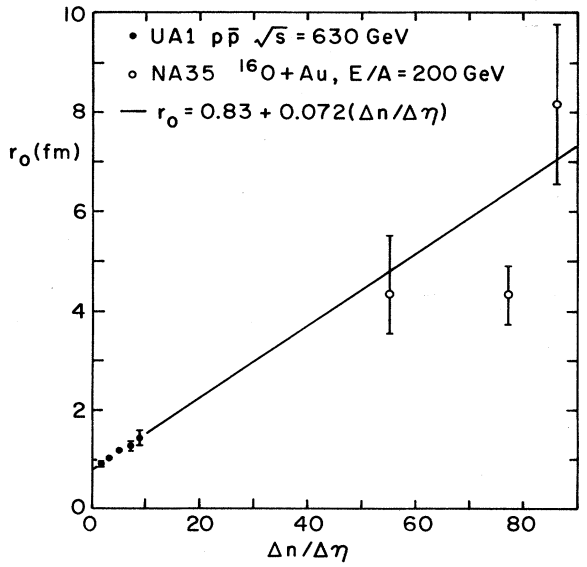

FIG. 9. Extracted Gaussian source radius r_0 as a function of charged-particle multiplcity per unit rapidity $\Delta n/\Delta\eta$ for high-energy reactions. Data are shown for $p\bar{p}$ reactions at $\sqrt{s}=630$ GeV (Albajar *et al.*, 1989) and O+Au at $E/A=200$ GeV (Bamberger *et al.*, 1988). The negative-pion multiplicities of Bamberger *et al.* have been multiplied by 2 to obtain a charged-particle multiplicity (from Albajar *et al.*, 1989).

for proton-proton correlations, by Chitwood *et al.* (1985), Boal and Shillcock (1986), Jennings, Boal, and Shillcock (1986), and Pochodzalla, Chitwood, *et al.* (1986) for a variety of particle pairs, and by Sato and Yazaki (1980) for $\alpha\alpha$ pairs. The predicted correlation functions are discussed in Sec. VI.A. Formalisms for handling two-particle final-state interactions in correlation functions are discussed in Sec. III.D.

Correlation functions can also provide information on the lifetime of the emitting region. However, statistically limited data sets have not allowed this aspect of the HBT effect to be exploited to its fullest. Consequences of the source's time evolution (Koonin, 1977; Boal and DeGuise, 1986; Pratt and Tsang, 1987) are discussed in Sec. VI.B. Contributions from resonance and compound nuclear decays (Grishin, Kopylov, and Podgoretskii, 1971a, 1971b; Kopylov and Podgoretskii, 1971, 1972; Kopylov, 1972; Grassberger, 1977; Thomas, 1977; Bernstein and Friedman, 1985; Koonin, Bauer, and Schäfer, 1989) are treated in Sec. VI.C.

The correlations due to final-state interactions depend on the nature of the source, which is the main focus of this review, and on the nature of the final-state interactions themselves. Indeed, we show in Sec. IV.A that certain deuteron-deuteron potentials are ruled out by the correlation function data. Peaks in the relative momentum distribution of a two-body system can given information on the existence, energy, and width of resonances. A perusal and the Review of Particle Properties (Particle Data Group, 1988) shows that much of the information on meson resonances comes from final-state interaction correlations. However, this topic is far removed from our main interest and we do not discuss it further in this review.

A. Strong-interaction effects

Almost all of the particles used to form correlation functions in nuclear reaction studies are charged and possess strong interactions. At the very least, Coulomb interactions must be taken into account when analyzing measured correlation functions. To illustrate the magnitude of the Coulomb effects we show in Fig. 10 the predicted correlation functions for *nonidentical* particle pairs emitted from a zero-lifetime Gaussian source and subject only to their mutual Coulomb interaction (Boal and Shillcock, 1986). Because these particles are not identical, there is no correlation arising from symmetrization. One can see that the range in $\mathbf{q}$ over which the Coulomb interaction manifests itself is significant: 10–20 MeV/c for hydrogen isotopes and even larger for helium isotopes. The curves for each particle pair are labeled by their Gaussian-source parameter r_0, and one can see that the correlation function becomes more negative as the size of the source decreases, as one would expect.

Koonin (1977) parametrizes the source distribution as a Gaussian distribution in space and time, so that the two-proton correlation function is

$$R(\mathbf{p}_1,\mathbf{p}_2)=\frac{1}{(2\pi)^{3/2}r_0^2 d}\int d^3r\,\exp\{-[r^2-(\mathbf{r}\cdot\mathbf{V}'\tau/d)^2]/2r_0^2\}[\tfrac{1}{4}|^1\psi_q(\mathbf{r})|^2+\tfrac{3}{4}|^3\psi_q(\mathbf{r})|^2-1]\ , \tag{6.1}$$

where $\mathbf{V}'=\mathbf{V}-\mathbf{V}_0$ is the difference between the velocity of the two-proton c.m. position $\mathbf{V}$ and the source velocity $\mathbf{V}_0$. The other quantities have the same definitions as in Eq. (3.12): $\mathbf{q}=(\mathbf{p}_1-\mathbf{p}_2)/2$ and $d=[r_0^2+(V'\tau)^2]^{1/2}$. The superscript on the wave function ψ is $2s+1$ and is used to indicate the spin state s of the two protons: 0 or 1. The weighting factors of $\frac{1}{4}$ and $\frac{3}{4}$ assume that the pairs are emitted with statistical probability (i.e., the dynamics does not favor a particular spin state). Typically, the wave functions in Eq. (6.1) are obtained by numerically integrating Schrödinger's equation. These numerical wave functions are themselves integrated over to obtain the correlation function. This procedure usually takes less than a minute on a fast computer to obtain numerically accurate results.

Koonin (1977) has investigated the effects on the corre-

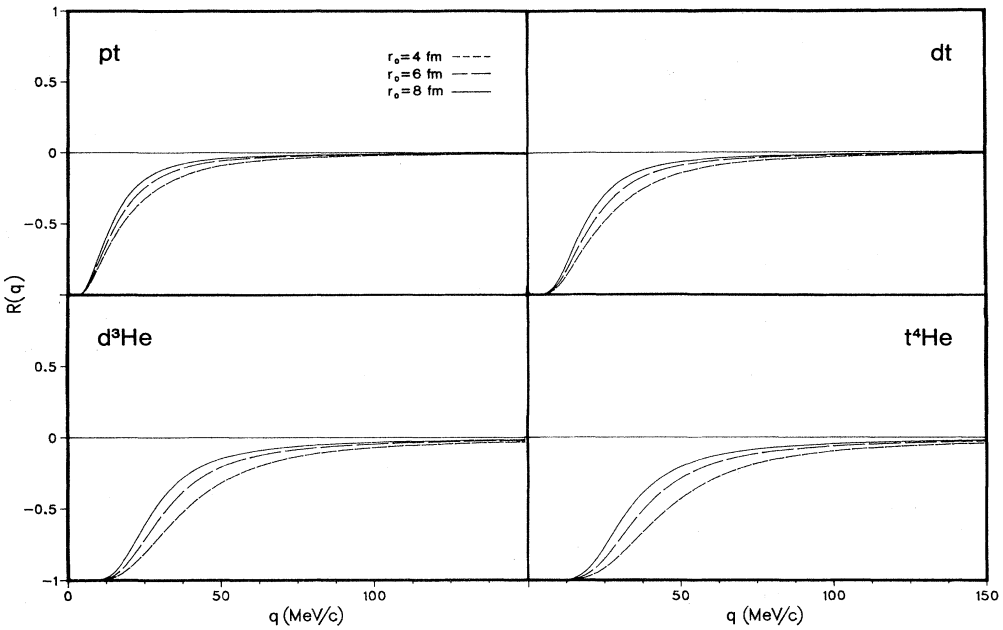

FIG. 10. Coulomb contributions to nonidentical particle correlation functions (from Boal and Shillcock, 1986).

lation function of several potentials for the proton-proton interaction. He finds that for the source sizes typically of interest, the correlation function is mainly determined by the Coulomb interaction and the s-wave strong interaction. Most calculations of two-proton correlations follow Koonin's prescription of using the Reid soft-core potential (Reid, 1968). This potential shows an enhancement in the correlation function around $q \approx 20$ MeV/c. A sample of the predicted zero-lifetime correlation function using the Koonin formulation is shown in Fig. 11 for a number of source radii (Boal and Shillcock, 1986). Shown for comparison is a measurement of the two-proton correlation function for the reaction $^{16}O+^{197}Au$ at $E/A=25$ MeV (Lynch *et al.*, 1983). One can see that the Reid soft-core potential provides a good description of the data (see also Fig. 16 below).

The strong interaction of two deuterons is more complicated than that of two protons. First of all, the spin of the *dd* system has three values: 0, 1, and 2. Hence, the zero-lifetime correlation function must be written as

$$R(\mathbf{p}_1,\mathbf{p}_2)=(2\pi r_0^2)^{-3/2}\int d^3r\,\exp(-r^2/r_0^2)[\tfrac{1}{9}|^1\psi_q(\mathbf{r})|^2+\tfrac{1}{3}|^3\psi_q(\mathbf{r})|^2+\tfrac{5}{9}|^2\psi_q(\mathbf{r})|^2-1]\ , \tag{6.2}$$

where the superscripts on the wave functions are equal to $2s+1$, as before. There are two partial-wave fits to the *dd* differential cross section, one performed using a coupled-channel R-matrix (RM) approach (Hale and Dodder, 1984) and one using a resonating group (RG) approach (Chwieroth *et al.*, 1972). Calculations based on both sets of phase shifts are shown in Fig. 12. The resonant structure at $q \approx 30$ MeV/c predicted by the RG phase-shift set does not appear to be supported by the data (see Fig. 24 below).

The phase shifts can be generated from Woods-Saxon potentials for each partial wave:

$$V(r)=V_{\rm WS}/\{1+\exp[-(r-R)/a]\}\ , \tag{6.3}$$

where $V_{\rm WS}$, R, and a are parameters. The values of these parameters for the RM phase shifts are shown in Table X (Chitwood *et al.*, 1985). A negative sign for $V_{\rm WS}$ in the table indicates an attractive potential term. Since most of the partial-wave potentials are observed to be repulsive, one expects that $R(\mathbf{p}_1,\mathbf{p}_2)$ should become more negative as the source size decreases. The calculations in the figure verify this behavior.

The spin structure of the triton-triton correlation function is identical in form to the proton-proton correlation function, Eq. (6.1). However, the interaction between tritons is less well known experimentally. The calculated *tt* correlation function shown in Fig. 12 uses only the Coulomb interaction between tritons. Calculations based on unpublished s-wave phase-shift analysis (G. M. Hale, private communication) have been performed (Pochodzalla, Chitwood, *et al.*, 1986) with the s-wave Woods-Saxon potential parameters given in Table X. Since the s-wave potential in the table is repulsive, one finds that the calculated value for $R(\mathbf{p}_1,\mathbf{p}_2)$ is more negative than that obtained from Coulomb wave functions.

Due to their Coulomb and strong interactions,

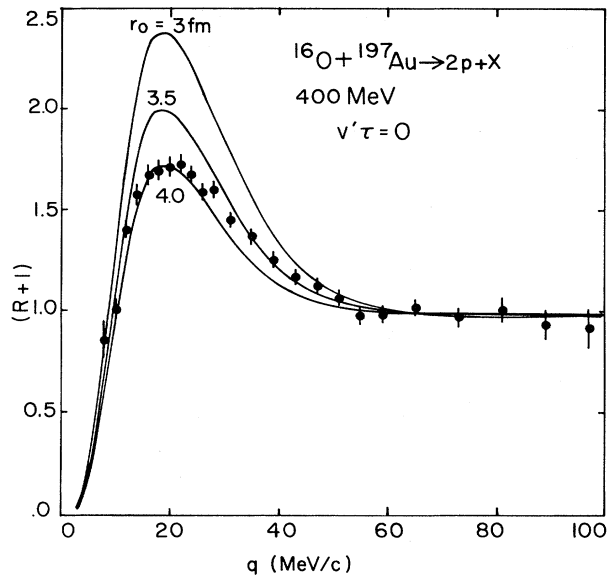

FIG. 11. Predicted two-proton correlation functions for source parameter $r_0=3$–4 fm. The data (Lynch *et al.*, 1983) are for the reaction $^{16}O+Au$ at $E/A=25$ MeV (from Boal and Shillcock, 1986).

nonidentical particle pairs also possess correlations that can yield geometrical information. Such correlations can provide useful analysis cross-checks because there are a much larger number of particle pairs. To date, strong-interaction contributions for only three nonidentical pairs have been treated in detail: *pd* (Jennings, Boal, and Shillcock, 1986) and $p\alpha$ and $d\alpha$ (Boal and Shillcock, 1986). Because sharp resonances are present in such cluster pairs, the strong-interaction potential parameters must be known accurately to ensure the accuracy of the correlation function obtained by numerical integration of numerically determined wave functions. In the three pairs investigated thus far, the original phase-shift data have been reanalyzed with Woods-Saxon partial-wave potentials. The results are shown in Table XI. Note the number of significant figures quoted for some of the parameters.

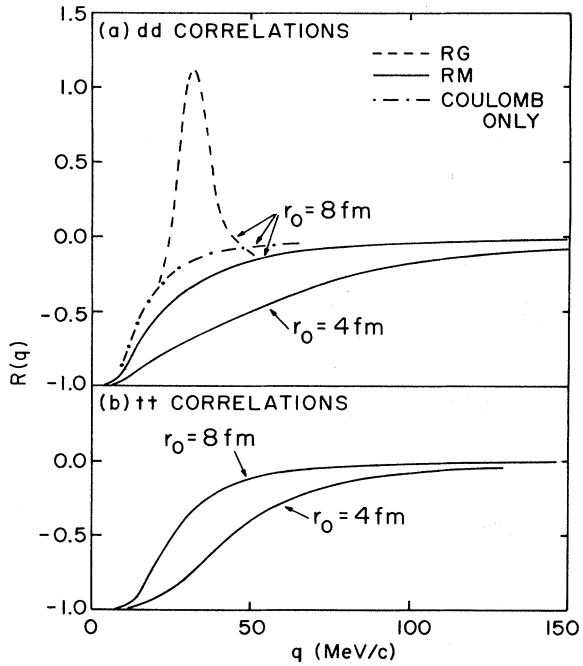

FIG. 12. (a) Predicted *dd* correlation functions based on *R*-matrix (RM) and resonating-group (RG) phase shifts (see text for definitions). The dot-dashed curve neglects the nuclear part of the potential. (b) Predicted *tt* correlation functions using Coulomb plus *s*-wave nuclear potentials. The radius parameter r_0 is indicated (after Chitwood *et al.*, 1985, and Pochodzalla, Chitwood, *et al.*, 1986).

TABLE X. Woods-Saxon potential parameters for the *dd* interaction (Chitwood *et al.*, 1985) and *tt* interaction (Pochodzalla, Chitwood, *et al.*, 1986) determined by fitting the *dd* phase shifts of the coupled-channel *R*-matrix approach (Hale and Dodder, 1984) and the *s*-wave *tt* phase shifts (Hale, private communication), respectively. Attractive potentials are denoted by negative V_{WS}. The rows with $j=3$ and 4 neglect the nuclear part of the interaction.

s	l	j	V_{WS} (MeV)	R (fm)	a (fm)
			dd interactions		
0	0		29.8	4.21	0.134
0	2		33.6	4.14	0.75
1	1	0	38.0	7.16	0.385
1	1	1	29.4	1.37	1.67
1	1	2	6.9	1.09	1.57
2	0		26.0	1.08	1.25
2	2	0	55.4	5.87	0.74
2	2	1	41.4	6.33	0.65
2	2	2	−11.5	1.85	1.65
2	2	3			
2	2	4			
			tt interactions		
0			30	4	0.6

As a first application of nonidentical pair correlations we demonstrate the prediction of Eq. (2.46) that the relevant factor in determining whether correlations are enhanced or suppressed is the derivative of the phase shift and not whether the potential is attractive or repulsive. The *pd* system has an attractive potential because of the presence of the ^3He bound state. Here, the phase shift at low momentum is π, and the phase shift decreases with increasing relative momentum. The behavior of the *pd* correlation function is shown in Fig. 13 for a zero-lifetime Gaussian-source parametrization (Jennings, Boal, and Shillcock, 1986). The predicted *pd* correlation function for Coulomb waves only is shown by the curves marked with a *C* in the figure, and one sees that the correlations become more negative with decreasing source size. However, even though Table XI shows the *pd* strong-interaction potentials to be mainly attractive, the behavior of the phase shift causes the correlation function to become more negative. This effect can be

TABLE XI. Woods-Saxon potential parameters found in analyses of phase-shift data for *pd* interactions (Jennings, Boal, and Shillcock, 1986) as well as $p\alpha$ and $d\alpha$ interactions (Boal and Shillcock, 1986). A negative sign for V_{WS} indicates an attractive potential.

l	j	V_{WS} (MeV)	R (fm)	a (fm)
		pd interactions		
$\frac{1}{2}$	0	−29.754	2.826	1.187
$\frac{1}{2}$	1	−8.214	2.962	0.259
$\frac{1}{2}$	2	−7.849	2.974	0.991
$\frac{3}{2}$	0	−18.115	2.837	0.9655
$\frac{3}{2}$	1	−13.10	2.067	1.578
$\frac{3}{2}$	2	+14.878	2.527	1.235
		$p\alpha$ interactions		
0	$\frac{1}{2}$	−25.575	3.050	0.938
1	$\frac{1}{2}$	−27.269	2.231	0.682
1	$\frac{3}{2}$	−30.929	2.700	0.488
2	$\frac{3}{2}$	−4.0	1.5	1.0
2	$\frac{5}{2}$	−3.4	2.0	1.0
		$d\alpha$ interactions		
0	1	−5.82	3.8767	0.1963
1	0	0.3586	5.57	0.55
1	1	0.749	4.14	0.566
1	2	1.147	3.848	0.551
2	1	−11.3646	4.1823	0.4712
2	2	−31.0	2.916	0.6386
2	3	−42.045	2.7648	0.70

seen by comparing curves C and $N+C$ in Fig. 13.

The two other pairs in Table XI both show resonant behavior at low q. The predicted zero-lifetime correlation function for the $p\alpha$ pair is shown in Fig. 14 (Boal and Shillcock, 1986). The peak near $q \approx 50$ MeV/c corresponds to the ^{5}Li ground state. Unfortunately, the unequal charge-to-mass ratio of this pair makes it susceptible to three-body interactions with the source region, as is discussed in Sec. VII.

The $d\alpha$ correlation function shows a very dramatic peak around $q \approx 40$ MeV/c arising from the d-wave resonance in ^{6}Li at 2.186 MeV ($J^\pi = 3^+$, $\Gamma = 24$ keV, $\Gamma_\alpha/\Gamma_{tot} = 1.00$) and a broad peak due to the overlapping states at 4.31 MeV ($J^\pi = 2^+$, $\Gamma = 1.3$ MeV, $\Gamma_\alpha/\Gamma_{tot} = 0.97$), and 5.65 MeV ($J^\pi = 1^+$, $\Gamma = 1.9$ MeV, $\Gamma_\alpha/\Gamma_{tot} = 0.74$). The predicted correlation function is shown in Fig. 15 (Boal and Shillcock, 1986). However, the true peak in the correlation function is so sharp that the use of an experimental resolution function is mandatory for data comparison. The $d\alpha$ system has a higher-lying resonance at $q \approx 80$ MeV/c, whose effect on the correlation function is shown in the inset. Results obtained from many of these pairs are discussed in Sec. VII.

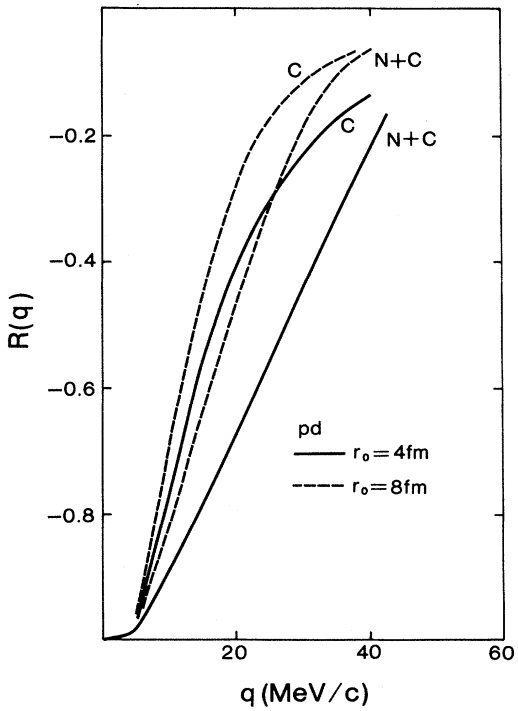

FIG. 13. Predictions of the *pd* correlation function with (*NC*) and without (*C*) the nuclear contribution to the two-particle wave function. The curves are shown for a zero-lifetime Gaussian source with $r_0 = 4$ or 8 fm (from Jennings, Boal, and Shillcock, 1986).

B. Emission time scales

Two different models for a fixed-geometry source of particles are discussed at length in Secs. III.A and III.B

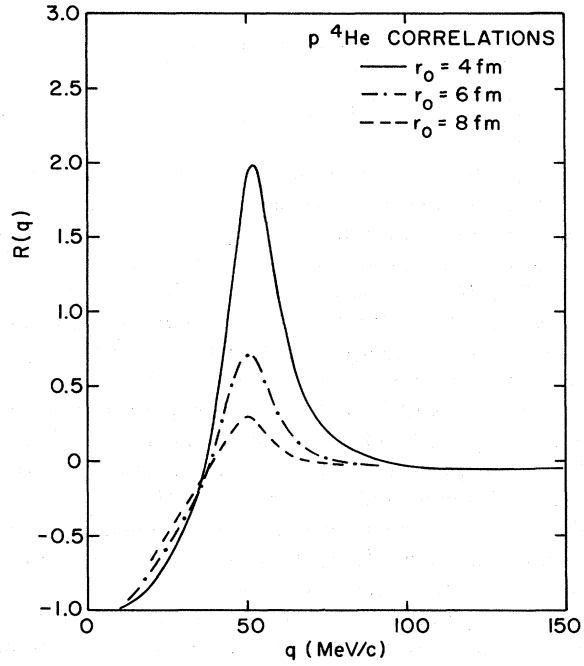

FIG. 14. Predictions of the $p\alpha$ correlation function for a zero-lifetime Gaussian source with $r_0=4$, 6, or 8 fm (after Boal and Shillcock, 1986).

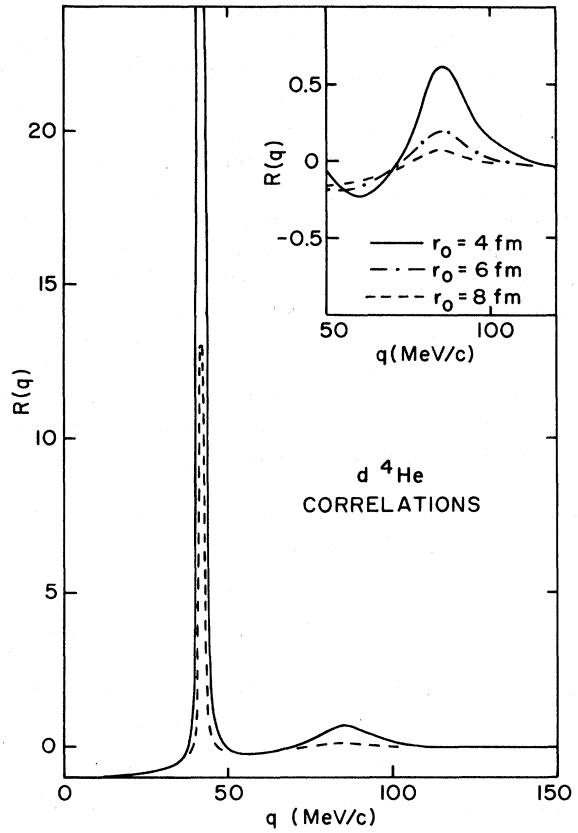

FIG. 15. Predicted $d\alpha$ correlation function for various values of the source parameter r_0. A more detailed view of the correlation function around $q\approx 80$ MeV/c is shown in the insert (after Boal and Shillcock, 1986).

and summarized by Eqs. (3.7), (3.24), and (3.25). In the equations the decay time of the source is conjugate to the energy difference of the particle pair, causing the source to appear elongated for $\mathbf{q}$ in the direction of $\mathbf{P}=\mathbf{p}_1+\mathbf{p}_2$ (Kopylov and Podgoretskii, 1972, 1973; Koonin, 1977; Pratt and Tsang, 1987). Naturally, the correlation function has to be measured at more than one angle for $\mathbf{P}$ in order to distinguish a lifetime effect from an anisotropic source. Generally speaking, obtaining sufficient statistics to determine the three parameters $r_{\parallel}$, $r_{\perp}$, and τ in an experimental fit is difficult, especially since these parameters exhibit a significant dependence on the total momentum of the coincident particle pair. Because of this we do not make comparisons between experimentally extracted lifetimes in Secs. IV, V, and VII.

Two calculations based in part on computer simulations have been performed to predict the magnitude of the lifetime effects. In one simulation (Boal and DeGuise, 1986), a hot classical gas of protons and neutrons is placed in a step-function attractive potential representing the nucleus and allowed to evolve according to Newton's equations. The nucleons can scatter from each other, and the protons also can interact through Coulomb's law. The fastest particles are observed to leave the system first, as one expects, and the source dimension obtained from the fast-particle correlation function in the computer simulation is very close to the size of the attractive potential. Slower particles continually reequilibrate and leave the system on longer time scales. Their correlation function shows a significantly larger source dimension. This qualitative behavior—source size decreasing with increasing energy of the emitted particles—is found experimentally over a wide range of reaction conditions (see Secs. V and VII), although the behavior may have many different causes.

Pratt and Tsang (1987) compare the Wigner functions for three different models of particle emission in heavy-ion reactions: evaporation from an equilibrated source, a Boltzmann-Uehling-Uhlenbeck transport equation model, and an explosive source (see also Sec. III.C). This calculation confirms that the apparent source size can change dramatically for emission energy ranges typically investigated in an intermediate-energy heavy-ion reaction. In the evaporative model, the true source size is obtained at high emission energies, and the source appears to be unreasonably large at low energies. This contrasts with the explosive source that measures the geometrical extent of the source at low energies, the source appearing smaller as the energy of the particle pair increases (see Fig. 2). The Boltzmann-Uehling-Uhlenbeck transport approach shows a more complicated rise and fall of the apparent source size with emission energy.

C. Resonance and compound-nuclear decays

A slightly different use of intensity interferometry is the determination of resonance lifetimes, either particle

resonances (Grishin, Kopylov, and Podgoretskii, 1971a; Kopylov and Podgoretskii, 1971; Kopylov, 1972), nuclear resonances (Grishin, Kopylov, and Podgoretskii, 1971b; Bernstein and Friedman, 1985), or compound-nuclear resonances (Kopylov and Podgoretskii, 1972; Koonin, Bauer, and Schäfer, 1989). In the latter case, spatial information is also obtained. The basic idea is to have a particle of type B emitted when the resonance is formed and another particle of the same type emitted when the resonance decays. The two particles of the same type can then interfere, and the extent of the interference can be used to determine the lifetime. Bernstein and Friedman (1985) use the effects of the Coulomb interaction rather than Pauli correlations to determine the lifetime of ^{2}H*. Owing to their difficulty of implementation, some of the formalisms presented in this subsection have not yet been applied to data analysis.

Following Grishin, Kopylov, and Podgoretskii (1971a), we consider a reaction of the type

$$I \rightarrow B + R^* \rightarrow B + B + X \ , \tag{6.4}$$

where I is an initial state, B is the detected particle, R^* is the resonance whose lifetime we want, and X is anything else. The amplitude A for this process can be written as

$$A \propto \frac{a(\mathbf{p}_1,\mathbf{p}_2,\mathbf{p}_3)}{m_{13}^2 - M^2 + iM\Gamma} + \frac{a(\mathbf{p}_2,\mathbf{p}_1,\mathbf{p}_3)}{m_{23}^2 - M^2 + iM\Gamma} \ , \tag{6.5}$$

where $\mathbf{p}_1$ and $\mathbf{p}_2$ are the momenta of the two identical particles and $\mathbf{p}_3$ is the momentum of X. The mass of the resonance R^* is M, and the effective masses of the particle pairs 13 and 23 are m_{13} and m_{23}, respectively. The plus sign corresponds to B having zero spin. It follows that interference is significant for $m_{13} \approx m_{23} \approx M$. For sufficiently narrow resonances these conditions may hold, together with $\mathbf{p}_1 \approx \mathbf{p}_2$, and we may assume $a(\mathbf{p}_1,\mathbf{p}_2,\mathbf{p}_3) = a(\mathbf{p}_2,\mathbf{p}_1,\mathbf{p}_3)$. Using the notation

$$x = \frac{m_{13}^2 + m_{23}^2 - 2M^2}{2M\Gamma} \ , \tag{6.6a}$$

$$y = \frac{m_{13}^2 - m_{23}^2}{2M\Gamma} \ , \tag{6.6b}$$

we can write the probability for two-particle emission as

$$\frac{d^2W}{dx\,dy} \propto \left| \frac{1}{x+y+i} + \frac{1}{x-y+i} \right|^2 \ . \tag{6.7}$$

Interference effects can now be found by studying $d^2W/dx\,dy$ as a function of x and y. For example, integrating over x or y yields

$$w(y) = \frac{dW}{dy} = \int_{-\infty}^{\infty} \frac{d^2W}{dx\,dy} dx = 2\pi \left[1 + \frac{1}{1+y^2} \right] \ , \tag{6.8a}$$

$$w(x) = \frac{dW}{dx} = \int_{-\infty}^{\infty} \frac{d^2W}{dx\,dy} dy = 2\pi \ . \tag{6.8b}$$

This result differs from other examples in this review because here we have only two sources. The dependence of the first of these two integrals on y gives information on the width of the resonance; the distribution is enhanced for small y. Notice that y depends on the resonance mass M as well as the width Γ. Thus, for narrow resonances, the correlation in energy will be wider than the natural width of the resonance, allowing for the determination of the resonance width with less energy resolution than might be expected. This is the main advantage of the interference approach to determining resonance lifetimes (Grishin, Kopylov, and Podgoretskii, 1971a).

The basic procedure can also be applied when two different resonances, decaying in parallel, produce identical particles; the reader is referred to Kopylov (1972) and Kopylov and Podgoretskii (1971) for more details. Extensions and further discussion can be found in Thomas (1977), who develops an S-matrix formulation for the calculation of two-particle correlations, and Grassberger (1977), who also investigates correlations between promptly produced particles and those arising from resonance decay. The work of Kopylov and Podgoretskii (1971) leads to the more general interferometry results (Kopylov and Podgoretskii, 1972, 1973; Kopylov, 1974) discussed in Sec. III.B.

A number of calculations dealing with the effects of specific resonance decays have also been performed. Biyajima (1983) considers modifications to the simple Gaussian-source model for two-proton correlations (Koonin, 1977) caused by adding a second source associated with the decay of two-proton quasiclusters. Bowler (1986) has investigated the role of η, η', and ω decays on two-pion correlations, while Thomas (1977) has considered ρ decays.

Compound-nucleus decay can be treated in a manner similar to resonance decay. Here we can also have identical particles emitted at successive stages of the reaction. Our presentation follows that of Koonin, Bauer, and Schäfer (1989). The reaction is assumed to proceed from the initial channel i through an equilibrated compound nucleus to an evaporative residue in state η by the sequential emission of identical particles of momenta $\mathbf{p}_1$ and $\mathbf{p}_2$, with energies E_1 and E_2. This is like sequential resonance decay. The corresponding T-matrix element is

$$T_{\eta i}(\mathbf{p}_1,\mathbf{p}_2) = \sum_{\alpha\beta} \gamma_{\eta\beta}(\mathbf{p}_2) \frac{1}{E - \varepsilon_\beta - i\Gamma_\beta/2 - E_1} \gamma_{\beta\alpha}(\mathbf{p}_1) \frac{1}{E - \varepsilon_\alpha - i\Gamma_\alpha/2} \gamma_{\alpha i} \ , \tag{6.9}$$

where E is the total energy. The intermediate compound-nucleus levels are labeled by α and β, with energies ε_α and ε_β and total widths Γ_α and Γ_β, respectively. The reduced width for the compound-nucleus state μ to decay to ν by the emission of a particle of momentum $\mathbf{p}$ is $\gamma_{\nu\mu}(\mathbf{p})$, while $\gamma_{\alpha i}$ is the reduced width for the entrance channel.

The two-particle inclusive cross section is proportional to the square of the coherent sum of the amplitudes corresponding to the two different orders of emission summed over final states η:

$$\sigma(\mathbf{p}_1,\mathbf{p}_2) \propto \sum_\eta |T_{\eta i}(\mathbf{p}_2,\mathbf{p}_1) \pm T_{\eta i}(\mathbf{p}_1,\mathbf{p}_2)|^2 2\pi\delta$$
$$= \sum_\eta [|T_{\eta i}(\mathbf{p}_2,\mathbf{p}_1)|^2 + |T_{\eta i}(\mathbf{p}_1,\mathbf{p}_2)|^2] 2\pi\delta \pm \sum_\eta 2\,\mathrm{Re}[T^*_{\eta i}(\mathbf{p}_2,\mathbf{p}_1) T_{\eta i}(\mathbf{p}_1,\mathbf{p}_2)] 2\pi\delta$$
$$\equiv \sigma_{\mathrm{dir}}(\mathbf{p}_1,\mathbf{p}_2) \pm \sigma_{\mathrm{int}}(\mathbf{p}_1,\mathbf{p}_2) \ . \tag{6.10}$$

The plus/minus signs correspond to spatially symmetric or antisymmetric particle emission, respectively. The energy-conserving delta function $2\pi\delta(E-E_\eta-E_1-E_2)$ is abbreviated to $2\pi\delta$. To this point we have followed the same procedure as for resonance decay. Now, however, we diverge and make the usual assumption for compound nuclei (Feshbach, Kerman, and Koonin, 1980), of maximal randomness of the widths. That is, only pairwise correlations of the widths are nontrivial, and these are given by expressions such as

$$\langle \gamma_{\eta\beta}(\mathbf{p}_2)\gamma^*_{\eta\beta'}(\mathbf{p}_1)\rangle \equiv \delta_{\beta\beta'}\langle \Gamma_{\eta\beta}(\bar{\mathbf{p}})\rangle g_{\eta\beta}(\mathbf{p}_2,\mathbf{p}_1) \ , \tag{6.11a}$$

$$\langle \gamma_{\beta\alpha}(\mathbf{p}_1)\gamma^*_{\beta\alpha'}(\mathbf{p}_2)\rangle \equiv \delta_{\alpha\alpha'}\langle \Gamma_{\beta\alpha}(\bar{\mathbf{p}})\rangle g_{\beta\alpha}(\mathbf{p}_1,\mathbf{p}_2) \ , \tag{6.11b}$$

which define the function g. The partial widths are defined by $\Gamma_{\nu\mu}=\gamma^2_{\nu\mu}$. The angular brackets denote averaging over the compound-nucleus states. The randomness is only with respect to the discrete states and not the continuous-momentum label $\bar{\mathbf{p}}$ [defined by $\bar{\mathbf{p}}=(\mathbf{p}_1+\mathbf{p}_2)/2\approx\mathbf{p}_1\approx\mathbf{p}_2$].

The quantity of interest is the ratio

$$R_{id}(\mathbf{p}_1,\mathbf{p}_2)$$
$$= \frac{\sigma_{\mathrm{int}}(\mathbf{p}_1,\mathbf{p}_2)}{\sigma_{\mathrm{dir}}(\mathbf{p}_1,\mathbf{p}_2)}$$
$$= g_{\alpha\beta}(\mathbf{p}_1,\mathbf{p}_2) g_{\beta\eta}(\mathbf{p}_2,\mathbf{p}_1) \frac{\langle\Gamma_\beta\rangle^2}{\langle\Gamma_\beta\rangle^2+(E_2-E_1)^2} \ . \tag{6.12}$$

This equals the correlation function R only if $\sigma_{\mathrm{dir}}(\mathbf{p}_1,\mathbf{p}_2)$ is just the product of the two single-particle cross sections. Otherwise, R contains other contributions from σ_{dir}. The spatial dependence is embodied in $g(\mathbf{p}_1,\mathbf{p}_2)$, which describes the coherence of the source. It is only the energy dependence that appears explicitly through the Lorentzian factor. Thus, in contrast to Sec. III where we encounter Gaussian sources, here we have Lorentzians that are more natural for resonance decay.

As one would expect, applications of this formalism are nontrivial. Koonin, Bauer, and Schäfer (1989) consider as an example the emission of two spinless neutrons from a rapidly rotating nucleus. They show that the extracted radii vary with the orientation of $\mathbf{P}$ and $\mathbf{q}$ with respect to the beam. This schematic calculation emphasizes the care that must be taken in interpreting interferometry results.

VII. PARTICLE EMISSION IN INTERMEDIATE-ENERGY NUCLEAR COLLISIONS

The transition from low-energy, mean-field-dominated nuclear reactions to high-energy, nucleon-nucleon-collision-dominated reactions is expected to take place at intermediate energies, $E/A=20-200$ MeV. Over this energy domain, particle emission from the early stages of the reaction becomes increasingly important. Through the use of two-particle correlation functions, we are able to obtain from such emission information concerning equilibration and the dynamics governing the early stages of the collision.

In this section we review results obtained from intermediate-energy heavy-ion reactions, $E/A=20-100$ MeV. We also include a brief discussion of data obtained at lower energies and for reactions induced by 500-MeV protons. At these energies, the cross sections for multipion emission are very small, and no attempts have yet been made to measure source dimensions via two-pion interferometry. At the same time, nucleons and complex light particles are emitted with sufficiently large multiplicities to make two-particle correlation measurements for these particles relatively straightforward.

Experimental techniques are discussed in Sec. VII.A. Results from two-proton correlation functions, integrated over various orientations between the total and relative momentum vectors ($\mathbf{P}$ and $\mathbf{q}$, respectively), are presented in Sec. VII.B. First measurements of longitudinal and transverse correlation functions and efforts to determine the importance of finite-lifetime effects are reviewed in Sec. VII.C. Correlations between complex particles are discussed in Sec. VII.D and the effects of reaction filters are described in Sec. VII.E.

A. Experimental techniques

In this energy range, most measurements of two-particle correlation functions employ hodoscopes composed of one or several dozen densely packed $\Delta E-E$ detector telescopes. Usually, single- and two-particle cross sections are measured simultaneously. The experimental two-particle correlation function $R(\mathbf{P},\mathbf{q})$ can then be defined in terms of the coincidence yield $Y_{12}(\mathbf{p}_1,\mathbf{p}_2)$ and the single-particle yield $Y_1(\mathbf{p}_1)$ and $Y_2(\mathbf{p}_2)$:

$$\sum Y_{12}(\mathbf{p}_1,\mathbf{p}_2) = C_{12}[1+R(\mathbf{P},\mathbf{q})] \sum Y_1(\mathbf{p}_1) Y_2(\mathbf{p}_2) \ . \tag{7.1}$$

The quantities **P** and **q** are the total and relative momenta of the pair, respectively. The normalization constant C_{12} is usually determined by the requirement that $R(\mathbf{q})=0$ for large **q**.

In order to obtain sufficient statistics, the sum in Eqs. (7.1) and (7.2) is performed over all detector and particle energy combinations satisfying a specific gating condition. In general, the experimental gating conditions correspond to implicit integrations over possible angular and other dependences of the two-particle correlation function. Most investigations explore the angle-integrated correlation function $R(q)$ (where by "angle-integrated" we mean averaged over the orientations of **q**, not necessarily over the orientations of **P**). There may also be a second averaging in which $R(q)$ is evaluated for a specific range of particle energies, E_1+E_2, with the implicit constraint that the particle energies E_1 and E_2 must lie above the detection threshold. For this special case the experimental correlation function is evaluated as

$$\sum Y_{12}(\mathbf{p}_1,\mathbf{p}_2)=C_{12}[1+R(q)]\sum Y_1(\mathbf{p}_1)Y_2(\mathbf{p}_2)\ . \qquad (7.2)$$

Accurate comparisons between experiment and theory can be performed by filtering the theoretical cross sections with the response of the experimental apparatus and by observing the appropriate gating and summation conventions. Since present microscopic theories cannot yet predict details of energy and other dependences of two-particle correlation functions, the correlation measurements have largely provided qualitative insight about the space-time evolution of the reaction zone. In most investigations, possible distortions arising from the applied gating conditions are neglected.

The definition of the experimental correlation function in terms of the ratio of single- and two-particle coincidence yields, Eq. (7.1), is meaningful when single- and two-particle yields correspond to the same class of collisions. Due to the stochastic nature of the particle emission process, this assumption is generally well satisfied. The definition of the experimental correlation function in terms of Eq. (7.1) has been employed by many authors (Lynch *et al.*, 1983; Chitwood *et al.*, 1985, 1986; Pochodzalla *et al.*, 1985a, 1985b, 1987; Kyanowski *et al.*, 1986; Pochodzalla, Chitwood *et al.*, 1986; Pochodzalla, Gelbke *et al.*, 1986; Chen *et al.*, 1987a, 1987b, 1987c, 1987d; Awes *et al.*, 1988).

A number of authors (Trockel *et al.*, 1987; Fox *et al.*, 1988; Cebra *et al.*, 1989; DeYoung *et al.*, 1989) have used alternative definitions of the experimental correlation function by generating an "uncorrelated" yield, $Y^*_{12}(\mathbf{p}_1,\mathbf{p}_2)$, via event mixing, e.g., by taking particle 1 from event n and particle 2 from event $n+k$, where k is chosen arbitrarily. The correlation function is then given by

$$R(q)+1=C^*_{12}Y_{12}(q)/Y^*_{12}(q)\ , \qquad (7.3)$$

where $Y_{12}(q)$ and $Y^*_{12}(q)$ are the coincidence and uncorrelated yields integrated over the specified gating conditions, and C^*_{12} is an appropriate normalization constant. The prescription of Eq. (7.3) ensures that the correlated and uncorrelated yields are taken from the same class of collisions. Because of the inherent simplicity of implementation, this method is often adopted in studies where special triggers make the definition of single-particle distributions more complicated or, simply, when single-particle data are not available. In many cases the two prescriptions yield virtually indistinguishable results (DeYoung *et al.*, 1989). When the phase-space acceptance of the experimental apparatus is narrow, however, the use of Eq. (7.3) can artificially reduce the correlation function since event mixing does not remove all correlations (Zajc *et al.*, 1984). Such effects can be assessed and corrected for by Monte Carlo simulations (Zajc *et al.*, 1984).

B. Inclusive two-proton correlations

The shape of the two-proton correlation function reflects the combined effects of the Pauli exclusion principle and the proton-proton interaction. The first measurements of two-proton correlation functions in intermediate-energy heavy-ion collisions performed by Lynch *et al.* (1983) provide evidence of particle emission from localized regions of high excitation. The magnitude of the measured correlations is found to exhibit a surprisingly strong dependence upon the total kinetic energy of the emitted protons: the measured correlations are more pronounced for particles emitted with higher kinetic energies. Similar dependences of the strengths of two-particle correlation functions have been observed in many subsequent investigations (Chitwood *et al.*, 1986; Pochodzalla, Chitwood, *et al.*, 1986; 1987; Chen *et al.*, 1987a, 1987b, 1987c, 1987d; Pochodzalla *et al.*, 1987; Awes *et al.*, 1988) and also in reactions at higher energies (see Sec. V).

As an example, Fig. 16 shows two-proton correlation functions measured (Pochodzalla, Chitwood, *et al.*, 1986) for the $^{14}N+^{197}Au$ reaction at $E/A=35$ MeV. The correlation functions are evaluated via Eq. (7.2) for the energy gates $E_1+E_2=24$–50, 50–75, and 75–100 MeV and energy thresholds of $E_1,E_2\geq 12$ MeV. The attractive singlet s-wave interaction between the two coincident protons gives rise to a pronounced maximum in the correlation function at a relative momentum of $q=20$ MeV/c. The minimum at small relative momenta, $q\approx 0$, results from the combined effects of the Pauli exclusion principle and the repulsive Coulomb interaction between the coincident protons. For two-proton correlation functions integrated over orientations of **q**, the magnitude of the maximum at $q\approx 20$ MeV/c is determined by the volume of the reaction zone. The maximum of the measured correlation function is observed to increase with increasing total kinetic energy, E_1+E_2, of the two coincident particles, indicating that more energetic particles are emitted from smaller sources or, alternatively, at shorter time intervals. The dashed, solid, and dotted curves represent theoretical correlation functions pre-

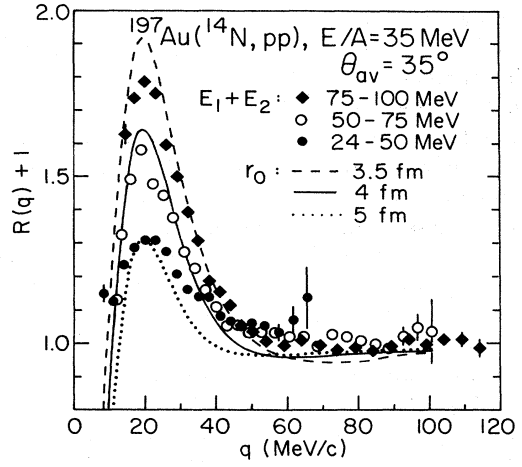

FIG. 16. Two-proton correlation functions measured for ^{14}N-induced reactions on ^{197}Au at $E/A=35$ MeV. The particles were detected at an average laboratory angle of $\theta_{av}=35°$; the energy gates are indicated in the figure. The curves represent theoretical correlation functions predicted for emission from sources of negligible lifetime and Gaussian density distribution with the radius parameters given in the figure (from Pochodazalla, Chitwood, *et al.*, 1986).

dicted for Gaussian sources of negligible lifetime, $\rho(r)=\rho_0\exp(-r^2/r_0^2)$, with $r_0=3.5$, 4, and 5 fm, respectively.

Such calculations provide upper bounds for the source dimensions, since finite lifetimes lead to reduced correlations (Koonin, 1977; Boal and DeGuise, 1986; Pratt and Tsang, 1987). For example, a computer simulation (Boal and DeGuise, 1986; see Sec. VI.B) of proton and neutron emission from a hot spherically symmetric source of radius 4.0 fm shows that the mean time between particle emission decreases with increasing energy of the measured pair of nucleons. In the simulation the apparent source size $d=[r_0^2+(v'\tau)^2]^{1/2}$ has the values 7.9, and 4.8, and 4.0 fm for the summed energy bins E_1+E_2 of 0–30, 30–60, and >60 MeV. Although this simulation treats nucleons semiclassically, it does provide an estimate of the order-of-magnitude change in apparent source size expected from finite-lifetime effects in this temperature range.

The calculated correlation functions shown in the figure do not represent best fits to the data; the source radii extracted from these data are (Pochodzalla, Chitwood, *et al.*, 1986): $r_0=3.8\pm0.2$ fm, 4.3 ± 0.3 fm, and 4.9 ± 0.5 fm, respectively. These parameters correspond to the equivalent rms radii of $r_{\rm rms}=4.7\pm0.3$ fm, 5.3 ± 0.4 fm, and 6.0 ± 0.6 fm, respectively. For comparison, the rms radii of ^{14}N and ^{197}Au are $r_{\rm rms}(^{14}\text{N})=2.54$ fm and $r_{\rm rms}(^{197}\text{Au})=5.43$ fm (Brown, Bronk, and Hodgson, 1984). The extracted source radii from the reactions are always larger than the radius of the projectile. Very energetic protons appear to be emitted from a reaction zone that is slightly smaller than the target nucleus, as may be expected for emission from the early stages of the reaction. For less energetic emissions, however, the extracted source radii are larger than the radius of the target (or the compound nucleus).

Figure 17 compares radius parameters for Gaussian sources of negligible lifetime determined from two-proton correlation functions measured for a number of intermediate-energy heavy-ion reactions: ^{14}N+^{197}Au at $E/A=35$ MeV, $\theta_{av}=35°$ (open circles, from Pochodzalla, Chitwood, *et al.*, 1986), ^{16}O+^{197}Au at $E/A=25$ MeV, $\theta_{av}=15°$ (open diamonds, from Lynch *et al.*, 1983), and at $E/A=94$ MeV, $\theta_{av}=45°$ (open squares, from Chen *et al.*, 1987c), ^{32}S+^{197}Au at $E/A=22.3$ MeV, $\theta_{av}=30°$ (solid squares, from Awes *et al.*, 1988), and ^{40}Ar+^{197}Au at $E/A=60$ MeV, $\theta_{av}=30°$ (solid circles, from Pochodzalla *et al.*, 1987). If finite-lifetime effects cannot be ignored, these source radii only provide upper limits for the spatial dimensions of the emitting system. Shown is the dependence of r_0 on the total kinetic energy per nucleon of the two coincident protons, measured in units of the projectile energy per nucleon $(E_1+E_2)A_p/[(A_1+A_2)E_p]$. This scaling (Chen *et al.*, 1987c) is interesting, but may not be unique. (To exclude contributions from evaporation residues, only the data for $E_1+E_2\geq70$ MeV are shown for the ^{16}O+Au reaction at $E/A=25$ MeV.) In all cases, smaller source radii are extracted for the emission of more energetic particles. For the most energetic particles emitted in ^{14}N- and ^{16}O-

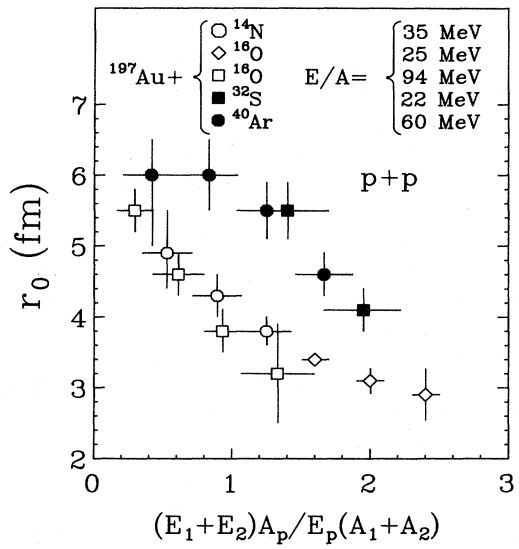

FIG. 17. Source parameters extracted from *pp* correlation functions measured for the following reactions: ○, ^{14}N+^{197}Au at $E/A=35$ MeV, $\theta_{av}=35°$ (from Pochodzalla, Chitwood, *et al.*, 1986); ◇, ^{16}O+^{197}Au at $E/A=25$ MeV, $\theta_{av}=15°$ (from Lynch *et al.*, 1983); □, ^{16}O+^{197}Au at $E/A=94$ MeV, $\theta_{av}=45°$ (from Chen *et al.*, 1987c); ■, ^{32}S+^{197}Au at $E/A=22.3$ MeV, $\theta_{av}=30°$ (from Awes *et al.*, 1988); ●, ^{40}Ar+^{197}Au at $E/A=60$ MeV, $\theta_{av}=30°$ (from Pochodzalla *et al.*, 1987). Shown is the dependence on the total kinetic energy per nucleon of the two coincident protons, measured in units of the projectile energy per nucleon $(E_1+E_2)A_p/[(A_1+A_2)E_p]$.

induced reactions, the extracted upper limits of the source dimensions are smaller than the size of the target nucleus [$r_0(\mathrm{Au})=(\frac{2}{3})^{1/2}r_{\mathrm{rms}}(\mathrm{Au})=4.3$ fm]. Larger values for r_0 are deduced for ^{32}S- and ^{40}Ar-induced reactions.

Unfortunately, angle-integrated two-proton correlation functions do not provide sufficient information to remove the interpretational ambiguities that arise from the interplay between source dimensions and source lifetimes (Awes *et al.* 1988). The observed attenuation of the correlation functions for the emission of lower-energy proton pairs could be caused by an expansion of the reaction zone or, alternatively, by increased time intervals between successive proton emissions as the reaction zone cools by particle emission. An attempt to clarify this issue experimentally (Awes *et al.,* 1988) is discussed in Sec. VII.C.

Dependences of two-proton correlation functions upon the average angle of the emitted protons have been investigated by Pochodzalla, Chitwood, *et al.* (1986) and Fox *et al.* (1988) for ^{14}N-induced reactions on ^{197}Au and $^{\mathrm{nat}}$Ag at $E/A=35$ MeV. Over an angular range of $\theta_{av}=35°-80°$, no significant angular dependence could be established within the experimental uncertainties. In these experiments, contributions from compound-nucleus evaporation are largely suppressed by the applied detection thresholds, and the detected protons are mainly emitted in fast noncompound emission processes from the early stages of the reaction. Different emission angles do not appear to select different average reaction geometries.

Correlation functions measured in regions of phase space that are dominated by emission from the later, equilibrated stages of the reactions appear to be strongly attenuated, possibly as a result of long time intervals between successive particle emissions. Such correlations can be investigated by measurements at low projectile energies, for which fast emission processes play an insignificant role, or at large emission angles, for which contributions from the early stages of the reaction are kinematically suppressed.

Measurements at large angles and with low detection thresholds have been performed by Ardouin *et al.* (1989) for the reactions ^{40}Ar+$^{\mathrm{nat}}$Ag, ^{197}Au at $E/A=44$ MeV, and ^{16}O+^{197}Au at $E/A=94$ MeV. The energy-integrated correlation functions are strongly suppressed as compared to those measured at more forward angles and higher detection thresholds (Lynch *et al.,* 1983; Chitwood *et al.,* 1986; Pochodzalla, Chitwood, *et al.,* 1986; Chen *et al.,* 1987a, 1987b, 1987c, 1987d; Pochodzalla, 1987; Awes *et al.,* 1988; Fox *et al.,* 1988). In addition, the magnitude of the observed correlations decreases with increasing detection angle, leading to a complete suppression of the maximum at $q\approx 20$ MeV/c at backward angles. This effect could be due to an implicit energy dependence: since the slopes of the single-particle energy spectra decrease with increasing detection angle, the average energy of the detected particles decreases at more backward angles.

Measurements for low projectile energies and with low detection thresholds have been performed by DeYoung *et al.* (1989) for the ^{16}O+^{27}Al reaction at $E/A=8.75$ MeV and $\theta_{av}=19.5°$. For this reaction, contributions from preequilibrium processes are small. The measured correlation function is shown in Fig. 18; it exhibits a narrow minimum at $q\approx 0$, but no maximum at $q\approx 20$ MeV/ c. It appears that $R(q=0)>-1$, an effect that could be due to the finite resolution of the experimental apparatus. The complete attenuation of the maximum at $q\approx 20$ MeV/ c is attributed to large time intervals for subsequent equilibrium emissions. The solid and dashed curves in Fig. 18 show correlation functions predicted by Coulomb trajectory calculations for particles randomly emitted from the surface of the compound nucleus. The time intervals between successive emissions are assumed to have a probability distribution $P(\Delta t)\approx\exp(-\Delta t/\tau)$. From these calculations an emission time scale of $1-5\times10^{-21}$ s is estimated (DeYoung *et al.,* 1989). For comparison, the dotted curve shows the correlation function expected for a Gaussian source of negligible lifetime with $r_0=4.5$ fm, a source that is clearly in disagreement with these data.

Only sparse experimental information exists on the dependence of two-particle correlation functions on the size of the target nucleus. For ^{16}O-induced reactions at $E/A=25$ MeV, two-proton correlation functions have been measured (Lynch *et al.,* 1983; Bernstein *et al.,* 1985) for three target nuclei, ^{12}C, ^{27}Al, and ^{197}Au. In contrast to simple geometrical expectations, more pronounced correlations are observed for reactions induced on heavier target nuclei. The reduced correlations for the lighter target nuclei, ^{12}C and ^{27}Al, are attributed to in-

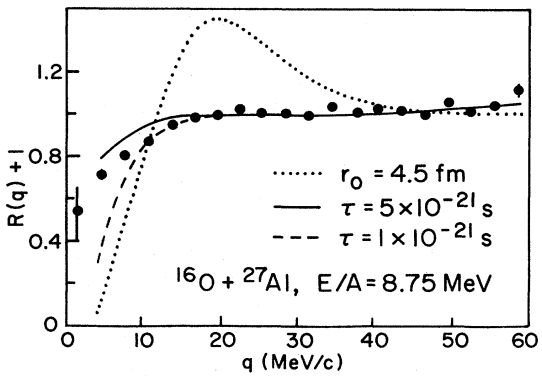

FIG. 18. Two-proton correlation function measured for the ^{16}O+^{27}Al reaction at $E/A=8.75$ MeV and $\theta_{av}=19.5°$; the detector threshold was $E_1,E_2\geq 2$ MeV. The curves show correlation functions predicted by Coulomb trajectory calculations for particles randomly emitted from the surface of the compound nucleus assuming a distribution of the time intervals between successive emissions of the form $\exp(-t/\tau)$: dashed curve, calculation with $\tau=1\times10^{-21}$ s; solid curve, $\tau=5\times10^{-21}$ s (from DeYoung *et al.,* 1989).

creased contributions from compound-nuclear decays. In fact, the correlation functions for the $^{16}O+^{12}C$ and $^{16}O+^{27}Al$ reactions can be quantitatively understood in terms of ^{2}He emission from fully equilibrated compound nuclei (Bernstein *et al.*, 1985). The large correlations measured (Lynch *et al.*, 1983) for the $^{16}O+^{197}Au$ reaction, on the other hand, are inconsistent with such an interpretation. A satisfactory explanation of the observed target dependence by a model that includes both equilibrium and nonequilibrium emissions does not yet exist.

At intermediate energies, most measurements of two-proton correlation functions have been performed for heavy-ion-induced reactions. Complementary measurements for reactions induced by 500-MeV protons have been made recently. No dramatic differences are observed (Cebra *et al.*, 1989) for the energy-integrated correlation functions measured for the reactions $p+$Be, $p+$Ag, and $^{14}N+$Ag at projectile energies of about 500 MeV (see Fig. 19). For Gaussian sources of negligible lifetime, radius parameters of $r_0(p+\text{Be})=3.3\pm1.1$ fm, $r_0(p+\text{Ag})=4.0\pm0.5$ fm, and $r_0(^{14}N+\text{Ag})=4.3-4.8$ fm are extracted. While there appears to be a tendency toward smaller source radii for lighter systems, the experimental uncertainties are too large to allow definitive conclusions. Since the magnitude of the experimental two-particle correlation functions exhibits a strong dependence on the energy of the detected particles, comparisons of the energy-integrated correlation functions contain only a reduced amount of information. Unfortunately, the dependence on the energy of the emitted particles has not yet been explored for proton-induced reactions. More detailed comparisons of proton- and heavy-ion-induced reactions, with higher statistical accuracy and as a function of the kinetic energy of the emitted particles, would clearly be valuable.

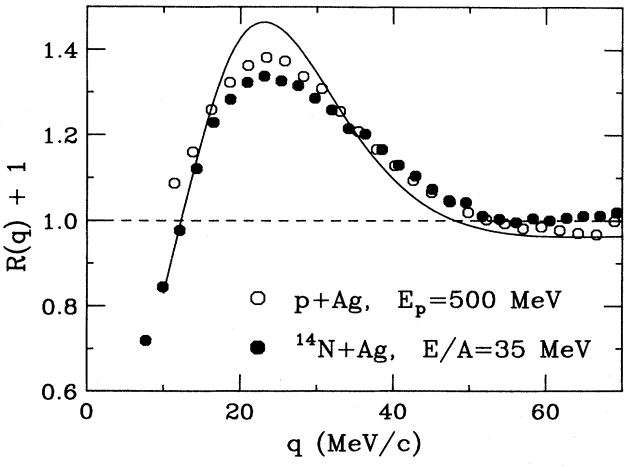

FIG. 19. Energy-integrated two-proton correlation functions measured for the reactions $p+^{nat}Ag$ at $E_p=500$ MeV and $^{14}N+^{nat}Ag$ at $E/A=35$ MeV; the energy threshold was $E_1, E_2 \geq 11.9$ MeV (from Cebra *et al.*, 1989).

C. Longitudinal and transverse two-proton correlations

The dependence of the two-particle correlation function on the angle between the vectors **q** and **P** can provide information on the source lifetime and shape (Kopylov and Podgoretskii, 1972, 1973; Koonin, 1977; Pratt, 1984; Pratt and Tsang, 1987; Awes *et al.*, 1988; see discussion in Secs. III.A, III.B, and VI.B). The two-proton correlation function is affected by the Coulomb and nuclear interactions of the emitted proton pair as well as by the requirement of antisymmetry. Because of the long range of the Couloumb interaction, Coulomb effects depend only weakly on the source size (see Sec. VI.A). For dimensions on the nuclear scale, the short-range attractive singlet *s*-wave interaction gives rise to the positive enhancement of the correlation function at $q=20$ MeV/*c*. To a first approximation the magnitude of this enhancement is inversely proportional to the volume of the emitting source. On the other hand, the effects of the Pauli exclusion principle depend on the shape of the reaction zone. Protons of identical spin projection will be suppressed from occupying relative momentum states over an interval of $\Delta p = h/\Delta x$, where Δx is the spread of the final Wigner distribution in the x direction [see Eqs. (3.42) and (3.43) for definition]. If the relative momentum of the two coincident protons is selected to lie along a specific direction, then the width of the suppression in the correlation function is predominantly sensitive to that particular spatial dimension. Measurements of the two-proton correlation function for three different directions of the relative momentum can, therefore, provide information about the shape of the relative Wigner function. The shape of the relative Wigner function depends on the lifetime of the emitting source: emission from a long-lived source would appear as a source that appears elongated in the direction of observation, i.e., in the direction parallel to the total momentum $\mathbf{P}=(\mathbf{p}_1+\mathbf{p}_2)$ of the two detected particles (Kopylov and Podgoretskii, 1972, 1973; Koonin, 1977; Pratt and Tsang, 1987; Awes *et al.*, 1988). Because of the stronger Pauli anticorrelation in the transverse direction, the transverse ($\mathbf{q}\perp\mathbf{P}$) correlation function of a long-lived source should exhibit a suppression relative to the longitudinal ($\mathbf{q}\parallel\mathbf{P}$) correlation function.

The directional dependence of two-proton correlation functions at intermediate energies was first investigated in experiments performed by Awes *et al.* (1988) for the $^{32}S+^{nat}Ag$ reaction at $E/A=22.3$ MeV and $\theta_{av}=30°$. The solid and open points in Fig. 20 show the measured longitudinal ($\theta[\mathbf{P},\mathbf{q}]=0°-30°$ or $150°-180°$) and transverse ($\theta[\mathbf{P},\mathbf{q}]=60°-120°$) two-proton correlation functions gated by total kinetic energies of $E_1+E_2=90-100$ MeV (part a) and $E_1+E_2=60-70$ MeV (part b). Within experimental errors, the longitudinal and the transverse correlation functions are very similar in shape, consistent with emission from a spherical source and inconsistent with emission from a long-lived compound nucleus (Awes *et al.*, 1988). To illustrate the correlations expected for

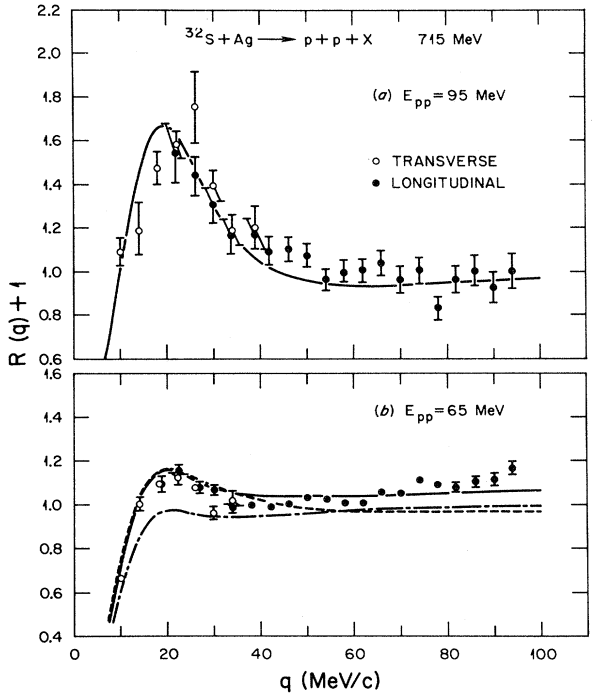

FIG. 20. Longitudinal (solid points) and transverse (open points) two-proton correlation functions measured for the ^{32}S+Ag reaction at $E/A=22.3$ MeV. (a) $E_1,E_2\geq 95\pm 5$ MeV; (b) $E_1,E_2\geq 65\pm 5$ MeV. Solid curves show predictions for spherical sources [(a) $r_{0L}=r_{0T}=4$ fm; (b) $r_{0L}=r_{0T}=6.5$ fm]. The dashed and dot-dashed curves show predictions for a nonspherical source $f\approx\exp[(x^2+y^2)/R_T^2+z^2/R_L^2]$ with $r_{0L}=20$ fm and $r_{0T}=4$ fm.

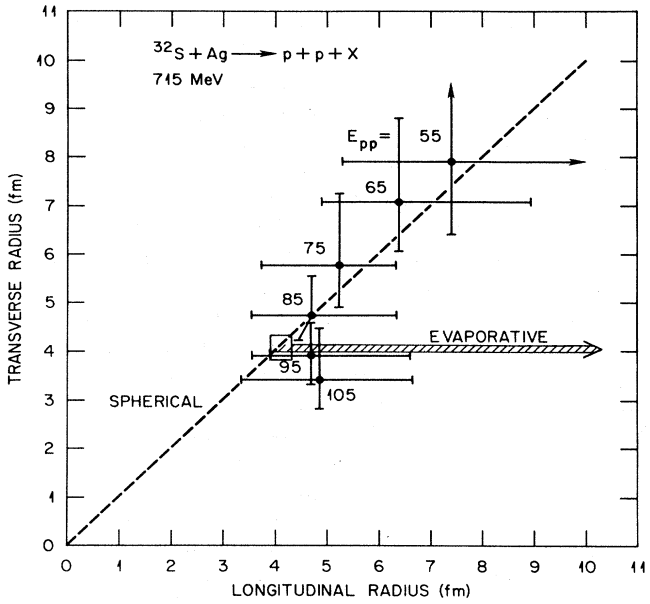

FIG. 21. Longitudinal and transverse radii extracted from the analysis of longitudinal and transverse two-proton correlation functions for the ^{32}S+^{nat}Ag reaction at $E/A=22.3$ MeV. The results are shown for different kinetic energies $E_{pp}=E_1+E_2$, ranging from 55 to 105 MeV. The errors reflect variations in the source dimensions which double the value of χ^2 (from Awes *et al.*, 1988).

nonspherical sources, part b of the figure shows calculations for an elongated source with longitudinal and transverse radii of $r_{0L}=20$ fm and $r_{0T}=4$ fm, respectively. The dashed curve shows the predicted longitudinal correlation function and the dot-dashed curve shows the predicted transverse correlation function, which clearly exhibits the enhanced Pauli suppression. The data are inconsistent with such a large ratio of the longitudinal to transverse dimensions of the source.

Figure 21 summarizes the energy dependence of the extracted source shapes (Awes *et al.*, 1988). High-energy protons appear to be emitted on a short time scale from a source of roughly compound-nuclear dimensions. Low-energy protons, on the other hand, appear to be emitted from a larger spherical source of up to twice the radius of the compound nucleus. This trend would not be expected for emission from a long-lived compound nucleus of lifetime τ and constant size. Such emissions would appear (Awes *et al.*, 1988) as an elongated source of fixed transverse dimension, $r_{0T}\approx 4$ fm, and elongated longitudinal dimension, $r_{0L}^2\approx r_{0T}^2+\tau^2P^2/4m_p^2$. Taken at face value, the measurements rule out lifetimes larger than $1-2\times 10^{-22}$ s.

In the exploding-source model of Pratt (1984), the correct geometry of the source is measured at low values of E_1+E_2. The system investigated in Fig. 2 shows $R_S(\mathbf{P}=0)\approx 0.8R_0$. The values of r_0 shown in Fig. 21 (particularly when extrapolated to small E_1+E_2) are much larger than the size of the target nucleus, making their interpretation in terms of an exploding source difficult. The understanding of these data awaits the development of more detailed microscopic descriptions of the reaction, particularly emission from compound nuclei (see Sec. VI.C).

D. Correlations between complex particles

Composite particles are emitted with large probability in intermediate-energy heavy-ion reactions. Because of their larger reaction cross sections, composite particles may be expected to interact for a longer reaction time and may be emitted from sources of lower densities than, for example, pions or protons (Boal and Shillcock, 1986). The simultaneous investigation of correlations between several light-particle pairs, including composite light particles, may offer a unique tool to investigate the dynamical expansion of the reaction zone.

Correlation functions involving composite light particles have been investigated by a number of authors (Kohmoto *et al.*, 1982; Chitwood *et al.*, 1985, 1986; Pochodzalla *et al.*, 1985b, 1987; Kyanowski *et al.*, 1986; Pochodzalla, Chitwood, *et al.*, 1986; Pochdzalla, Gelbke, *et al.*, 1986; Chen *et al.*, 1987a, 1987b, 1987c, 1987d; Trockel *et al.*, 1987; Fox *et al.*, 1988; Cebra *et al.*, 1989;

DeYoung *et al.*, 1989). A number of investigations have exploited the long-range Coulomb interaction between the emitted particles to extract information about the lifetime of the emitting system (Kohmoto *et al.*, 1982; Trockel *et al.*, 1987; DeYoung *et al.*, 1989). However, most measurements have been performed for fast, nonequilibrium emission processes with the intent of extracting source dimensions.

Figure 22 gives an example for αd correlation functions, measured (Chen *et al.*, 1987c) for the $^{16}O+^{197}Au$ reaction at $E/A=94$ MeV. The αd correlation functions exhibit a sharp peak due to the 2.186-MeV state in ^6Li ($J^\pi=3^+$, $\Gamma=24$ keV, $\Gamma_\alpha/\Gamma_{tot}=1.00$) and a broad peak due to the overlapping states at 4.31 MeV ($J^\pi=2^+$, $\Gamma=1.3$ MeV, $\Gamma_\alpha/\Gamma_{tot}=0.97$) and 5.65 MeV ($J^\pi=1^+$, $\Gamma=1.9$ MeV, $\Gamma_\alpha/\Gamma_{tot}=0.74$); see Sec. VI.A. Consistent with the qualitative trend established for two-proton correlation functions, these peaks increase in magnitude for more energetic αd pairs. Theoretical correlation functions, calculated for Gaussian sources of negligible lifetime (Boal and Shillcock, 1986), are shown by the solid and dashed curves. Because of the narrow width of the 2.186-MeV state in ^6Li, the theoretical αd correlation function is corrected in the figure for the finite resolution of the experimental apparatus (Chen *et al.*, 1987c) by folding the original calculation with a Gaussian of appropriate width. Source radii have been extracted (Chen *et al.*, 1987c) from the integrated αd correlation $R_{eff}=\int R(q)dq$ with the integration performed over the range of $q=30$–60 MeV/c; this procedure is less sensitive to uncertainties of the experimental line shape (Chen *et al.*, 1987d). Source radii extracted from the broad peak of the αd correlation function at $q=85$ MeV/c are larger by about 1 fm than those extracted from the sharp peak at $q=40$ MeV/c; such discrepancies have also been noted by Chen *et al.* (1987d) and Pochodzalla, Chitwood, *et al.* (1986), but they are not yet understood.

Figure 23 compares source radii extracted from pp (left-hand side) and αd (right-hand side) correlation functions measured for ^{14}N-, ^{40}Ar-, and ^{16}O-induced reactions on ^{197}Au at $E/A=35$, 60, and 94 MeV, respectively (Pochodzalla, Chitwood, *et al.*, 1986; Pochodzalla *et al.*, 1987; Chen *et al.*, 1987c). In all cases, smaller source radii are extracted for more energetic particles, indicating that these particles are emitted at shorter time intervals and/or from smaller sources. Because of the strong energy dependence, direct comparisons between the source radii extracted from αd and pp correlation functions cannot be performed without a certain level of ambiguity. Nevertheless, radii extracted from the sharp peak of the αd correlation function (at $q\approx40$ MeV/c) tend to be slightly smaller than those extracted from pp correlation functions. Note, however, that slightly larger values of r_0 are extracted from the broad peak of the αd correlation function (at $q\approx85$ MeV/c).

Significant correlations are also observed between two particles for which the interaction does not exhibit resonant features. As an example, Fig. 24 shows two-deuteron correlation functions measured for ^{40}Ar-induced reactions on ^{197}Au at $E/A=60$ MeV (Pochodzalla *et al.*, 1987). The correlation functions exhibit a pronounced minimum at small relative momenta, which becomes more pronounced with increasing energy of the emitted particles. The curves show several calculations

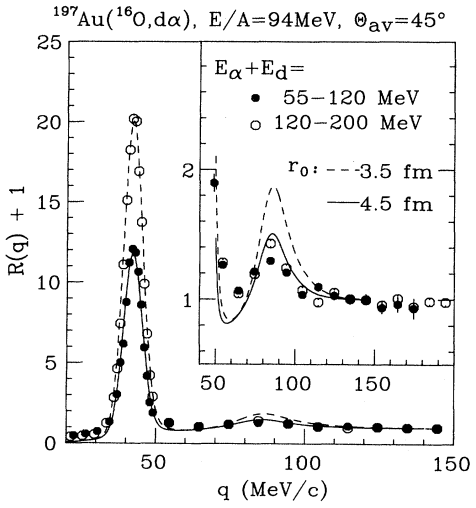

FIG. 22. Correlation functions for the αd pair measured for the $^{16}O+^{197}Au$ reaction at $E/A=94$ MeV and $\theta_{av}=45°$. The constraints on the total kinetic energy, E_1+E_2, of the αd pair are indicated in the figure. The curves show calculations (Boal and Shillcock, 1986) for Gaussian sources of negligible lifetime with the radius parameters indicated in the figure (from Chen *et al.*, 1987c).

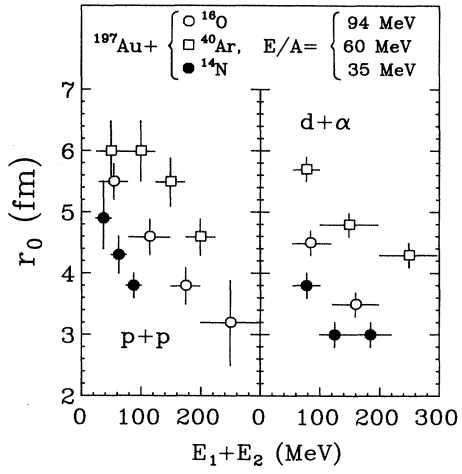

FIG. 23. Source parameters r_0 extracted from pp correlation functions (left-hand side) and αd correlation functions (right-hand side) for the following reactions: ●, $^{14}N+^{197}Au$ at $E/A=35$ MeV and $\theta_{av}=35°$ (from Pochodazalla, Chitwood, *et al.*, 1986); □, $^{40}Ar+^{197}Au$ at $E/A=60$ MeV and $\theta_{av}=30°$ (from Pochodzalla *et al.*, 1987); ○, $^{16}O+^{197}Au$ at $E/A=94$ MeV and $\theta_{av}=45°$ (from Chen *et al.*, 1987c). The dependence on the total kinetic energy, E_1+E_2, of the two coincident particles is shown (from Chen *et al.*, 1987c).

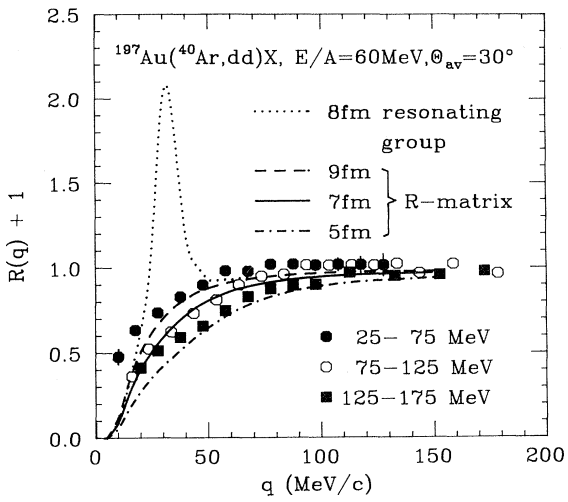

FIG. 24. Two-deuteron correlation functions measured for the ^{40}Ar+^{197}Au reaction at $E/A=60$ MeV and $\theta_{av}=30°$. The constraints on the sum energy, E_1+E_2, are given in the figure. The calculations are explained in the text (from Pochodzalla *et al.*, 1987).

(Chitwood *et al.*, 1985; see Sec. VI.A) for Gaussian sources of negligible lifetime. The dotted curve represents calculations based on deuteron-deuteron phase shifts extracted by the resonating group method (Chwieroth, Tang, and Thompson, 1972). These phase shifts exhibit a resonant behavior in the $l=1$ partial wave at energies below 2 MeV. The predicted maximum of the correlation function at low relative momenta is not, however, observed experimentally. The dashed, solid, and dot-dashed curves represent calculations based on the phase shifts of Hale and Dodder (1984) and are seen to be in better agreement with the data. Radius parameters extracted from two-deuteron correlation functions are considerably large than those extracted from *pp* or *αd* correlation functions (Chitwood *et al.*, 1985; Pochodzalla, Chitwood, *et al.*, 1986; Pochodzalla *et al.*, 1987; Chen *et al.*, 1987c; Fox *et al.*, 1988; Cebra *et al.*, 1989). Such differences could indicate that correlations between different light-particle pairs are sensitive to different stages of the reaction. They could, however, also reflect uncertainties in the *dd* interaction for which coupled-channel effects may not be negligible.

The shapes of two-triton correlation functions are qualitatively similar to those of two-deuteron correlation functions. A number of authors have extracted source parameters from *tt* correlation functions (Pochodzalla, Chitwood, *et al.*, 1986; Pochodzalla *et al.*, 1987; Fox *et al.*, 1988; Cebra *et al.*, 1989), using calculations based on Coulomb interactions only or on Coulomb plus *s*-wave nuclear interactions between the tritons (see Sec. VI.A). The extracted source radii are generally larger than those extracted from *pp* and *αd* correlations and are comparable to those extracted from *dd* correlations. However, the uncertainties of the triton-triton interaction are even larger than those for the deuteron-deuteron interaction. The resulting errors are unknown.

Quantitative analyses of two-particle correlation functions generally neglect distortions of the relative wave function by the Coulomb field of the residual nuclear system (Gyulassy, Kauffmann, and Wilson, 1979; see Sec. III.D). Such Coulomb distortions are expected to be less important for the case of narrow resonances, which decay at large distances from the emitting nuclear system, or for particles with identical charge-to-mass ratios, which experience similar accelerations in the Coulomb field. Coulomb distortions, however, are not negligible for light particles of different charge-to-mass ratio when their interaction at small relative momenta is dominated by short-lived resonances or when their interaction is nonresonant (Pochodzalla *et al.*, 1985b, 1987; Pochodzalla, Gelbke, *et al.*, 1986).

An example of line-shape distortions due to final-state interactions with the Coulomb field of the residual nuclear system is given in Fig. 25 (Pochodzalla, Gelbke, *et al.*, 1985). The figure shows $p\alpha$ correlation functions measured for ^{40}Ar-induced reactions on ^{197}Au at $E/A=60$ MeV and $\theta_{av}=30°$. For these correlation functions the summation in Eq. (7.2) is performed with the constraints $v_\alpha<v_p$ (open points) and $v_\alpha>v_p$ (solid points), where v_α and v_p denote the laboratory velocities of alpha particles and protons, respectively. The experimental correlation functions exhibit two pronounced maxima located at $q=15$ and 50 MeV/c. While the location of the first maximum ($q=15$ MeV/c) is the same for both kinematic branches, the location of the second maximum ($q=50$ MeV/c) is not. The peak near $q=15$ MeV/c is due to the detection of two of the three fragments from the two-stage decay $^9\mathrm{B}\rightarrow p+^8\mathrm{Be}\rightarrow p+(\alpha+\alpha)$; it is a result of the small decay energies and the narrow widths of the ground states of ^{9}B and ^{8}Be (Po-

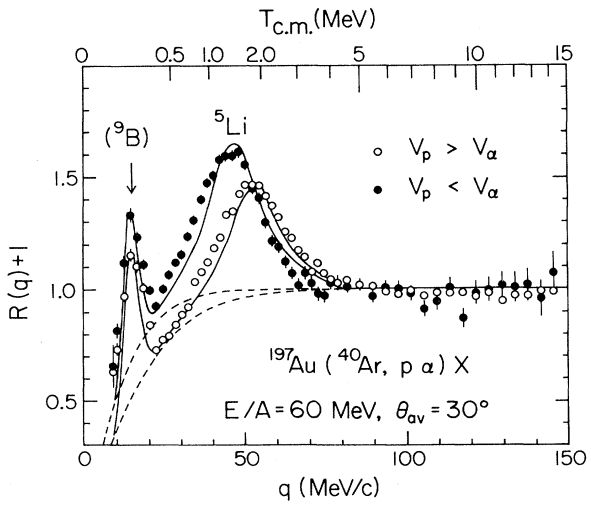

FIG. 25. Correlation function for coincident protons and alpha particles for the ^{40}Ar+^{197}Ar reaction at $E/A=60$ MeV and $\theta_{av}=30°$. Open and solid points correspond to the constraints $v_\alpha<v_p$ and $v_\alpha>v_p$, respectively (from Pochodzalla, Gelbke, *et al.*, 1985).

chodzalla, Gelbke, *et al.*, 1985). Because of the long lifetimes of these states, distortions in the Coulomb field of the residual nucleus are negligible. The peak near $q=50$ MeV/c is related to the unbound ground state of ^{6}Li, which has a width of about 1.5 MeV corresponding to a short mean life of about $\tau=130$ fm/c (see Sec. VI.A). Since the charge-to-mass ratio of protons is greater than that of alpha particles, the former will experience greater accelerations in the Coulomb field of the residual nuclear system. As a consequence, the asymptotic velocity difference between protons and alpha particles will be decreased if $v_\alpha > v_p$ at the time of decay and increased if $v_\alpha < v_p$. The solid lines in Fig. 25 show the results of simple classical calculations for this effect (Pochodzalla, Gelbke, *et al.*, 1985). Source radii can be extracted from the αp correlation function with fair accuracy when these line-shape distortions are taken into account. However, one should bear in mind that such corrections can be associated with considerable uncertainties, especially when the charge distribution of the emitting system is unknown.

The situation is even more complicated for proton-deuteron correlations. These two particles have different charge-to-mass ratios and experience nonresonant final-state interactions (see Sec. VI.A). For nonresonant systems, the Coulomb distortion already sets in at the point of emission, where the Coulomb force is strongest. Since the correlation functions for nonresonant systems are rather featureless, the effects of the Coulomb distortions are more difficult to unravel. A number of investigations have revealed significant distortions of the shapes of the experimental *pd* correlation functions due to Coulomb interactions with the residual nuclear system (Pochodzalla, Gelbke, *et al.*, 1986; Pochodzalla *et al.*, 1987). In those cases, a quantitative extraction of source dimensions from *pd* correlation functions has not been possible. Some analyses of *pd* correlation functions ignore these complications (Cebra *et al.*, 1989; Fox *et al.*, 1988) and extract radii even larger than the radii for the *dd* correlations.

Source radii extracted from correlations between different particle pairs are compared by Pochodzalla, Chitwood, *et al.* (1986), Pochodzalla *et al.* (1987), Fox *et al.* (1988), and Cebra *et al.* (1989). Table XII summarizes the results of Cebra *et al.* (1989) and Fox *et al.* (1988), who investigate energy-integrated correlation functions. Cebra *et al.* (1989) concluded that the observed correlations are insensitive to the details of the emitting system. This conclusion may be premature. Energy-integrated correlation functions depend strongly on the detection threshold and contain less information than energy-dependent correlation functions. In addition, the uncertainties in the extracted source radii are large, and more accurate measurements are needed to firmly establish similarities or differences between the two reactions.

TABLE XII. Source radii extracted from energy-integrated two-particle correlation functions measured for the reactions $p+{}^9$Be and $p+$Ag at $E_p=500$ MeV and $\theta_{av}=65°$ (Cebra *et al.*, 1989) and ^{14}N+Ag at $E/A=35$ MeV and $\theta_{av}=45°$ (Fox *et al.*, 1988).

Particle pair	r_0 (fm) $p+$Be	$p+$Ag	^{14}N+Ag
pp	3.3±1.1	4.0±0.5	4.5±0.3
dd	9±5	9.4±2.1	7.3±0.7
tt	10±6	11±8	5.9±0.8
pd	12.2±2.6	11.8±1.6	9.1±0.7
$p\alpha$	1.6±1.8	1.8±1.2	4.6±0.3
$d\alpha$	1.9±1.2	2.0±1.1	4.9±0.4

Energy-dependent two-particle correlation functions have been measured for the reactions ^{14}N+^{197}Au at $E/A=35$ MeV and $\theta_{av}=35°$ (Pochodzalla, Chitwood, *et al.*, 1986) and ^{40}Ar+^{197}Au at $E/A=60$ MeV and $\theta_{av}=30°$ (Pochodzalla *et al.*, 1987). The results are summarized in Table XIII. The extracted source parameters exhibit considerable dependences on the reaction, the particular particle pair, and the kinetic energy of the emitted particles. However, the wealth of information contained in the various experimental correlation functions cannot yet be fully exploited since present microscopic treatments of intermediate-energy nucleus-nucleus collisions have not yet been used to calculate two-particle correlations. The detailed interpretation of the energy dependence of the two-particle correlations remains a challenging theoretical problem.

E. Filtered correlation functions

While inclusive two-particle correlations provide insight into the average properties of the emitting system, more detailed information must be obtained from more exclusive measurements in which specific classes of reactions can be suppressed or enhanced. Ideal reaction filters would allow the determination of the impact parameter and the orientation of the reaction plane. For intermediate-energy heavy-ion reactions, the development and calibration of various possible reaction filters is still a topic of ongoing research (Ogilvie *et al.*, 1989; Tsang, Bertsch, *et al.*, 1989; Tsang, Kim, *et al.*, 1989). One can for example, discriminate between quasielastic and more violent, fusionlike projectile-target interaction by measuring the linear momentum transfer to the heavy reaction residue. Alternatively, one can classify the violence of the projectile-target interactions in terms of the light-particle multiplicity. At lower energies, $E/A<50$ MeV, the two techniques provide similar selectivities (Tsang, Kim, *et al.*, 1989): Violent collisions involving a large overlap between projectile and target nuclei can be selected by large linear momentum transfers or large particle multiplicities. Less violent peripheral interactions can be selected by small linear momentum transfers or small charged-particle multiplicities. With increasing projectile energy, however, multiplicity measurements become the tool of choice (Tsang, Bertsch, *et al.*, 1989).

TABLE XIII. Source radii extracted from two-particle correlation functions measured for the reactions $^{14}N+^{197}Au$ at $E/A=35$ MeV and $\theta_{av}=35°$ (Pochodzalla, Chitwood, *et al.*, 1986) and $^{40}Ar+^{197}Au$ at $E/A=60$ MeV and $\theta_{av}=30°$ (Pochodzalla *et al.*, 1987). The analysis of the αd correlation function is based on fits to the peak at $q\approx 40$ MeV/c. The errors include normalization uncertainties for the different energy gates; theoretical uncertainties are not assessed. Note that nuclear interactions for $l>0$ were omitted in the calculations of the tt correlation function.

Particle pair	$^{14}N+^{197}Au$ $E/A=35$ MeV E_1+E_2 (MeV)	r_0 (fm)	$^{40}Ar+^{197}Au$ $E/A=60$ MeV E_1+E_2 (MeV)	r_0 (fm)
pp	24–50	4.9±0.5	25–75	$6.0^{+0.5}_{-1.0}$
	50–75	4.3±0.3	75–125	6.0±0.5
	75–100	3.8±0.2	125–175	5.5±0.4
			175–225	4.6±0.3
dd	30–80	8±2	25–75	10±3
	80–160	5.5±1	75–125	7±2
			125–175	6±2
			175–225	5±1
			225–275	4±1
tt	36–120	6.5±1	36–100	7.5±1.5
	120–200	5.5±1	100–180	6±1.5
			180–260	6±1.5
$p\alpha$	52–100	6±0.5	52–125	$7.5^{+0.5}_{-1.0}$
	100–150	5±0.5	125–200	6.7±0.4
	150–200	4±0.5	200–300	5.9±0.3
$d\alpha$	55–100	3.8±0.2	55–100	5.7±0.2
	100–150	3.0±0.2	100–200	4.8±0.2
	150–220	3.0±0.2	200–300	4.3±0.2
			300–400	4.4±0.2

The dependence of two-particle correlation functions on the multiplicity of the emitted light particles has not yet been measured for intermediate-energy nucleus-nucleus collisions. A first step in this direction has been undertaken by Kyanowski *et al.* (1986) for the $^{40}Ar+^{197}Au$ reaction at $E/A=60$ MeV and $\theta_{av}=30°$. They classify the reactions in terms of the number ν of charged particles detected in a forward-angle scintillator array covering an angular range of about $\theta_{av}=5°-30°$. The αd correlation function is found to depend strongly on ν. Correlation functions gated on small values of ν exhibit very pronounced maxima, whereas correlations gated on large values of ν are strongly suppressed. Source radii extracted from energy-integrated correlation functions vary from $r_0\approx 4.5$ fm for $\nu=0$ to $r_0\approx 8$ fm for $\nu=11$. Unfortunately, the number of particles emitted at forward angles does not exhibit a unique dependence on impact parameter (Tsang, Bertsch, *et al.*, 1989; Tsang, Kim, *et al.*, 1989). The interpretation of these results remains unclear.

Information about the linear momentum transfer can be extracted from the folding angle θ_{ff} between two coincident fission fragments (Sikkeland, Haines, and Viola, 1962; Back *et al.*, 1980). Because of kinematic focusing, small folding angles ($\theta_{ff}\ll 180°$) correspond to large linear momentum transfers, and large folding angles ($\theta_{\rm eff}\approx 180°$) represent small momentum transfers. Two-particle correlation functions gated on folding angles have been measured by Chen *et al.* (1987a, 1987d) for the $^{14}N+^{197}Au$ reaction at $E/A=35$ MeV and $\theta_{av}=20°$. Figures 26 and 27 show pp and αd correlation functions,

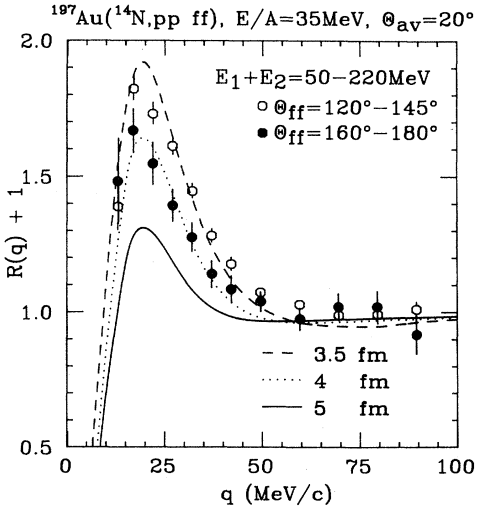

FIG. 26. Two-proton correlation functions gated on large ($\theta_{ff}=120°-145°$, open points) and small ($\theta_{ff}=160°-180°$, solid points) linear momentum transfers to the heavy reaction residue. The gate on the total kinetic energy is indicated in the figure (from Chen *et al.*, 1987d).

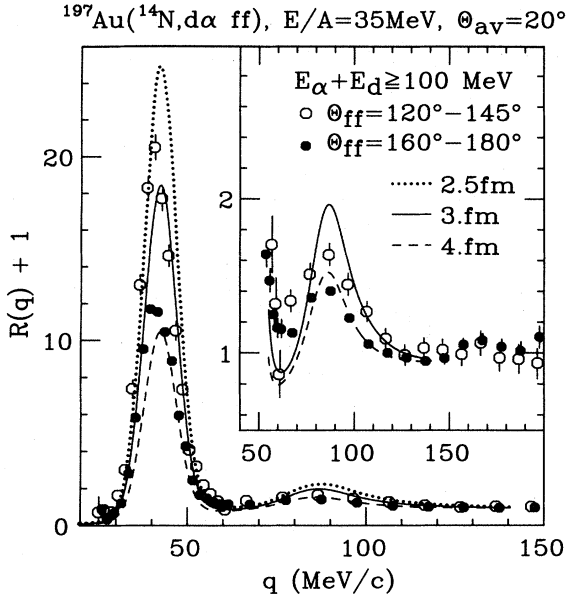

FIG. 27. Correlation functions for the αd pair gated on large ($\theta_{ff}=120°-145°$, open points) and small ($\theta_{ff}=160°-180°$, solid points) linear momentum transfers to the heavy reaction residue. The gate on the total kinetic energy is indicated in the figure (from Chen *et al.*, 1987d).

respectively, gated on small ($\theta_{ff}=160°-180°$, solid points) and large ($\theta_{ff}=120°-145°$ open points) linear momentum transfers (Chen *et al.*, 1987d). In order to reduce contributions from later stages of the reaction for which sequential emission of low-energy particles from the fully equilibrated composite system may be important, these correlations are gated on total energies well above the compound-nucleus Coulomb barrier. In both cases the selection of events with large linear momentum transfer produces enhanced correlations. For orientation the curves show theoretical correlation functions for Gaussian sources of negligible lifetime with the radius parameters indicated in the figures. From the two-proton correlation functions shown in Fig. 26, source radii of $r_0=3.7$ and 4.0 fm are extracted for the central and peripheral collisions gates; from the sharp peak of the αd correlation functions shown in Fig. 27, source radii of $r_0=2.8$ and 3.6 fm are extracted (Chen *et al.*, 1987d). Source radii extracted from the broad peak at $q=85$ MeV/c are larger by about 0.8 fm. Consistent with the results from inclusive measurements these source dimensions are slightly smaller than the size of the target nucleus [$r_0(\mathrm{Au})=4.4$ fm].

A strictly geometric interpretation of the correlation functions would imply that quasielastic collisions are characterized by sources significantly larger than the size of the projectile nucleus [$r_0(\mathrm{N})\approx 2.1$ fm]; furthermore, it would imply that quasielastic collisions produce sources of larger dimensions than fusionlike collisions. Such implications are difficult to understand. The observation of reduced correlations for peripheral processes could also reflect longer emission time scales rather than larger source dimensions. For example, sequential decays of excited and fully equilibrated projectile residues could involve longer emission time scales than preequilibrium reactions; such longer emission time scales would lead to reduced correlations (Chen *et al.*, 1987d). Measurements of longitudinal and transverse two-proton correlation functions could clarify this issue.

Figure 28 summarizes the present information about the dependences of αd correlation functions on the total energy per nucleon, $(E/A)_{\mathrm{tot}}=[E_\alpha+E_d]/6$, of the two coincident particles, on emission angle, and on reaction type for $^{14}\mathrm{N}+^{197}\mathrm{Au}$ collisions at $E/A=35$ MeV (Chen *et al.*, 1987a). Inclusive correlations and correlations measured in coincidence with fission fragments are shown in the right- and left-hand parts of the figure, respectively. The left-hand scale of the figure gives the integral correlation $R_{\mathrm{eff}}=\int R(q)dq$ with the integration range of $q=30-60$ MeV/c. The right-hand scale of the figure gives Gaussian source radii r_0, extracted in the limit of negligible lifetime. At low energies, the αd correlations are of comparable magnitude. For small linear momentum transfers, they are nearly independent of energy. For larger linear momentum transfers, on the other hand, the αd correlations depend strongly on energy. For inclusive correlations shown in the right-hand part of the figure, a similar energy dependence exists. It becomes more pronounced at larger emission angles, where contributions from quasielastic processes become less important, thus lending support to the previous conclusion that contributions from the decay of equilibrated projectile residues lead to reduced two-particle correlations.

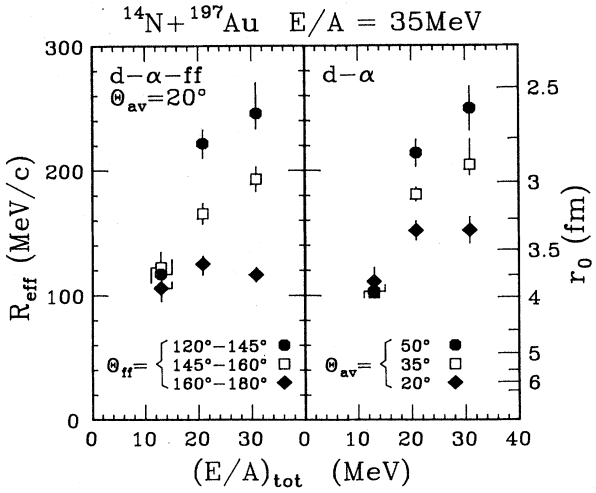

FIG. 28. Dependence of αd correlations on the total energy per nucleon of the outgoing particles. Correlations measured inclusively and in coincidence with fission fragments are shown in the right-hand and left-hand parts, respectively. The left-hand scale corresponding to $R_{\mathrm{eff}}=\int R(q)dq$, with the integration performed over the range of $q=30-60$ MeV. The right-hand scale gives source radii r_0 for Gaussian sources of negligible lifetime (from Chen *et al.*, 1987a).

VIII. SUMMARY AND DISCUSSION

Two-particle correlation functions contain useful information about the space-time characteristics of radiation sources when the emitted radiation is at least partially incoherent. Such incoherence could arise from a complete randomization of the phase relation between the wave functions describing individual emission processes, as should be the case for emission from thermal systems. It would also apply if, at least in principle, the contributions from individual emission processes could be determined by a more complete experiment performed on the remainder of the system. Coherent emission destroys such information. For example, in optical applications, intensity interferometric techniques can be applied to measure the dimensions of stars and galaxies for which the individual photons are emitted incoherently. In contrast, the diameter of a coherent laser beam can be measured through a correlation function if the beam is first made incoherent, for example, by passage through a ground-glass screen.

For subatomic particles, measurable two-particle correlations arise from final-state interactions and, for the case of identical particles, from the required symmetrization (or antisymmetrization) of the two-particle wave function. Both effects depend on the size of the emitting system. The correlation function can be written as the sum of an interaction term and a plane-wave term. Roughly speaking, the interaction term corresponds to the ratio of the number of resonances (which is independent of the source volume) to the number of standing waves (which does depend on the source volume). The plane-wave term is the Fourier transform of the source function.

Present microscopic theories do not yet allow the calculation of two-particle correlation functions. Insights gleaned from measured two-particle correlations are, therefore, largely qualitative. Existing experimental information is still scarce, and only a few attempts have been made to explore the systematic dependence of two-particle correlation functions on various reaction parameters, such as the incident energy, the mass of target and projectile, the energy dependence of the emitted particles, or the impact parameter of the collision. Nevertheless, some systematic dependences begin to emerge.

In general, the measured two-particle correlation functions depend on the total momentum of the emitted particle pair. The magnitude of the correlations increases with increasing total momentum or, equivalently, with increasing kinetic energy of the coincident particles. Accordingly, the extracted source dimensions decrease when more energetic particles are detected. Such a dependence has been observed in nucleus-nucleus collisions at both high and intermediate energies. It cannot be understood in terms of emission from a single stationary source. Qualitatively, these observations have been associated with the expansion of the reaction zone or, for reactions at lower energies, with increasing time intervals between successive emission processes. More quantitative tests of existing reaction models have been performed only at lower energies.

The dependence of the experimental two-particle correlation functions on the impact parameter of the collision remains largely unexplored. A number of investigations performed for nucleus-nucleus and elementary-particle collisions at relativistic energies report source dimensions that increase as a function of the associated charged-particle multiplicity. But not all experiments confirm this effect. At lower energies the situation is less clear due to difficulties in finding observables that are uniquely related to the impact parameter and due to the possible importance of temporal effects.

A number of groups have extracted source dimensions in directions parallel and perpendicular to the beam axis from two-pion correlation functions measured for nucleus-nucleus collisions at relativistic energies. The individual results are difficult to reconcile: different groups find evidence for sources of rather different shapes for rather similar systems and incident energies. More experiments with better statistical accuracy are needed to clarify the situation.

Information on the degree of incoherence of the emitting system has been obtained from two-pion correlation measurements at relativistic energies. In these investigations the magnitude of the experimental correlation function at zero relative momentum has been characterized in terms of an incoherence parameter λ. Most experimental investigations find that λ is less than unity. Unfortunately, this potentially interesting finding has not yet been brought into contact with some more fundamental property of the emitting system. Distortions due to impact-parameter averaging, contributions from resonance decays and many other aspects of reaction history and measurement may have non-negligible effects on the extraction of λ; these effects are largely unknown. At the present time it is unclear whether the concept of incoherence is useful in nucleus-nucleus collisions.

Interesting similarities exist between two-pion correlation measurements performed for ultrarelativistic p-p and nucleus-nucleus collisions. Within the experimental uncertainties both reactions show the same functional relation between extracted source radii and associated multiplicity per unit rapidity. This relationship must be understood in depth before two-pion interferometry measurements can be used as a diagnostic tool to signal the formation of the quark-gluon plasma.

At relativistic energies few attempts have been made to cross calibrate the two-pion and two-proton correlation experiments. Quantitative comparisons of existing data are hampered by large experimental uncertainties and different gating conditions applied to individual measurements. In most cases the dependence of the extracted source radii on the total momentum of the emitted particle pair is not sufficiently well known to allow definitive conclusions. A detailed comparison for one specific reaction would be highly valuable.

For nucleus-nucleus collisions at intermediate energies, source radii have been extracted for a number of different particle combinations emitted in the same reaction. Different source radii were extracted for different particle pairs even when dependences upon the energy of the emitted particle pair have been taken into account. Such differences may be related to the sequential freeze-out of different degrees of freedom, which could be expected for realistic treatments of the final stages of the reaction. Specific degrees of freedom are expected to freeze out at different average densities because of differences in the interaction cross sections between individual constituents. Quantitative calculations that take such effects into account have not yet been compared to the data.

Finite-lifetime effects may give information on reaction dynamics in intermediate-energy heavy-ion collisions. For example, the latent heat of a first-order phase transition would affect the apparent source lifetime. First measurements of longitudinal and transverse correlation functions find evidence for spherical systems whose apparent size decreases with total pair momentum and whose lifetimes are shorter than $1-2\times10^{-22}$ s. Yet a number of observations are difficult to reconcile with purely geometric interpretations of the measured two-proton correlation functions: Correlation functions measured in regions of phase space for which compound-nucleus decays are expected to dominate are strongly attenuated. In such cases purely geometric interpretations are clearly unphysical. For low-energy nucleus-nucleus collisions, compound-nucleus lifetimes were estimated via Coulomb trajectory calculations. The determination of shorter time scales believed to prevail for noncompound emission in intermediate-energy heavy-ion reactions remains a challenge.

ACKNOWLEDGMENTS

The authors wish to thank G. Bertsch, M. Gyulassy, and S. Pratt for many useful discussions and M. Fincke-Keeler for providing data and figures from the UA1 experiment. This work is supported in part by the Natural Sciences and Engineering Research Council of Canada and by the National Science Foundation.

REFERENCES

Abramowitz, M., and I. A. Stegun, 1964, *Handbook of Mathematical Functions* (National Bureau of Standards, Washington, D.C.).

Adamus, M., I. V. Ajinenko, Yu. A. Belokopytov, V. A. Berezhnoy, H. Bottcher, P. V. Chliapnikov, F. Crijns, A. De Roeck, E. A. De Wolf, K. Dziunikowska, A. M. F. Endler, P. F. Ermolov, A. Eskreys, H. Graessler, R. Sh. Hakobyan, P. van Hal, T. Haupt, L. P. Kishinevskaya, W. Kittel, A. I. Kurnosenko, B. B. Levchenko, J. Makela, F. Meijers, A. B. Michalowska, V. I. Nikolaenko, L. C. S. Oliveira, K. Olkiewicz, E. Riipinen, H. F. Roloff, V. M. Ronjin, A. M. Rybin, H. M. T. Saarikko, W. Schmitz, L. Scholten, J. Stepaniak, O. G. Tchikilev, A. G. Tomaradze, V. A. Uvarov, F. Verbeure, R. Wischnewski, and S. A. Zotkin, 1988, Z. Phys. C **37**, 347.

Agakishiev, G. N., D. Armutaliiski, N. Akhababyan, E. Bartke, E. Bogdanovich, A. P. Gasparyan, N. S. Grigalashvili, V. G. Grishin, L. A. Didenko, I. A. Ivanovskaya, T. Kanarek, E. N. Kladnitskaya, M. Kowalski, D. K. Kopylova, V. B. Lyubimov, Z. V. Metreveli, R. R. Mekhtiev, V. F. Nikitina, V. M. Popova, M. I. Solov'ev, A. N. Solomin, G. P. Toneeva, A. P. Cheplakov, and L. M. Shcheglova, 1984, Yad. Fiz. **39**, 543 [Sov. J. Nucl. Phys. **39**, 344 (1984)].

Aihara, H., M. Alston-Garnjost, J. A. Bakken, A. Barbaro-Galtieri, A. V. Barnes, B. A. Barnett, H.-U. Bengtsson, B. J. Blumenfeld, A. D. Bross, C. D. Buchanan, O. Chamberlain, C-Y. Chien, A. R. Clark, A. Cordier, O. I. Dahl, C. T. Day, K. A. Derby, P. H. Eberhard, D. L. Fancher, H. Fujii, T. Fujii, B. Gabioud, J. W. Gary, W. Gorn, N. J. Hadley, J. M. Hauptman, W. Hofmann, J. E. Huth, J. Hylen, T. Kamae, H. S. Kaye, R. W. Kenney, L. T. Kerth, R. I. Koda, R. R. Kofler, K. K. Kwong, J. G. Layter, C. S. Lindsey, S. C. Loken, X. Q. Lu, G. R. Lynch, L. Madansky, R. J. Madaras, K. Maruyama, J. N. Marx, J. A. J. Matthews, S. O. Melnikoff, W. Moses, P. Nemethy, D. R. Nygren, P. J. Oddone, D. A. Park, A. Pevsner, M. Pripstein, P. R. Robrish, M. T. Ronan, R. R. Ross, F. R. Rouse, R. R. Sauerwein, G. Shapiro, M. D. Shapiro, B. C. Shen, W. E. Slater, M. L. Stevenson, D. H. Stork, H. K. Ticho, N. Toge, R. F. van Daalen Wetters, G. J. VanDalen, R. van Tyen, E. M. Wang, M. R. Wayne, W. A. Wenzel, H. Yamamoto, M. Yamauchi, and W.-M. Zhang, 1985, Phys. Rev. D **31**, 996.

Åkesson, T., M. G. Albrow, S. Almehed, R. Batley, O. Benary, H. Boggild, O. Botner, H. Breuker, H. Brody, V. Burkert, A. A. Carter, J. R. Carter, P. Cecil, S. U. Chung, W. E. Cleland, D. Cockerill, S. Dagan, E. Dahl-Jensen, I. Dahl-Jensen, P. Dam, G. Damgaard, S. Eidelman, W. M. Evans, C. W. Fabjan, P. Frandsen, S. Frankel, W. Frati, M. Gibson, U. Goerlach, H. Gordon, K. H. Hansen, B. Heck, V. Hedberg, J. Hiddleston, H. J. Hilke, J. Hooper, G. Jarlskog, P. Jeffreys, A. Kalinovsky, G. Kesseler, T. Killian, R. Kroeger, K. Kulka, J. van der Lans, J. Lindsay, D. Lissauer, B. Lorstad, T. Ludlam, A. Markou, N. A. McCubbin, U. Mjornmark, R. Moller, W. Molzon, B. S. Nielson, A. Nilsson, L. H. Olsen, Y. Oren, L. Rosselet, E. Rosso, A. Rudge, R. Schindler, M. Sullivan, G. Thorstenson, E. Vella, J. Williamson, W. J. Willis, M. Winik, W. Witzeling, C. Woody, and W. A. Zajc, 1983, Phys. Lett. **129B**, 269.

Åkesson, T., M. G. Albrow, S. Almehed, R. Batley, O. Benary, H. Boggild, O. Botner, H. Breuker, H. Brody, V. Burkert, A. A. Carter, J. R. Carter, P. Cecil, S. U. Chung, W. E. Cleland, D. Cockerill, S. Dagan, E. Dahl-Jensen, I. Dahl-Jensen, P. Dam, G. Damgaard, S. Eidelman, W. M. Evans, C. W. Fabjan, P. Frandsen, S. Frankel, W. Frati, M. Gibson, U. Goerlach, H. Gordon, K. H. Hansen, B. Heck, V. Hedberg, J. Hiddleston, H. J. Hilke, J. Hooper, G. Jarlskog, P. Jeffreys, A. Kalinovsky, G. Kesseler, T. Killian, R. Kroeger, K. Kulka, J. van der Lans, J. Lindsay, D. Lissauer, B. Lorstad, T. Ludlam, A. Markou, N. A. McCubbin, U. Mjornmark, R. Moller, W. Molzon, B. S. Nielson, A. Nilsson, L. H. Olsen, Y. Oren, L. Rosselet, E. Rosso, A. Rudge, R. Schindler, M. Sullivan, J. A. Thompson, G. Thorstenson, E. Vella, J. Williamson, W. J. Willis, M. Winik, W. Witzeling, C. Woody, and W. A. Zajc, 1985, Phys. Lett. B **155**, 128.

Åkesson, T., M. G. Albrow, S. Almehed, O. Benary, H. Boggild, O. Botner, H. Breuker, V. Burkert, A. A. Carter, J. R. Carter, W. E. Cleland, S. Dagan, E. Dahl-Jensen, I. Dahl-Jensen, G. Damgaard, C. W. Fabjan, U. Goerlach, K. H. Han-

sen, V. Hedberg, G. Jarlskog, R. Kroeger, K. Kulka, D. Lissauer, B. Lorstad, A. Markou, N. A. McCubbin, U. Mjornmark, R. Moller, W. Molzon, B. S. Nielson, L. H. Olsen, Y. Oren, I. Stumer, M. Sullivan, J. A. Thompson, E. Vella, J. Williamson, W. J. Willis, and W. A. Zajc, 1987a, Phys. Lett. B **187**, 420.

Åkesson, T., M. G. Albrow, S. Almehed, O. Benary, H. Boggild, O. Botner, H. Breuker, V. Burkert, A. A. Carter, J. R. Carter, W. E. Cleland, S. Dagan, E. Dahl-Jensen, I. Dahl-Jensen, G. Damgaard, C. W. Fabjan, S. Frankel, U. Goerlach, K. H. Hansen, V. Hedberg, G. Jarlskog, N. Kjaer, R. Kroeger, K. Kulka, D. Lissauer, B. Lorstad, A. Markou, N. A. McCubbin, U. Mjornmark, R. Moller, W. Molzon, B. S. Nielson, L. H. Olsen, Y. Oren, J. Schukraft, K. Spang, I. Stumer, M. Sullivan, J. A. Thompson, H. H. Thodberg, E. Vella, J. Williamson, W. J. Willis, and W. A. Zajc, 1987b, Z. Phys. C **36**, 517.

Akhababian, N., J. Bartke, V. G. Grinshin, and M. Kowalski, 1984, Z. Phys. C **26**, 245.

Albajar, C., M. G. Albrow, O. C. Allkofer, B. Andrieu, K. Ankoviak, R. Apsimon, A. Astbury, C. Bacci, T. Bacon, N. Bains, G. Bauer, S. Beingessner, A. Bettini, A. Bezaguet, P. Biddulph, H. Bohn, A. Bohrer, R. Bonino, K. Bos, M. Botlo, B. Buschbeck, G. Busetto, A. Caner, P. Casoli, F. Cavanna, P. Cennini, S. Centro, F. Ceradini, D. G. Charlton, G. Ciapetti, S. Cittolin, E. Clayton, D. Cline, J. Colas, P. Colas, R. Conte, J. A. Coughlan, G. Cox, D. Dau, J. P. Debrion, M. Degiorgi, M. Della Negra, M. Demoulin, D. Denegri, H. Dibon, A. Diciaccio, F. J. Diez Hedo, L. Dobrzynski, J. Dorenbosch, J. D. Dowell, K. Eggert, E. Eisenhandler, N. Ellis, P. Erhard, H. Faissner, I. F. Fensome, A. Ferrando, M. Fincke-Keeler, L. Fortson, T. Fuess, J. Garvey, S. Geer, A. Geiser, C. Ghiglino, Y. Giroud-Heraud, A. Givernaud, A. Gonidec, J. M. Gregory, W. Haynes, D. J. Holthuizen, M. Ikeda, W. Jank, M. Jimack, G. Jorat, D. Joyce, P. I. P. Kalmus, V. Karimaki, R. Keeler, I. Kenyon, A. Kernan, A. Khan, W. Kienzle, R. Kinnunen, M. Krammer, J. Kroll, D. Kryn, F. Lacava, S. Lammel, M. Landon, R. Leuchs, S. Levegrun, M. Lindgren, D. Linglin, P. Lipa, C. Markou, M. Markytan, M. A. Marquina, G. Maurin, S. McMahon, J.-P. Mendiburu, A. Meneguzzo, J. P. Merlo, T. Meyer, T. Moers, M. Mohammadi, K. Morgan, H.-G. Moser, A. Moulin, B. Mours, Th. Muller, L. Naumann, P. Nedelec, M. Nikitas, A. Nisati, A. Norton, V. O'Dell, G. Pancheri, F. Pauss, E. Petrolo, G. Piano Mortari, E. Pietarinen, M. Pimia, A. Placci, J.-P. Porte, M. Preischl, R. Prosi, E. Radermacher, T. Redelberger, H. Reithler, J.-P. Revol. D. Robinson, T. Rodrigo, J. Rohlf, C. Rubbia, G. Sajot, G. Salvini, J. Sass, D. Samyn, D. Schinzel, M. Schroder, A. Schwartz, W. Scott, C. Seez, T. P. Shah, I. Siotis, D. Smith, P. Sphicas, C. Stubenrauch, K. Sumorok, F. Szoncso, A. Taurok, L. Taylor, I. Ten Have, S. Tether, G. Thompson, E. Tscheslog, J. Tuominiemi, W. van de Guchte, A. van Dijk, S. Veneziano, J. P. Vialle, T. S. Virdee, W. von Schlippe, J. Vrana, V. Vuillemin, K. Wacker, G. Walzel, I. Wingerter, X. Wu, C.-E. Wulz, M. Yvert, C. Zaccardelli, I. Zacharov, L. Zanello, and P. Zotto, 1989, Phys. Lett. B **226**, 410.

Allasia, D., C. Angelini, A. Baldini, L. Bertanza, F. Bianchi, A. Bigi, F. Bobisut, A. Borg, P. Capiluppi, R. Cirio, J. Derkaoui, M. L. Faccini-Turluer, A. G. Frodesen, D. Gamba, G. Giacomelli, B. Jongejans, G. Mandrioli, A. Margiotta-Neri, A. Marzari-Chiesa, R. Pazzi, L. Patrizii, C. Petri, F. Predieri, A. Romero, A. M. Rossi, A. Sconza, P. Serra-Lugaresi, M. Spurio, A. G. Tenner, G. W. van Apeldoorn, P. H. A. van Dam, N. A. M. van Eijndhoven, and D. Vignaud, 1988, Z. Phys. C **37**, 527.

Althoff, M., W. Braunschweig, F. J. Kirschfink, H.-U. Martyn, P. Rosskamp, H. Siebke, W. Wallraff, J. Eisenmann, H. M. Fischer, H. Hartmann, A. Jocksch, G. Knop, H. Kolanoski, H. Kuck, V. Mertens, R. Wedemeyer, B. Foster, A. Wood, E. Bernardi, Y. Eisenberg, A. Eskreys, R. Fohrmann, K. Gather, H. Hultschig, P. Joos, B. Klima, U. Kotz, H. Kowalski, A. Lagage, B. Lohr, D. Luke, P. Mattig, G. Mikenberg, D. Notz, D. Revel, D. Trines, T. Tymieniecka, G. Wolf, W. Zeuner, E. Hilger, T. Kracht, H. L. Krasemann, E. Lohrmann, G. Poelz, K.-U. Posnecker, D. M. Binnie, P. J. Dornan, D. A. Garbutt, C. Jenkins, W. G. Jones, J. K. Sedgbeer, D. Su, J. Thomas, W. A. T. Wan Abdullah, F. Barriero, L. Labarga, E. Ros, M. G. Bowler, P. Bull, R. J. Cashmore, P. Dauncey, R. Devenish, C. M. Hawkes, G. Heath, D. J. Mellor, P. Ratoff, S. L. Lloyd, K. W. Bell, G. E. Forden, J. C. Hart, D. K. Hasell, D. H. Saxon, S. Brandt, M. Dittmar, M. Holder, G. Kreutz, B. Neumann, E. Duchovni, U. Karshon, A. Montag, R. Mir, E. Ronat, G. Yekutieli, A. Shapira, G. Baranko, A. Caldwell, M. Cherney, M. Hildebrandt, J. M. Izen, M. Mermikides, S. Ritz, D. Strom, M. Takashima, H. Venkataramania, E. Wicklund, S. L. Wu, and G. Zobernig, 1985, Z. Phys. C **29**, 347.

Althoff, M., W. Braunschweig, F. J. Kirschfink, H.-U. Martyn, P. Rosskamp, W. Wallraff, J. Eisenmann, H. M. Fischer, H. Hartmann, A. Jocksch, G. Knop, H. Kolanoski, H. Kuck, V. Mertens, R. Wedemeyer, B. Foster, A. Wood, E. Bernardi, A. Eskreys, R. Fohrmann, K. Gather, H. Hultschig, P. Joos, U. Karshon, B. Klima, U. Kotz, H. Kowalski, A. Lagage, B. Lohr, D. Luke, P. Mattig, D. Notz, D. Revel, A. Shapira, D. Trines, T. Tymieniecka, G. Wolf, W. Zeuner, E. Hilger, T. Kracht, H. L. Krasemann, E. Lohrmann, G. Poelz, K.-U. Posnecker, D. M. Binnie, P. J. Dornan, D. A. Garbutt, C. Jenkins, W. G. Jones, J. K. Sedgbeer, D. Su, J. Thomas, W. A. T. Wan Abdullah, F. Barriero, L. Labarga, E. Ros, M. G. Bowler, P. Bull, R. J. Cashmore, P. Dauncey, R. Devenish, C. M. Hawkes, G. Heath, D. J. Mellor, P. Ratoff, S. L. Lloyd, G. E. Forden, J. C. Hart, D. K. Hasell, D. H. Saxon, S. Brandt, M. Dittmar, M. Holder, G. Kreutz, B. Neumann, Y. Eisenberg, A. Montag, G. Mikenberg, R. Mir, E. Ronat, G. Yekutieli, G. Baranko, A. Caldwell, M. Cherney, M. Hildebrandt, J. M. Izen, M. Mermikides, S. Ritz, D. Strom, M. Takashima, H. Venkataramania, E. Wicklund, Sau Lan Wu, and G. Zobernig, 1986, Z. Phys. C **30**, 355.

Andersson, B., and W. Hofmann, 1986, Phys. Lett. B **169**, 364.

Angelini, C., L. Bertanza, A. Bigi, R. Casali, R. Pazzi, C. Petri, P. Espigat, P. Ladron, de Guevara, and M. Laloum, 1977, Lett. Nuovo Cimento **19**, 279.

Angelov, N., S. Backovic, V. G. Grishin, S. V. Dzhmukhadze, L. A. Didenko, I. A. Ivanovskaya, T. Ya. Inogamova, T. Kanarek, E. N. Kladnitskaya, V. B. Lyubimov, N. N. Mel'nikova, Yu. Nady, R. M. Nazargulov, V. F. Nikitina, V. M. Popova, A. N. Solomin, Kh. Semerdzhiev, M. I. Solov'ev, M. K. Suleimanov, D. Tuvdendorzh, E. T. Tsivtsivadze, and L. M. Scheglova, 1977, Yad. Fiz. **26**, 796 [Sov. J. Nucl. Phys. **26**, 419 (1977)].

Angelov, N., N. Akhababyan, Ts. Baatar, E. Bartke, A. P. Gasparyan, N. S. Grigalashvili, V. G. Grishin, S. V. Dzhmukhadze, I. A. Ivanovskaya, L. Jenik, T. Kanarek, E. N. Kladnitskaya, D. K. Kopylova, V. B. Lyubimov, V. F. Nikitina, V. M. Popova, S. I. Lyutov, A. N. Solomin, M. I. Solov'ev, M. K. Suleimanov, G. P. Toneeva, D. Tuvdendorzh, A. P. Cheplakov, A. I. Shklovskaya, and L. M. Shcheglova, 1980, Yad. Fiz. **31**, 411 [Sov. J. Nucl. Phys. **31**, 215 (1980)].

Angelov, N., N. O. Akhababyan, O. Balea, V. Boldea, V. G. Grishin, M. Kowalski, T. Ponta, L. Simic, and S. Khakman,

1981, Yad. Fiz. **33**, 1257 [Sov. J. Nucl. Phys. **33**, 671 (1981)].
Ardouin, D., D. Goujdami, P. Lautridou, R. Boisgard, F. Guilbault, C. Lebrun, A. Peghaire, J. Quebert, F. Saint-Laurent, B. Erazmus, N. Carjan, H. Dabrowski, and D. Durand, 1989, University of Nantes, Internal Report LPN-89-02.
Arneodo, M., A. Arvidson, J. J. Aubert, B. Badelek, J. Beaufays, C. P. Bee, C. Benchouk, G. Berghoff, I. Bird, D. Blum, E. Bohm, X. de Bouard, F. W. Brasse, H. Braun, C. Broll, S. Brown, H. Bruck, H. Calen, J. S. Chima, J. Ciborowski, R. Clifft, G. Coignet, F. Combley, J. Coughlan, G. D'Agostini, S. Dahlgren, F. Dengler, I. Derado, T. Dreyer, J. Drees, M. Duren, V. Eckardt, A. Edwards, M. Edwards, T. Ernst, G. Eszes, J. Favier, M. I. Ferrero, J. Figiel, W. Flauger, J. Foster, E. Gabathuler, J. Gajewski, R. Gamet, J. Gayler, N. Geddes, P. Grafstrom, F. Grard, J. Haas, E. Hagberg, F. J. Hasert, P. Hayman, P. Heusse, M. Jaffre, A. Jacholkowska, F. Janata, G. Jancso, A. S. Johnson, E. M. Kabuss, G. Kellner, V. Korbel, J. Kruger, S. Kullander, U. Landgraf, D. Lanske, J. Loken, K. Long, M. Maire, P. Malecki, A. Manz, S. Maselli, W. Mohr, F. Montanet, H. E. Montgomery, E. Nagy, J. Nassalski, P. R. Norton, F. G. Oakham, A. M. Osborne, L. S. Osborne, C. Pascaud, B. Pawlik, P. Payre, C. Peroni, H. Peschel, H. Pessard, J. Pettingale, B. Pietrzyk, B. Ponsgen, M. Potsch, P. Renton, P. Ribarics, K. Rith, E. Rondio, A. Sandacz, M. Scheer, A. Schlagbohmer, H. Schiemann, N. Schmitz, M. Schneegans, M. Sholz, T. Schroder, M. Schouten, K. Schultze, T. Sloan, H. E. Stier, M. Studt, G. N. Taylor, J. M. Thenard, J. C. Thompson, A. de la Torre, J. Toth, L. Urban, W. Wallucks, M. Whalley, S. Wheeler, W. S. C. Williams, S. J. Wimpenny, R. Windmolders, and G. Wolf, 1986, Z. Phys. C **32**, 1.
Averchenkov, V. A., A. N. Makhlin, and Yu. M. Sinyukov, 1987, Yad. Fiz. **46**, 1525 [Sov. J. Nucl. Phys. **46**, 905 (1987)].
Avery, P., C. Bebek, K. Berkelman, D. G. Cassel, T. Copie, R. Desalvo, J. W. DeWire, R. Ehrlich, R. S. Galik, M. G. D. Gilchriese, B. Gittelman, S. W. Gray, A. M. Halling, D. L. Hartill, B. K. Heltsley, S. Holzner, M. Ito, J. Kandaswamy, D. L. Kreinick, Y. Kubota, N. B. Mistry, E. Nordberg, M. Ogg, D. Peterson, D. Perticone, M. Pisharody, K. Read, A. Silverman, P. C. Stein, S. Stone, Xu Kezun, A. J. Sadoff, T. Bowcock, R. T. Giles, J. Hassard, K. Kinoshita, F. M. Pipkin, R. Wilson, P. Haas, M. Hempstead, T. Jensen, H. Kagan, R. Kass, S. Behrends, T. Gentile, Jan M. Guida, Joan A. Guida, F. Morrow, G. Parkhurst, R. Poling, C. Rosenfeld, E. H. Thorndike, P. Tipton, D. Besson, J. Green, R. Namjoshi, F. Sannes, P. Skubic, R. Stone, D. Bortoletto, A. Chen, M. Goldberg, N. Horwitz, A. Jawahery, P. Lipari, P. Lubrano, G. C. Moneti, C. G. Trahern, H. van Hecke, S. E. Csorna, L. Garren, M. D. Mestayer, R. S. Panvini, G. B. Word, Xia Yi, M. S. Alam, A. Bean, and T. Ferguson, 1985, Phys. Rev. D **32**, 2294.
Awes, T. C., R. L. Ferguson, F. E. Obenshain, F. Plasil, G. R. Young, S. Pratt, Z. Chen, C. K. Gelbke, W. G. Lynch, J. Pochodzalla, and H. M. Xu, 1988, Phys. Rev. Lett. **61**, 2665.
Azimov, S. A., M. L. Allaberdin, S. Edgorov, Sh. V. Inogamov, E. A. Kosonowski, V. D. Lipin, S. L. Lutpullaev, K. Olimov, T. P. Tarasova, K. T. Turdaliev, A. A. Yuldashev, B. S. Yuldashev, A. R. Erwin, R. J. Loveless, and D. D. Reeder, 1984, Phys. Rev. D **29**, 1304.
Back, B. B., K. L. Wolf, A. C. Mignerey, C. K. Gelbke, H. Breuer, V. E. Viola, Jr., and P. Dyer, 1980, Phys. Rev. C **22**, 1927.
Bamberger, A., D. Bangert, J. Bartke, H. Bialkowska, R. Bock, R. Brockmann, S. I. Chase, C. DeMarzo, M. DePalma, I. Derado, V. Eckardt, C. Favuzzi, J. Fent, D. Ferenc, H. Fessler, P. Freund, M. Gazdzicki, H. J. Gebauer, K. Geissler, E. Gladysz, C. Guerra, J. W. Harris, W. Heck, T. J. Humanic, K. Kadija, A. Karabarbounis, R. Keidel, J. Koisiec, M. Kowalski, S. Margetis, E. Nappi. G. Odyniec, G. Paic, A. Panagiotou, A. Petridis, J. Pfennig, F. Posa, K. P. Pretzl, H. B. Pugh, F. Puhlhofer, G. Rai, A. Ranieri, W. Rauch, R. Renfordt, D. Rohrich, K. Runge, A. Sandoval, D. Schall, N. Schmitz, L. S. Schroeder, G. Selvaggi, P. Seyboth, J. Seyerlein, E. Skrzypczak, P. Spinelli, R. Stock, H. Strobele, A. Thomas, M. Tincknell, L. Teitelbaum, G. Vesztergombi, D. Vranic, and S. Wenig, 1988, Phys. Lett. B **203**, 320 [also in Z. Phys. **38**, 79 (1988)].
Barshay, S., 1983, Phys. Lett. B **130**, 220.
Bartke, J., O. Czyzewski, J. A. Danysz, A. Eskreys, J. Loskiewicz, P. Malecki, J. Zaorska, K. Eskreys, K. Juszczak, D. Kisielewska, W. Zielinski, M. Szeptycka, K. Zalewski, G. Pichon, and M. Rumpf, 1967, Phys. Lett. B **24**, 163.
Bartke, J., 1986, Phys. Lett. B **174**, 32.
Bartke, J., and M. Kowalski, 1984, Phys. Rev. C **30**, 1341.
Bartnik, E. A., and K. Rzazewski, 1978, Phys. Rev. D **18**, 4308.
Beavis, D., S. Y. Fung, W. Gorn, A. Huie, D. Keane, J. J. Lu, R. T. Poe, B. C. Shen, and G. VanDalen, 1983a, Phys. Rev. C **27**, 910.
Beavis, D., S. Y. Chu, S. Y. Fung, W. Gorn, D. Keane, R. T. Poe, G. VanDalen, and M. Vient, 1983b, Phys. Rev. C **28**, 2561.
Beavis, D., S. Y. Chu, S. Y. Fung, D. Keane, Y. M. Liu, G. VanDalen, and M. Vient, 1986, Phys. Rev. C **34**, 757.
Becker, U., J. Burger, M. Chen, G. Everhart, F. H. Heimlich, T. Lagerlund, J. Leong, D. Novikoff, L. Rosenson, W. Toki, M. Weimer, and D. I. Lowenstein, 1979, Nucl. Phys. **B151**, 357.
Bernstein, M. A., W. A. Friedman, W. G. Lynch, C. B. Chitwood, D. J. Fields, C. K. Gelbke, M. B. Tsang, T. C. Awes, R. L. Ferguson, F. E. Obenshain, F. Plasil, R. L. Robinson, and G. R. Young, 1985, Phys. Rev. Lett. **54**, 402.
Bernstein, M. A., and W. A. Friedman, 1985, Phys. Rev. C **31**, 843.
Bertsch, G. F., 1989, Nucl. Phys. **A498**, 173c.
Bertsch, G., M. Gong, and M. Tohyama, 1988, Phys. Rev. C **37**, 1896.
Bilic, N., I. Dadic, and M. Martinis, 1978, Phys. Rev. D **18**, 4313.
Biswas, N. N., J. M. Bishop, N. M. Cason, V. P. Kenney, W. D. Shephard, L. R. Fortney, A. T. Goshaw, J. W. Lamsa, J. S. Loos, W. J. Robertson, W. D. Walker, G. Levman, V. A. Sreedhar, T. S. Yoon, G. Hartner, and P. M. Patel, 1976, Phys. Rev. Lett. **37**, 175.
Biyajima, M., 1980, Phys. Lett. B **92**, 193.
Biyajima, M., 1981, Prog. Theor. Phys. **66**, 1378.
Biyajima, M., 1982, Prog. Theor. Phys. **68**, 1273.
Biyajima, M., 1983, Phys. Lett. B **132**, 299 [also published as Phys. Lett B **128**, 24 (1983)].
Biyajima, M., and O. Miyamura, 1974, Phys. Lett. B **53**, 181.
Biyajima, M., and O. Miyamura, 1978, Prog. Theor. Phys. **60**, 302.
Bjorken, J. D., and S. D. Drell, 1965, *Relativistic Quantum Fields* (McGraw-Hill, New York).
Boal, D. H., 1987, Annu. Rev. Nucl. Part. Sci. **37**, 1.
Boal, D. H., and H. DeGuise, 1986, Phys. Rev. Lett. **57**, 2901.
Boal, D. H., and J. C. Shillcock, 1986, Phys. Rev. C **33**, 549.
Bock, R., G. Claesson, K. G. R. Doss, H.-A. Gustafsson, H. H. Gutbrod, K.-H. Kampert, B. W. Kolb, P. Kristiansson, A. M. Poskanzer, H. G. Ritter, H. R. Schmidt, T. Siemiarczuk, H. Wieman, and W. Wislicki, 1988, Mod. Phys. Lett. A **3**, 1745.
Boesebeck, K., G. Kraus, K. Rumpf, P. Kostka, J. Schreiber,

K. Bockmann, H. Drevermann, H. Plothow, B. U. Stocker, P. F. Dalpiaz, W. Kittel, D. R. O. Morrison, R. Stroynowski, H. Wahl, T. Coghen, K. Dziunikowska, J. Loskiewicz, J. Zaorska, A. Wroblewski, and W. Wojcik, 1973, Nucl. Phys. **B52**, 189.

Borreani, G., F. Marchetto, E. Morrone, B. Quassiati, and G. Rinaudo, 1976, Nuovo Cimento **A36**, 245.

Bowler, M. G., 1985, Z. Phys. C **29**, 617.

Bowler, M. G., 1986, Phys. Lett. B **180**, 299.

Bowler, M. G., 1987a, Phys. Lett. B **185**, 205.

Bowler, M. G., 1987b, Phys. Lett. B **197**, 443.

Bowler, M. G., 1988, Z. Phys. C **39**, 81.

Breakstone, A., R. Campanini, H. B. Crawley, G. M. Dallavalle, M. M. Deninno, K. Doroba, D. Drijard, F. Fabbri, A. Firestone, H. G. Fischer, H. Frehse, W. Geist, L. Gesswein, G. Giacomelli, R. Gokieli, M. Gorbics, P. Hanke, M. Heiden, W. Herr, D. Isenhower, E. E. Kluge, J. W. Lamsa, T. Lohse, R. Mankel, W. T. Meyer, T. Nakada, M. Panter, A. Putzer, K. Rauschnabel, B. Rensch, F. Rimondi, M. Schmelling, G. Siroli, R. Sosnowski, M. Szczekowski, O. Ullaland, D. Wegener, and S. Zuchelli, 1985, Phys. Lett. B **162**, 400.

Breakstone, A., R. Campanini, H. B. Crawley, M. Cuffiani, G. M. Dallavalle, M. M. Deninno, K. Doroba, D. Drijard, F. Fabbri, A. Firestone, H. G. Fischer, H. Frehse, W. Geist, H. Floge, L. Gesswein, G. Giacomelli, R. Gokieli, M. Gorbics, M. Gorski, P. Hanke, M. Heiden, W. Herr, D. Isenhower, E. E. Kluge, J. W. Lamsa, T. Lohse, R. Mankel, W. T. Meyer, T. Nakada, M. Panter, A. Putzer, K. Rauschnabel, B. Rensch, F. Rimondi, M. Schmelling, G. Siroli, R. Sosnowski, M. Szczekowski, O. Ullaland, D. Wegener, and R. Young, 1987, Z. Phys. C **33**, 333.

Brown, B. A., C. R. Bronk, and P. E. Hodgson, 1984, J. Phys. G **10**, 1683.

Calligarich, E., G. Cecchet, R. Dolfini, A. Giovannini, S. Ratti, M. Tirelli, R. Gessaroli, G. Parrini, S. Squarcia, G. Costa, L. Perini, J. L. Lloyd, and R. G. Thompson, 1976, Lett. Nuovo Cimento **16**, 129.

Capella, A., and A. Krzywicki, 1989, Z. Phys. C **41**, 659.

Carruthers, P., and C. C. Shih, 1983, Phys. Lett. B **127**, 242.

Carruthers, P., and C. C. Shih, 1984, Phys. Lett. B **137**, 425.

Cebra, D. A., W. Benenson, Y. Chen, E. Kashy, A. Pradhan, A. Vander Molen, G. D. Westfall, W. K. Wilson, D. J. Morrissey, R. S. Tickle, R. Korteling, and R. L. Helmer, 1989, Phys. Lett. B **227**, 336.

Chacon, A. D., J. A. Bistirlich, R. R. Bossingham, H. R. Bowman, C. W. Clawson, K. M. Crowe, T. J. Humanic, J. M. Kurck, C. A. Meyer, J. O. Rasmussen, O. Hashimoto, W. McHarris, J. P. Sullivan, and W. A. Zajc, 1988, Phys. Rev. Lett. **60**, 780.

Chen, Z., C. K. Gelbke, J. Pochodzalla, C. B. Chitwood, D. J. Fields, W. G. Gong, W. G. Lynch, and M. B. Tsang, 1987a, Nucl. Phys. **A473**, 564.

Chen, Z., C. K. Gelbke, W. G. Gong, Y. D. Kim, W. G. Lynch, M. R. Maier, J. Pochodzalla, M. B. Tsang, F. Saint-Laurent, D. Ardouin, H. Delagrange, H. Doubre, J. Kasagi, A. Kyanowski, A. Peghaire, J. Peter, E. Rosato, G. Bizard, F. Lefebvres, B. Tamain, J. Quebert, and Y. P. Viyogi, 1987b, Phys. Lett. B **199**, 171.

Chen, Z., C. K. Gelbke, W. G. Gong, Y. D. Kim, W. G. Lynch, M. R. Maier, J. Pochodzalla, M. B. Tsang, F. Saint-Laurent, D. Ardouin, H. Delagrange, H. Doubre, J. Kasagi, A. Kyanowski, A. Peghaire, J. Peter, E. Rosato, G. Bizard, F. Lefebvres, B. Tamain, J. Quebert, and Y. P. Viyogi, 1987c, Phys. Rev. C **36**, 2297.

Chen, Z., C. K. Gelbke, J. Pochodzalla, C. B. Chitwood, D. J. Fields, W. G. Lynch, and M. B. Tsang, 1987d, Phys. Lett. B **186**, 280.

Chitwood, C. B., J. Aichelin, D. H. Boal, G. Bertsch, D. J. Fields, C. K. Gelbke, W. G. Lynch, M. B. Tsang, J. C. Shillcock, T. C. Awes, R. L. Ferguson, F. E. Obenshain, F. Plasil, R. L. Robinson, and G. R. Young, 1985, Phys. Rev. Lett. **54**, 302.

Chitwood, C. B., C. K. Gelbke, J. Pochodzalla, Z. Chen, D. J. Fields, W. G. Lynch, R. Morse, M. B. Tsang, D. H. Boal, and J. C. Shillcock, 1986, Phys. Lett. B **172**, 27.

Chwieroth, F. S., Y. C. Tang, and D. R. Thompson, 1972, Nucl. Phys. **A189**, 1.

Cocconi, G., 1974, Phys. Lett. B **49**, 459.

Cooper, A. M., S. N. Ganguli, P. K. Malhotra, R. Raghavan, A. Subramanian, A. Gurtu, L. Montanet, L. Dobrzynski, R. Nacasch, M. Aguilar-Benitez, J. A. Garcon, and J. A. Rubio, 1978, Nucl. Phys. **B139**, 45.

De Baere, W., J. Debaisieux, E. De Wolf, P. Dufour, F. Grard, P. Herquet, J. Heughebaert, L. Pape, P. Peeters, F. Verbeure, G. Charriere, D. Drijard, W. M. Dunwoodie, A. Eskreys, Y. Goldschmidt-Clermont, A. Grant, V. P. Henri, F. Muller, Z. Sekera, J. K. Tuominiemi, 1970, Nucl. Phys. **B22**, 131.

De Marzo, C., M. De Palma, A. Distante, C. Favuzzi, P. Lavopa, G. Maggi, F. Posa, A. Ranieri, G. Selvaggi, P. Spinelli, F. Waldner, A. Eskreys, K. Eskreys, D. Kisielewski, B. Madeyski, P. Malecki, K. Olkiewicz, B. Pawlick, P. Stopa, J. R. Fry, M. Houlden, A. Moreton, S. L. Wong, M. Antic, F. Dengler, I. Derado, V. Eckardt, J. Fent, P. Freund, H. J. Gebauer, T. Kahl, A. Manz, K. Miller, P. Polakos, K. P. Pretzl, N. Schmitz, T. Schouten, P. Seyboth, J. Seyerlein, J. Shiers, D. Vranic, G. Wolf, F. Crijns, W. J. Metzger, C. Pols, and T. Spuijbrock, 1984, Phys. Rev. D **29**, 363.

Deutschmann, M., R. Honecker, H. Kirk, M. Klein, R. Nahnhauer, R. Hartmann, H. Plothow, V. T. Cocconi, M. J. Counihan, S. Humble, G. Kellner, D. R. O. Morrison, P. Schmid, R. Stroynowski, L. Aniola, T. Coghen, K. Dziunikowska, J. Figiel, A. Zalewska, E. Leitner, J. Stiewe, J. Krolikowski, A. Para, and A. K. Wroblewski, 1976, Nucl. Phys. **B103**, 198.

Deutschmann, M., P. Kostka, R. Nahnhauer, K. Bockmann, V. T. Cocconi, D. R. O. Morrison, J. Bartke, T. Coghen, J. Figiel, P. Stopa, K. J. W. Barnham, B. Pollock, B. Buschbeck, M. Markytan, A. Para, and A. K. Wroblewski, 1982, Nucl. Phys. **B204**, 333.

De Wolf, E., D. Johnson, F. Vergeure, F. Grard, Ph. Herquet, V. P. Henri, R. Windmolders, J. N. Carney, D. C. Colley, G. T. Jones, J. B. Kinson, J. B. Kinson, K. M. Storr, D. C. Watkins, A. Grant, Y. Goldschmidt-Clermont, H. Johnstad, and A. Stergiou, 1978, Nucl. Phys. **B132**, 383.

DeYoung, P. A., M. S. Gordon, Xiu qin Lu, R. L. McGrath, J. M. Alexander, D. M. de Castro Rizzo, and L. C. Vaz, 1989, Phys. Rev. C **39**, 128.

Donald, R. A., D. N. Edwards, R. S. Moore, E. J. C. Read, S. Reucroft, T. Buran, A. G. Frodesen, S. Sire, P. Saetre, A. Bettini, S. Limentani, L. Peruzzo, R. Santangelo, and S. Sartori, 1969, Nucl. Phys. **B11**, 551.

Drijard, D., H. G. Fischer, R. Gokieli, P. G. Innocenti, V. Korbel, A. Minten, A. Norton, R. Sosnowski, S. Stein, O. Ullaland, H. D. Wahl, P. Burland, M. Della Negra, G. Fontaine, P. Frenkiel, C. Ghesquire, D. Linglin, G. Sajot, H. Frehse, E. E. Kluge, A. Putzer, J. Stiewe, P. Hanke, W. Hofmann, W. Isenbeck, J. Spengler, and D. Wegener, 1979, Nucl. Phys. **B155**, 269.

Dupieux, P., J. P. Alard, J. Augerat, R. Babinet, N. Bastid, F.

Brochard, P. Charmensat, N. De Marco, H. Fanet, Z. Fodor, L. Fraysse, J. Girard, P. Gorodetzky, J. Gosset, C. Laspalles, M. C. Lemaire, D. L'Hote, B. Lucas, J. Marroncle, G. Montarou, M. J. Parizet, J. Poitou, D. Qassoud, C. Racca, A. Rahmani, W. Schimmerling, and O. Valette, 1988, Phys. Lett. B **200**, 17.

Engles, J., and K. Schilling, 1978, Nucl. Phys. **B136**, 349.

Ernst, D. J., M. R. Strayer, and A. S. Umar, 1985, Phys. Rev. Lett. **55**, 584.

Ezell, C., L. J. Gutay, A. T. Laasanen, F. T. Dao, P. Schubelin, and F. Turkot, 1977, Phys. Rev. Lett. **38**, 873.

Feshbach, H. H., A. Kerman, and S. E. Koonin, 1980, Ann. Phys. (N.Y.) **125**, 429.

Fowler, G. N., E. M. Friedlander, F. W. Pottag, R. M. Weiner, J. Wheeler, and G. Wilk, 1988, Phys. Rev. D **37**, 3127.

Fowler, G. N., and R. M. Weiner, 1977, Phys. Lett. B **70**, 201.

Fowler, G. N., and R. M. Weiner, 1978, Phys. Rev. D **17**, 3118.

Fowler, G. N., and R. M. Weiner, 1985, Phys. Rev. Lett. **55**, 1373.

Fowler, G. N., N. Stelte, and R. M. Weiner, 1979, Nucl. Phys. **A319**, 349.

Fox, D., D. A. Cebra, J. Karn, C. Parks, A. Pradhan, A. Vander Molen, J. van der Plicht, G. D. Westfall, W. K. Wilson, and R. S. Tickle, 1988, Phys. Rev. C **38**, 146.

Fung, S. Y. W. Gorn, G. P. Kiernan, J. J. Lu, Y. T. Oh, and R. T. Poe, 1978, Phys. Rev. Lett. **41**, 1592.

Gamow, G., 1928, Z. Phys. **51**, 204.

Gersch, H.-U., 1987, Z. Phys. A **327**, 115.

Giovannini, A., and G. Veneziano, 1977, Nucl. Phys. **B130**, 61.

Goldberger, M. L., H. W. Lewis, and K. M. Watson, 1963, Phys. Rev. **132**, 2764.

Goldberger, M. L., H. W. Lewis, and K. M. Watson, 1966, Phys. Rev. **142**, 25.

Goldhaber, G., W. B. Fowler, S. Goldhaber, T. F. Hoang, T. E. Kalogeropoulos, and W. M. Powell, 1959, Phys. Rev. Lett. **3**, 181.

Goldhaber, G., S. Goldhaber, W. Lee, and A. Pais, 1960, Phys. Rev. **120**, 300.

Goossens, M., E. De Wolf, J. J. Dumont, M. Gysen, C. Dujardin, F. Grard, H. Blumenfeld, N. K. Nguyen, Z. Strachman, J. P. Laugier, I. V. Ajinenko, G. N. Khromova, V. M. Kubic, S. B. Lugovsky, N. G. Minaev, and V. A. Riadovikov, 1978, Nuovo Cimento **48**, 469.

Grard, F., V. P. Henri, J. Schlesinger, R. Windmolders, E. De Wolf, F. Verbeure, D. Drijard, Y. Goldschmidt-Clermont, A. Grant, and A. Stergiou, 1976, Nucl. Phys. **B102**, 221.

Grassberger, P., 1977, Nucl. Phys. **B120**, 231.

Grishin, V. G., G. I. Kopylov, and M. I. Podgoretskii, 1971a, Yad. Fiz. **13**, 1116 [Sov. J. Nucl. Phys. **13**, 638 (1971)].

Grishin, V. G., G. I. Kopylov, and M. I. Podgoretskii, 1971b, Yad. Fiz. **14**, 600 [Sov. J. Nucl. Phys. **14**, 335 (1972)].

Gurney, R. W., and E. U. Condon, 1929, Phys. Rev. **33**, 127.

Gustafsson, H. A., H. H. Gutbrod, B. Kolb, H. Lohner, B. Ludewigt, A. M. Poskanzer, T. Renner, H. Riedesel, H. G. Ritter, A. Warwick, F. Weik, and H. Weiman, 1984, Phys. Rev. Lett. **53**, 544.

Gyulassy, M., 1982, Phys. Rev. Lett. **48**, 454.

Gyulassy, M., 1990, private communication.

Gyulassy, M., and S. K. Kauffmann, 1981, Nucl. Phys. **A362**, 503.

Gyulassy, M., S. K. Kauffmann, and L. W. Wilson, 1979, Phys. Rev. C **20**, 2267.

Gyulassy, M., and S. S. Padula, 1988, Phys. Lett. B **217**, 181.

Hale, G. M., and B. C. Dodder, 1984, in *Few-Body Problems in Physics,* edited by B. Zeitnitz (Elsevier, Amsterdam), Vol. 2, p. 433.

Hama, Y., and S. S. Padula, 1988, Phys. Rev. D **37**, 3237.

Hanbury-Brown, R., R. C. Jennison, and M. K. Das Gupta, 1952, Nature (London) **170**, 1061.

Hanbury-Brown, R., and R. Q. Twiss, 1954, Philos. Mag. **45**, 633.

Hanbury-Brown, R., and R. Q. Twiss, 1956a, Nature (London) **177**, 27.

Hanbury-Brown, R., and R. Q. Twiss, 1956b, Nature (London) **178**, 1046.

Hanbury-Brown, R., and R. Q. Twiss, 1956c, Nature (London) **178**, 1447.

Hanbury-Brown, R., and R. Q. Twiss, 1957a, Proc. R. Soc. London Ser. A **242**, 300.

Hanbury-Brown, R., and R. Q. Twiss, 1957b, Proc. R. Soc. London Ser. A **243**, 291.

Horn, D., and R. Silver, 1971, Ann. Phys. (N.Y.) **66**, 509.

Humanic, T., 1986, Phys. Rev. C **34**, 191.

Jennings, B. K., D. H. Boal, and J. C. Shillcock, 1986, Phys. Rev. C **33**, 1303.

Juricic, I., G. Goldhaber, G. Gidal, G. S. Abrams, D. Amidei, A. R. Baden, J. Boyer, F. Butler, W. C. Carithers, M. S. Gold, L. Golding, J. Haggerty, D. Herrup, J. A. Kadyk, M. E. Levi, M. E. Nelson, P. C. Rowson, H. Schellman, W. B. Schmidke, P. D. Sheldon, G. Trilling, D. R. Wood, T. Barklow, A. Boyarski, M. Breidenbach, P. Burchat, D. L. Burke, D. Cords, J. M. Dorfan, G. J. Feldman, L. Gladney, G. Hanson, K. Hayes, D. G. Hitlin, R. J. Hollebeek, W. R. Innes, J. A. Jaros, D. Karlen, S. R. Klein, A. J. Lankford, R. R. Larsen, B. LeClaire, N. Lockyer, V. Luth, R. A. Ong, M. L. Perl. B. Richter, K. Riles, M. C. Ross, R. H. Schindler, J. M. Yelton, T. Schaad, and R. Schwitters, 1989, Phys. Rev. D **39**, 1.

Klauder, J. R., and E. C. G. Sudarshan, 1968, *Fundamentals of Quantum Optics* (Benjamin, New York).

Kohmoto, S., M. Ishihara, H. Kamitsubo, T. Nomura, Y. Gono, H. Utsunomiya, T. Sugitate, and K. Ieki, 1982, Phys. Lett. B **114**, 107.

Kolehmainen, K., and M. Gyulassy, 1986, Phys. Lett. B **180**, 203.

Koonin, S. E., 1977, Phys. Lett. B **70**, 43.

Koonin, S. E., W. Bauer, and A. Schäfer, 1989, Phys. Rev. Lett. **62**, 1247.

Kopylov, G. I., 1972, Yad. Fiz. **15**, 178 [Sov. J. Nucl. Phys. **15**, 103 (1972)].

Kopylov, G. I., 1974, Phys. Lett. B **50**, 472.

Kopylov, G. I., and M. I. Podgoretskii, 1971, Yad. Fiz. **14**, 1081 [Sov. J. Nucl. Phys. **14**, 604 (1972)].

Kopylov, G. I., and M. I. Podgoretskii, 1972, Yad. Fiz. **15**, 392 [Sov. J. Nucl. Phys. **15**, 219 (1972)].

Kopylov, G. I., and M. I. Podgoretskii, 1973, Yad. Fiz. **18**, 656 [Sov. J. Nucl. Phys. **18**, 336 (1973)].

Kvatadze, R. A., R. Moller, and B. Lorstad, 1988, Z. Phys. C **38**, 551.

Kyanowski, A., F. Saint-Laurent, D. Ardouin, H. Delagrange, H. Doubre, C. Gregoire, W. Mittig, A. Peghaire, J. Peter, Y. P. Viyogi, B. Zwieglinski, J. Quebert, G. Bizard, F. Lefebvres, B. Tamain, J. Pochadzalla, C. K. Gelbke, W. Lynch, and M. Maier, 1986, Phys. Lett. B **181**, 43.

Lednicky, R., and M. I. Podgoretskii, 1979, Yad. Fiz. **39**, 837 [Sov. J. Nucl. Phys. **30**, 432 (1979)].

Liu, Y. M., D. Beavis, S. Y. Chu, S. Y. Fung, D. Keane, G. VanDalen, and M. Vient, 1986, Phys. Rev. C **34**, 1667.

Loktionov, A. A., Zh. S. Takibaev, V. V. Filippova, T.

Temiraliev, B. V. Batyunya, I. V. Boguslavskii, A. Valkarova, V. Vrba, I. M. Gramenitskii, Z. Zlatonov, P. Lednicky, L. A. Tkihonova, T. P. Topuriya, T. A. Garanina, R. K. Dement'ev, E. M. Leiken, N. A. Pozhidaeva, V. I. Rud, J. Zacek, L. Rob, J. Ridky, I. Gerenek, P. Raimer, J. Cwach, W. Simak, S.-B. Liung, R. Orawa, and E. Ervanne, 1978, Yad. Fiz. **27**, 1556 [Sov. J. Nucl. Phys. **27**, 819 (1978)].

Lopez, J. A., J. C. Parikh, and P. J. Siemens, 1984, Phys. Rev. Lett. **53**, 1216.

Lu, J. J., D. Beavis, S. Y. Fung, W. Gorn, A. Huie, G. P. Kiernan, R. T. Poe, and G. VanDalen, 1981, Phys. Rev. Lett. **46**, 898.

Lynch, W. G., C. B. Chitwood, M. B. Tsang, D. J. Fields, D. R. Klesch, C. K. Gelbke, G. R. Young, T. C. Awes, R. L. Ferguson, F. E. Obenshain, F. Plasil, R. L. Robinson, and A. D. Panagiotou, 1983, Phys. Rev. Lett. **51**, 1850.

Machlin, A. N., and Yu. M. Sinyukov, 1987, Yad. Fiz. **46**, 354 [Sov. J. Nucl. Phys. **46**, 354 (1987)].

Makhlin, A. N., 1987, Pis'ma Zh. Eksp. Teor. Fiz. **46**, 49 [JETP Lett. **46**, 55 (1987)].

Miyamura, O., and M. Biyajima, 1975, Phys. Lett. B **57**, 376.

Nakai, T., and H. Yokomi, 1981, Prog. Theor. Phys. **66**, 1328.

Nayak, T. K., T. Murakami, W. G. Lynch, K. Swartz, D. J. Fields, C. K. Gelbke, Y. D. Kim, J. Pochodzalla, M. B. Tsang, F. Zhu, and K. Kwiatkowski, 1989, Phys. Rev. Lett. **62**, 1021.

Neuhauser, D., 1986, Phys. Lett. B **182**, 289.

Ogilvie, C. A., D. A. Cebra, J. Clayton, S. Howden, J, Karn, A. VanderMolen, G. D. Westfall, W. K. Wilson, and J. S. Winfield, 1989, Phys. Rev. C **40**, 654.

Oh, B. Y., W. Morris, D. L. Parker, G. A. Smith, J. Whitmore, R. J. Miller, J. J. Phelan, P. F. Schultz, L. Voyvodic, R. Walker, R. Yaari, E. W. Anderson, H. B. Crawley, W. J. Kernan, F. Ogino, R. G. Glasser, D. G. Hill, G. McClellan, H. L. Price, B. Sechi-Zorn, G. A. Snow, and F. Svrcek, 1975, Phys. Lett. B **56**, 400.

Osborne, L. S., 1988, Phys. Rev. Lett. **60**, 987.

Particle Data Group, 1988, Phys. Lett. B **204**, 1.

Pochodzalla, J., C. B. Chitwood, D. J. Fields, C. K. Gelbke, W. G. Lynch, M. B. Tsang, D. H. Boal, and J. C. Shillcock, 1986, Phys. Lett. B **174**, 36.

Pochodzalla, J., W. A. Friedman, C. K. Gelbke, W. G. Lynch, M. Maier, D. Ardouin, H. Delagrange, H. Doubre, C. Gregoire, A. Kyanowski, W. Mittig, A. Peghaire, J. Peter, F. Saint-Laurent, Y. P. Viyogi, B. Zwieglinski, G. Bizard, F. Lefebvres, B. Tamain, and J. Quebert, 1985a, Phys. Rev. Lett. **55**, 177.

Pochodzalla, J., W. A. Friedman, C. K. Gelbke, W. G. Lynch, M. Maier, D. Ardouin, H. Delagrange, H. Doubre, C. Gregoire, A. Kyanowski, W. Mittig, A. Peghaire, J. Peter, F. Saint-Laurent, Y. P. Viyogi, B. Zwieglinski, G. Bizard, F. Lefebvres, B. Tamain, and J. Quebert, 1985b, Phys. Lett. B **161**, 256.

Pochodzalla, J., W. A. Friedman, C. K. Gelbke, W. G. Lynch, M. Maier, D. Ardouin, H. Delagrange, H. Doubre, C. Gregoire, A. Kyanowski, W. Mittig, A. Peghaire, J. Peter, F. Saint-Laurent, Y. P. Viyogi, B. Zwieglinski, G. Bizard, F. Lefebvres, B. Tamain, and J. Quebert, 1985c, Phys. Lett. B **161**, 275.

Pochodzalla, J., C. K. Gelbke, C. B. Chitwood, D. J. Fields, W. G. Lynch, M. B. Tsang, and W. A. Friedman, 1986, Phys. Lett. B **175**, 275.

Pochodzalla, J., C. K. Gelbke, W. G. Lynch, M. Maier, D. Ardouin, H. Delagrange, H. Doubre, C. Gregoire, A. Kyanowski, W. Mittig, A. Peghaire, J. Peter, F. Saint-Laurent, B. Zwieglinski, G. Bizard, F. Lefebvres, B. Tamain, J. Quebert, Y. P. Viyogi, W. A. Friedman, and D. H. Boal, 1987, Phys. Rev. C **35**, 1695.

Podgoretskii, M. I., and A. P. Cheplakov, 1986, Yad. Fiz. **44**, 1285 [Sov. J. Nucl. Phys. **44**, 835].

Pratt, S., 1984, Phys. Rev. Lett. **53**, 1219.

Pratt, S., 1986a, Phys. Rev. D **33**, 72.

Pratt, S., 1986b, Phys. Rev. D **33**, 1314.

Pratt, S., and M. B. Tsang, 1987, Phys. Rev. C **36**, 2390.

Preston, M. A., and R. K. Bhaduri, 1975, *Structure of the Nucleus* (Addison-Wesley, Reading, Mass.).

Purcell, E. M., 1956, Nature (London) **178**, 1449.

Ranft, J., and G. Ranft, 1975a, Nucl. Phys. **B92**, 207.

Ranft, J., and G. Ranft, 1975b, Phys. Lett. B **57**, 373.

Reid, R. V., Jr., 1968, Ann. Phys. (N.Y.) **50**, 411.

Sato, H., and K. Yazaki, 1980, in *High Energy Interactions and Properties of Dense Matter,* edited by K. Nakai and A. S. Goldhaber (Hakone seminar).

Schiff, L. I., 1955, *Quantum Mechanics* (McGraw-Hill, New York).

Shuryak, E. V., 1973a, Phys. Lett. B **44**, 387.

Shuryak, E. V., 1973b, Yad. Fiz. **18**, 1302 [Sov. J. Nucl. Phys. **18**, 667 (1973)].

Sikkeland, T., E. L. Haines, and V. E. Viola, Jr., 1962, Phys. Rev. **125**, 150.

Suzuki, M., 1987, Phys. Rev. D **35**, 3359.

Thomas, G. H., 1977, Phys. Rev. D **15**, 2636.

Trockel, R., U. Lynen, J. Pochodzalla, W. Trautmann, N. Brummund, E. Eckert, R. Glasow, K. D. Hildenbrand, K. H. Kampert, W. F. J. Muller, D. Pelte, H. J. Rabe, H. Sann, R. Santo, H. Stelzer, and R. Wada, 1987, Phys. Rev. Lett. **59**, 2844.

Tsang, M. B., G. F. Bertsch, W. G. Lynch, and M. Tohyama, 1989, Phys. Rev. C **40**, 1685.

Tsang, M. B., Y. D. Kim, N. Carlin, Z. Chen, R. Fox, C. K. Gelbke, W. G. Gong, W. G. Lynch, T. Murakami, T. K. Nayak, R. M. Ronningen, H. M. Xu, F. Zhu, L. Sobotka, D. Stracener, D. G. Sarantites, Z. Majka, V. Abenante, and H. Griffin, 1989, Phys. Lett. B **220**, 492.

Vourdas, A., and R. M. Weiner, 1988, Phys. Rev. D **38**, 2209.

Xu, H. M., W. G. Lynch, C. K. Gelbke, M. B. Tsang, D. J. Fields, M. R. Maier, D. J. Morrissey, T. K. Nayak, J. Pochodzalla, D. G. Sarantites, L. G. Sobotka, M. L. Halbert, and D. C. Hensley, 1989, Phys. Rev. C **40**, 186.

Xuong, N.-H., and G. R. Lynch, 1962, Phys. Rev. **128**, 1849.

Yano, F. B., and S. E. Koonin, 1978, Phys. Lett. B **78**, 556.

Zajc, W. A., 1987a, Phys. Rev. D **35**, 3396.

Zajc, W. A., 1987b, in *Hadronic Multiparticle Production,* edited by P. Carruthers (World Scientific, Singapore), p. 235.

Zajc, W. A., J. A. Bistirlich, R. R. Bossingham, H. R. Bowman, C. W. Clawson, K. M. Crowe, K. A. Frankel, J. G. Ingersoll, J. M. Kurck, C. J. Martoff, D. L. Murphy, J. O. Rasmussen, J. P. Sullivan, E. Yoo, O. Hashimoto, M. Koike, W. J. MacDonald, J. P. Miller, and P. Truol, 1984, Phys. Rev. C **29**, 2173.

Zarbakhsh, F., A. L. Sagle, F. Brochard, T. A. Mulera, V. Perez-Mendez, R. Talaga, I. Tanihata, J. B. Carroll, K. S. Ganezer, G. Igo, J. Oostens, D. Woodard, and R. Sutter, 1981, Phys. Rev. Lett. **46**, 1268.